

**MICROSTRUCTURAL AND GEOCHEMICAL INVESTIGATION
OF NORTH AMERICAN LOWER-MIDDLE PALEOZOIC TRILOBITES
AND RECENT ARTHROPODS**

A Thesis Presented to
the Department of Geological Sciences
Brock University

In partial fulfillment of
the requirements for the degree
Master of Science in Geology

Graduated Fall, 1989

By
John E. McAllister, B. Sc. Hons.

© 1989

Dr. U. Brand

Thesis Supervisor

"Upon the whole, I was sadly vexed and puzzled, but, at length, I concluded to make a virtue of necessity—to dig with a good will, and thus the sooner to convince the visionary, by ocular demonstration, of the fallacy of the opinions he entertained."

Edgar Allen Poe
The Gold Bug

ABSTRACT

Trilobites were collected from Ordovician and Devonian formations of Ontario, New York, Ohio, Oklahoma, and Indiana. Diversity was generally low, but *Isotelus* and *Phacops* were the most abundant species from the Ordovician and Devonian, respectively. Recent marine arthropods were collected from the Atlantic shore of the middle Florida Keys, and from the Pacific and lagoonal waters at Cape Beale, B. C. Fresh-water arthropods were collected along the shore of the Severn River in north-central Ontario. Cuticles were analyzed for major, minor and trace elements, ^{18}O and ^{13}C isotopes, as well as examined by scanning electron microscope to identify original and diagenetic fabrics.

Examination of trilobite cuticles by scanning electron microscope revealed several microstructures consistent with those observed in Recent arthropods. Microstructures, such as setae and tegumental gland duct openings, in like sized *Limulus* and Isoteline trilobites may indicate common ancestral origins for these organisms, or simply parallel cuticle evolutions. The dendritic microstructure, originally thought to be a diagenetic indicator, was found in Recent specimens and therefore its presence in trilobites may be suggestive of the delicate nature of diagenesis in trilobites. The absence of other primary microstructures in trilobites may indicate alteration, taxonomic control, or that there is some inherent feature of SEM examination which may not allow detection of some features, while others are apparently visible only under SEM. The region of the cuticle sampled for examination is also a major influence in detecting pristine microstructures, as not all areas of trilobite and Recent arthropod cuticles will have microstructures identifiable in a SEM study. Subtleties in the process of alteration, however, may leave pristine microstructures in cuticles that are partially silicified or dolomitized, and degree and type of alteration may vary stratigraphically and longitudinally within a unit. The presence of fused matrices, angular calcite rhombs, and

pyrite in the cuticle are thought to be indicative of altered cuticles, although pyritization may not affect the entire cuticle.

Natural processes in Recent arthropods, such as molting, lead to variations in cuticle chemistries, and are thought to reflect the area of concentration of the elements during calcification. The level of sodium in Recent arthropods was found to be higher than that in trilobites, but highly mobile when subjected to the actions of weathering. Less saline water produced lower magnesium and higher calcium values in Recent specimens, and metal variations in pristine Ordovician trilobite cuticle appears to follow the constraints outlined for Recent arthropods, of regulation due to the chemistry of the surrounding medium. In diagenetic analysis, sodium, strontium and magnesium proved most beneficial in separating altered from least altered trilobites. Using this criterion, specimens from shale show the least amount of geochemical alteration, and have an original mineralogy of 1.7 — 2.4 mole % MgCO_3 (8000 to 9500 ppm magnesium) for both *Isotelus maximus* and *Pseudogygites latimarginatus*, and 2.8 — 3.3 mole % MgCO_3 (5000 to 7000 ppm magnesium) for *Phacops*. This is slightly lower than the mineralogy of Recent marine arthropods (4.43 — 12.1 mole % MgCO_3), and slightly higher than that of fresh-water crayfish (0.96 — 1.82 mole % MgCO_3). Geochemically pristine trilobites were also found to possess primary microstructures. Stable isotope values and trends support the assertion that marine-meteoric/burial fluids were responsible for the alteration observed in a number of the trilobite specimens.

The results of this study suggest that fossil material has to be evaluated separately along taxonomic and lithological lines to arrive at sensible diagenetic and environmental interpretations.

ACKNOWLEDGEMENTS

The author wishes to sincerely thank the following people for their contributions to this work. I thank my supervisor Dr. U. Brand for patiently listening to my ramblings on the pros and cons of arthropod chemistry. I thank Dr. Steve Westrop for having contributed greatly to this thesis by reading early drafts and suggesting changes to concepts, and making available his vast reference library. I truly appreciated the time that he spent on this thesis, and I hope that I will be able to work with him in the future. I'd like to also thank Dr. Terasmae, who's conversations and courses on paleoecology greatly contributed to the approach that this thesis took. His kindness and suggestions will stay with me always. I thank my external examiner, Dr. Rodney Feldman of Kent State University, and Dean Cade for making my incamera defense stimulating and actually quite fun.

I thank my family and friends for having tolerated my indulgence in fossils, and particularly my room-mate Gary dal Bianco for having put up with tons of material scattered liberally about our living room, and forever imbedded in our carpet. I thank Cynthia Forster McAllister for her support and having the strength to put me in my place and pull me through the darkest hours of thesis writing. Her help in reading and making corrections to the various versions of this work, and in sample preparation is greatly appreciated.

To not mention the trip to Ohio, Indiana and Missouri that I made with my mother (the Mary Leakey of trilobite geochemistry) would somehow lessen the sacrifice of the heat that put the misery in Missouri. I also thank (in no particular order) Peter Brown, Denis Tetrault, Nick Bates, Cynthia Forster McAllister, John V. and Cynthia McAllister, Mark and Carolyn Culp, Douglas and Diane Peterson, Bill and Ilse Forster, Uwe Brand, Bill Hessin, James Tremblay, Ian Colquhoun, Eugene Myciak, Neno Testano, John Zorz, and Leonard the-Wonder-Kitty for their friendship and assistance in field work over the past few seasons. I thank Dr. James Stitt (University of Missouri at Columbia) for his

contribution of material from the now closed exposures of the Silica Formation near Sylvania, Ohio and the Bromide Formation in Oklahoma. Dr. Stig Bergström (Ohio State University at Columbus) is thanked for his suggestions of contacts and for releasing, at a small price, some specimens from the Silica Formation. N. Brand and family are thanked for collecting and mailing the specimens from Cape Beale, B. C., thus making much of the Recent arthropod section possible. Thomas Johnson is thanked for his aid in obtaining fragments of *Isotelus maximus* and his suggestion of other, although less fruitful, localities in the Cincinnati region. I thank Mike Lozon for drafting the scales on the SEM photos, and for his competent aid in creating the presentation slides. All other drafted figures were created by the author on a Macintosh Plus computer with SuperPaint software. Howard Melleville is thanked for demonstrating how to pilot the mini-SEM into the bowels of many a trilobite cuticle, and for being an ace reliever when the machine decided to self-destruct; and Candice Kramer is thanked for providing razor blades necessary to separate cuticle from matrix, and an easy way out if things got too bad. And a very special thanks to Nick Bates, my office mate and human wall to bounce ideas. He more than anyone else understands where I'm coming from with this work, and has contributed more than his fair share of ideas. The world needs more Nick Bates'.

Lastly I dedicate this to my grandfather, Edmund P. Peterson, who had wanted to pursue a Masters degree and teach, but due to the onset of the 1930's was robbed of his chance. Although he died before this was completed, he had faith in me and my ability to do anything I put my mind to. He and my grandmother, Violetta, have had more influence on me and my direction in life than they will ever know.

Table of Contents

	Page Number
Abstract	i
Acknowledgements	iii
Table of Contents	v
List of Figures	viii
List of Tables	x
Introduction	xi
Chapter 1—General Geology and Environment	1
Introduction	2
Recent	2
Cape Beale, B. C.	4
Middle Florida Keys	4
North-Central Ontario	4
Devonian	5
Ontario	5
Ohio	9
New York	9
Life Mode of Devonian Trilobites	12
Ordovician	13
Oklahoma	13
Ontario	17
Ohio	20
Life Mode of Ordovician Trilobites	21
Chapter 2 — Methods of Analysis	22
Introduction	23
Scanning Electron Microscopy (SEM)	23
Atomic Absorption Spectrometry (AAS)	25
Trilobites	25
Recent Arthropods	26
X-ray Diffractometry (XRD)	27
Mass Spectrometry	27
Trilobites	27

Statistical Analyses	28
Chapter 3 — Recent Arthropods	29
Introduction	30
Microstructures	30
Laminae	31
Pore Canals and Tegumental Ducts	31
Setae	36
Dendritic Microstructures	39
General Surface Features	39
Trace Element Geochemistry	39
Pristine Composition	43
Molting in Recent Arthropods	43
Environmental Influences on Recent Arthropods	48
Salinity	48
Sediment	49
Mineralogy	52
Chapter 4 — Trilobites	57
Introduction	58
Microstructures	58
Pristine Microstructures	59
Surface Features	59
Osmólska Cavities	62
Pore Canals and Setae	62
Dendritic Microstructures	65
Laminae	70
Biomineralization Structures	72
Diagenetic Microstructures	72
Replacement and Pyritization Microstructures	75
Trace Element Geochemistry	77
Diagenesis in Trilobites	79
Devonian Trilobites	80
Ordovician Trilobites	88
Mineralogy	96
Stable Isotopes	101

Diagenetic Evaluation	101
Chapter 5 — Summary and Conclusions	104
References	109
Appendix I — Species, Locality, Sample Information	125
Appendix II — Ecology of Recent Arthropods	133
Appendix III — Geochemical Data	136
Appendix IV — Statistical Calculations	159
Appendix V — XRD Evaluation	168

List of Figures

	Page Number
Figure 1 — North America locality map	3
Figure 2 — Devonian locality map	6
Figure 3 — Middle Devonian plate positions	7
Figure 4 — Idealized correlation of Devonian units	8
Figure 5 — Correlation of sections in the Devonian of New York	11
Figure 6 — Ordovician locality map	14
Figure 7 — Ordovician plate positions	15
Figure 8 — Idealized correlation of Ordovician units	16
Figure 9 — Section at Craigeith Ontario	19
Figure 10 — Separation of layers in <i>Orconectes</i> sp.	24
Figure 11 — Laminae in <i>Panulirus argus</i>	32
Figure 12 — Tegumental gland ducts on inside surface of <i>Limulus polyphemus</i>	33
Figure 13 — Detail of openings on inside surface of <i>Limulus polyphemus</i>	33
Figure 14 — Dendritics on tegumental gland duct in <i>Limulus polyphemus</i>	34
Figure 15 — Cross-section of tegumental gland duct in <i>Limulus polyphemus</i>	34
Figure 16 — Tegumental duct opening on dorsal surface of <i>Limulus</i>	35
Figure 17 — Detail of tegumental duct opening in <i>Limulus polyphemus</i>	35
Figure 18 — Setae opening on dorsal surface of <i>Limulus polyphemus</i>	37
Figure 19 — Opening on surface of <i>Limulus polyphemus</i>	37
Figure 20 — Receptors in a claw of <i>Orconectes</i> sp.	38
Figure 21 — Setae in a claw of <i>Orconectes</i> sp.	38
Figure 22 — Detail of dendritic microstructure in <i>Limulus</i>	40
Figure 23 — Dendritic microstructures on claw of <i>Callinectes</i> sp.	41
Figure 24 — Dendritic microstructures on <i>Orconectes</i> sp.	41
Figure 25 — Surface texture of the lobster <i>Panulirus argus</i>	42
Figure 26 — Abrasion marks of ventral surface of <i>Callinectes</i> sp.	42
Figure 27 — Iron versus manganese for molt and carcass <i>Orconectes</i> sp.	45
Figure 28 — Calcium versus strontium for molt and carcass <i>Orconectes</i> sp.	45
Figure 29 — 1000 strontium/calcium versus sodium for molt and carcass <i>O.</i> sp.	47
Figure 30 — Iron versus manganese in crabs from Cape Beale, B. C.	51
Figure 31 — Iron versus manganese in <i>Cancer</i> and <i>Callinectes</i>	51
Figure 32 — 1000 strontium/calcium versus magnesium for Recent specimens	53

Figure 33 — Calcim versus magnesium in <i>Cancer</i> and <i>Hemigrapsus</i>	53
Figure 34 — 1000 strontium/calcium versus magnesium in Florida arthropods	54
Figure 35 — Calcium versus magnesium in <i>Callinectes</i> and <i>Cancer</i>	54
Figure 36 — Calcium versus magnesium in Recent arthropods	56
Figure 37 — Striated prismatic layer in pristine <i>Phacops rana</i>	60
Figure 38 — Calcite rhombs on the surface of pristine <i>Phacops rana</i>	61
Figure 39 — Detail of the calcite rhombs on pristine <i>Phacops rana</i>	61
Figure 40 — Angular calcite crystals on the surface of <i>Isotelus maximus</i>	63
Figure 41 — Detail of the angular calcite crystals on <i>Isotelus maximus</i>	63
Figure 42 — Osmólska cavities in pristine <i>Phacops rana</i>	64
Figure 43 — Detail of Osmólska cavities in <i>Phacops rana</i>	64
Figure 44 — Hexagonal surface opening in <i>Isotelus maximus</i>	66
Figure 45 — Large opening on cephalon of <i>Isotelus gigas</i>	66
Figure 46 — Cluster of possible setae openings on cephalon of <i>Vogdesia</i>	67
Figure 47 — Detail of possible setae opening on cephalon of <i>Vogdesia</i>	67
Figure 48 — Tubercles on pygidium of <i>Greenops boothi</i>	68
Figure 49 — Detail of tubercles on <i>Greenops boothi</i>	68
Figure 50 — Possible setae openings at base of tubercles in <i>Greenops boothi</i>	69
Figure 51 — Dendritic microstructures in <i>Phacops rana</i>	71
Figure 52 — Dendritic microstructures in <i>Isotelus maximus</i>	71
Figure 53 — Biomineralization structures in cephalon of <i>Isotelus maximus</i>	73
Figure 54 — Biomineralization structures in thorax of <i>Isotelus maximus</i>	73
Figure 55 — Detail of biomineralization structures in <i>Isotelus maximus</i>	74
Figure 56 — Biomineralization structures in <i>Isotelus</i> sp.	74
Figure 57 — Fused calcite rhombs in <i>Phacops rana</i>	76
Figure 58 — Cubic pyrite crystals in <i>Phacops rana</i>	78
Figure 59 — Pyritohedron pyrite crystals in <i>Isotelus maximus</i>	78
Figure 60 — 1000 strontium/calcium versus manganese in Devonian trilobites	81
Figure 61 — Strontium versus sodium concentrations in Devonian trilobites	81
Figure 62 — <i>Phacops</i> iron and manganese in the Demissa Bed	82
Figure 63 — <i>Phacops</i> strontium and sodium in the Demissa Bed	82
Figure 64 — Strontium and sodium in Smoke Creek <i>Phacops</i>	84
Figure 65 — 1000 strontium/calcium and magnesium in Smoke Cr. <i>Phacops</i>	84
Figure 66 — Stratigraphic variation in cuticle iron and manganese	85
Figure 67 — Stratigraphic variation in cuticle strontium and sodium	85
Figure 68 — 1000 Sr/Ca versus Mg for Devonian trilobites in shale	87

Figure 69 — 1000 Sr/Ca versus Mg for all Devonian trilobites	87
Figure 70 — 1000 Sr/Ca versus Mn for all Ordovician trilobites	89
Figure 71 — 1000 Sr/Ca versus Mn showing facies influence in Ordovician	90
Figure 72 — Stratigraphic variations of sodium and manganese in <i>Isotelus</i>	91
Figure 73 — Stratigraphic variations of Sr/Ca and Mg in <i>Isotelus</i>	91
Figure 74 — Strontium and sodium in <i>Isotelus</i> from equivalent units	93
Figure 75 — Iron and manganese in <i>Isotelus</i> from laterally equivalent units	93
Figure 76 — Iron differences in <i>Vogdesia</i> and <i>Isotelus</i>	94
Figure 77 — Strontium and sodium in <i>Vogdesia</i> and <i>Isotelus</i>	94
Figure 78 — Iron and manganese in <i>Isotelus</i> and <i>Pseudogygites</i>	97
Figure 79 — Strontium and sodium in <i>Isotelus</i> and <i>Pseudogygites</i>	97
Figure 80 — Strontium and sodium in all Ordovician trilobites	98
Figure 81 — 1000 Sr/Ca and magnesium in 'pristine' trilobites	100
Figure 82 — $\delta^{13}\text{C}$ and $\delta^{18}\text{O}$ in Ordovician trilobites	102
Figure 83 — $\delta^{13}\text{C}$ and $\delta^{18}\text{O}$ in Devonian <i>Phacops</i>	102

List of Tables

Table 2.1: Dilutions of sample solutions	26
Table 1: Species Numbers	126
Table 2: Sample Numbers	127
Table 3: Old Sample Numbers	128
Table 4: Locality Numbers	129

INTRODUCTION

In comparison studies with trilobites, Recent arthropods have been used extensively in suggesting the function of microstructures (e. g. Dalingwater and Miller, 1977), morphologic features (e. g. Eldredge, 1970), methods of feeding (e. g. Thayer, 1979) and circulatory systems (e. g. Bergström, 1975). Due to apparent similarities in molting and cuticle formation, Recent arthropods may also be used as a model for the emplacement, and chemistry, of cuticular calcite. This is tempered by the knowledge that cuticle similarities between trilobites and Recent arthropods may be the product of parallel evolution, rather than a common ancestry. Establishing Recent arthropod cuticular chemistry will provide a basis for determining what similarities and differences there may be between taxa, and physical and chemical environmental influences. A comparison with the chemistry of trilobites should then allow the removal of the diagenetic imprint, suggest an original chemistry and mineralogy, and indicate possible environmental influences.

In order to attain as great a diversity of information as possible, Recent specimens were sampled from marine detrital and carbonate environments, as well as fresh water. The species obtained inhabited similar ecological niches, and are limited in diversity. Ordovician and Devonian trilobites, also limited in diversity, were obtained from limestone and shale facies. This was done in order to establish the influence that facies exerts in the diagenesis of these organisms, as well as presenting the possibility of a variety of environmental influences. Different degrees and modes of alteration were also desirable in trilobites to facilitate identification of geochemical changes that could be associated with the diagenesis. This necessitated that localities known to possess altered specimens be sampled.

Few researchers have examined in detail the composition of trilobite, or Recent arthropod cuticular calcite. Studies on Recent arthropod cuticle have generally concentrated on microstructures (e. g. Neville and Berg, 1971; Kennaugh, 1965; Neville

and Luke, 1969), biophysiology (Travis, 1954; Passano, 1960; Quackenbush and Herrnkind, 1983), or chemistry (Brannon and Rao, 1979; Huner *et al.*, 1979a and b; Vigh and Dendinger, 1982; Greenaway, 1983; Quackenbush and Herrnkind, 1983; Dendinger and Alterman, 1983; Engel, 1987) of the cuticle. Detailed studies of the cuticle are rare, and geochemical analyses even less. Examinations of trilobite cuticle has been likewise sporadic. Using X-ray diffraction (XRD), Stehli (1956) examined one trilobite pygidium from the Middle Pennsylvanian Boggy Formation of Oklahoma, U. S. A. and supported Bøggild's (1930 in Stehli, 1956) suggestion of a calcitic trilobite cuticle. Lowenstam (1963) expanded on this proposition and suggested a MgCO_3 composition of 2–14 mole % (recorded maximum—5 mole %) for the cuticle of Proetid trilobites (Lower Pennsylvanian), and 6–14 mole% for Recent Decapoda. He indicated that additional data were needed to comment on the original mineralogy of ancient arthropods and trilobites. Dalingwater (1973) and Towe (1973) also inferred that the original mineralogy of trilobites was calcite. Kanip (1986) examined the elemental composition of ten trilobite fragments from the Kashong Shale of the Middle Devonian Hamilton Group and concluded that trilobite cuticles were originally low-Mg calcite. Subsequently, McAllister (1987, 1988) and McAllister and Brand (1987, 1989, In press) reported preliminary elemental and isotopic results, and provided information on both diagenetic and pristine microstructures in trilobite cuticles.

Chapter 1

General Geology and Environment

INTRODUCTION

Due to adaptation and natural selection, marine arthropods live in a wide range of environments. The impact of the surrounding medium on the chemistry and preservation of the cuticle of Recent and fossil arthropods is largely unknown. Thus localities with contrasting environments were chosen to be representative of these influences. Paleozoic trilobite cuticles were collected from formations of different lithologic compositions such as limestone and shale, which originated in contrasting environments. In order to compensate for possible age influences on specimen exoskeletal geochemistry, trilobites were obtained from Ordovician and Devonian units.

RECENT

The localities, from which Recent material was obtained, were chosen to provide as great a contrast in physical and chemical environmental settings as possible. Marine samples were procured from the temperate waters off Cape Beale, B. C (loc. 28, Fig. 1), and the subtropical waters of the middle Florida Keys (loc. 29, 30; Fig. 1). Fresh water species were obtained from the Severn River in north-central Ontario (loc. 27; Fig. 1). For a complete listing and description of localities see Appendix I.II.

Aside from the physical and chemical environmental constraints, the life habits and habitats of the species must be taken into consideration before attempting to interpret their respective chemistries (see Appendix II). For example, the chemistry of a burrowing mud crab might be different than that of a crab from a high energy carbonate environment, due to differences in sediment and water compositions, and biological fractionation for or against specific elements.

Cape Beale, B. C.

Specimens obtained from Cape Beale, B. C. matured in a detrital environment with a water temperature range of 6.2°C to 12.8°C, a salinity range of 28.5‰ to 31.0‰

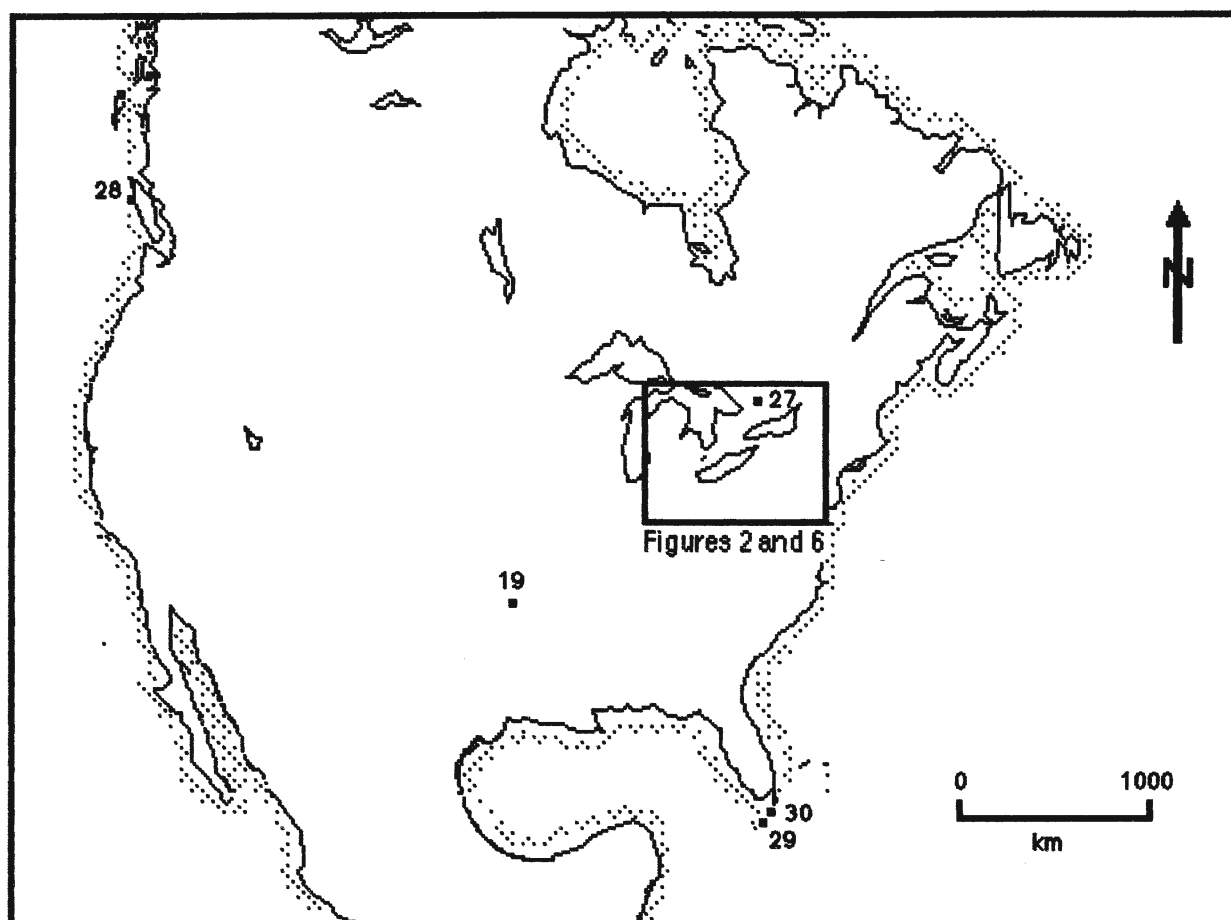


Figure 1: General locality diagram of Recent material (27—Severn River, Washago, ON; 28—Cape Beale, BC; 29—Bahia Honda Key, FL; and 30—Long Key, FL) and an extraneous Middle Ordovician sample site (19—Bromide Formation, Ardmore, OK). Devonian and Ordovician localities are illustrated in figures 2 and 6.

TDS, and a $\delta^{18}\text{O}$ composition of -1.7‰ to -0.7‰ (SMOW; Brand *et al.*, 1987). Specimens of *Cancer productus* and *Cancer magister* were collected from the high energy beach front, while specimens of *Hemigrapsus nudis* were obtained from the lower energy, less saline lagoonal waters. Individuals were dead for only a few days, because the high energy actions of the surf at Cape Beale combined with bacterial feeding quickly disarticulates the arthropods. More detailed information is found in Appendix II.

Middle Florida Keys, Florida

The modern marine arthropods obtained from the middle Florida Keys matured in a carbonate environment with an average water pH of 7.5 and a surf temperature of 19.5°C (on the date of collection in mid-November, 1987). However, the water temperature range for the Florida Keys is 15°C to 33°C (Bathurst, 1975, p. 149). Salinity within 9 m of the water surface in the Florida Keys ranges from approximately 32‰ to 38‰ (Bathurst, 1975, p. 149), and $\delta^{18}\text{O}$ values range from +0.91‰ to +1.74‰ (SMOW; Brand, unpublished data). Carcasses of *Limulus polyphemus*, *Panulirus argus*, *Callinectes sapidus* and *Callinectes* sp. were obtained from the beach and near-shore surf. Several of the specimens of *Panulirus argus* had died recently, as indicated by their lack of disarticulation and presence of adhering tissue.

North-Central Ontario

Specimens of the crayfish *Orconectes* sp. were obtained, during the spring and summer of 1988, from the Severn River, Ontario. These organisms matured in an environment that, due to its proximity to the town of Washago and highways 11 and 169, may have received spring run-off with large quantities of silt and dissolved road salt. Secondary sources for elevated, short-term salinities would be run-off from cities and highways draining into Lakes Simcoe and Couchiching, which in turn drain into the Severn River. Unlike its water source, the river does not freeze in winter. In summer, the

surface water temperature of the Severn River may be as high as 30°C, whereas the temperature at the water/sediment interface is closer to 22°C. The river bottom consists of a combination of mud and fractured Precambrian rock, with high concentrations of vegetation in areas with a soft stratum. Carcasses were collected along the river shore, and collected daily as fragments from a floating wooden platform used for feeding by birds.

DEVONIAN

Ten localities from north-central New York State, southern Ontario, and north-western Ohio (Fig. 2) were selected for this study based on their facies, age and repeated exposure of beds. All of the Devonian units are located within 2 to 3 degrees paleolatitude of each other, and at the time of deposition, the region was within 15 degrees of the equator (Fig. 3; Scotese and Dunham, 1988). The constrained latitudinal positions of the units has likely minimized habitat effects, such as wide variations in water temperature, on trilobite cuticle geochemistry (e.g., Brand, 1989). For a complete listing and description of localities see Appendix I.II.

Ontario

The oldest Devonian unit examined is the Edgecliff Member of the Onondaga Formation (Fig. 4), which forms a minor escarpment extending from Lake Huron across southern Ontario into northern New York State. This unit represents a reef complex deposited in a warm, shallow subtidal, normal marine environment (Laporte, 1971; Parkins, 1977; Feldman, 1980) that is believed to have been quite similar to that of the present Bermuda coral reefs (Reimann, 1940). The trilobites of this unit range in size from the large *Terataspis grandis* to the not-so-large *Phacops rana*.

The Widder Formation (Tioughiogon) is younger than the Onondaga Formation (Onesquethawan) (Fig. 4) and outcrops in gorges cut by the Ausable River, and in

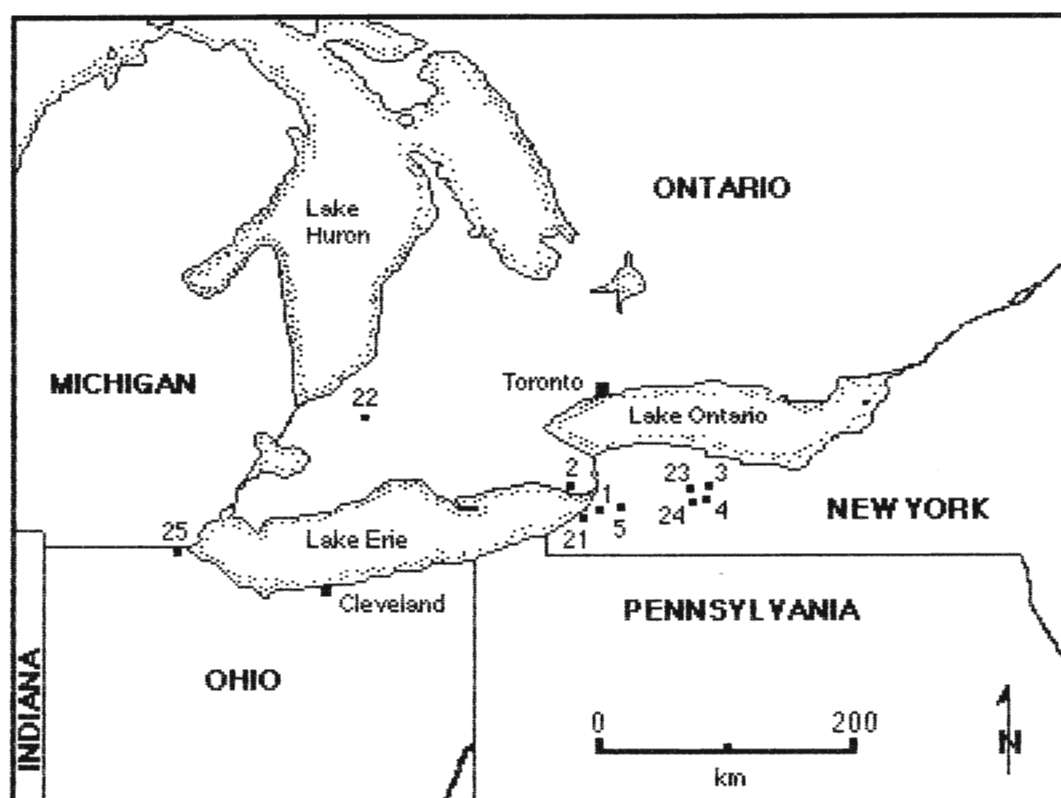


Figure 2: Locality diagram of sample sights for Devonian trilobites in Ontario, Canada and Ohio and New York State, U.S.A. Localities are: Erian (Givetian) Moscow Formation (1—Bayview, NY; 3—Fall Brook, Genesee, NY; 23—Retsof, NY; 24—Wheeler Gully, Genesee, NY); Erian Widder Formation (22—Arcona, ON); Erian Silica Formation (25—Sylvania, OH); Erian Ludlowville Formation (1—Bayview, NY; 4—Jaycox Creek, NY; 5—Spring Brook, NY; 21—Eighteen Mile Creek, Wanakah, NY); Erian (Eifelian) Onondaga Formation (2—Pt. Colbourne, ON).

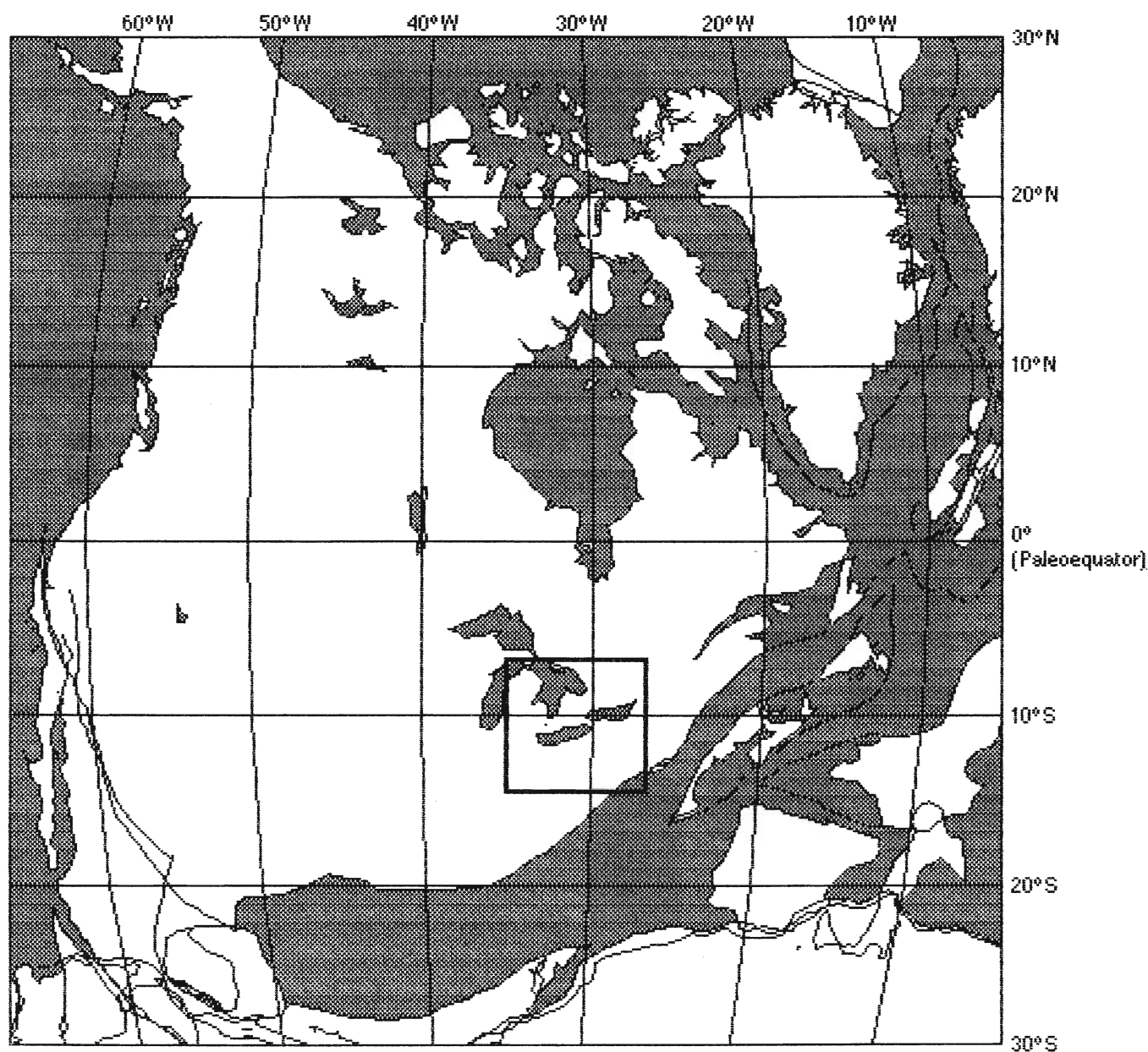


Figure 3: Orthographic projection of the relative continental plate positions (modified from Scotese and Dunham, 1988) during the deposition of the Middle Devonian units of this study 383 to 373 ma (Rickard, 1975; Harland et al., 1982). The area outlined is shown in more detail in figure 2. Paleoshorelines are not suggested by this diagram.

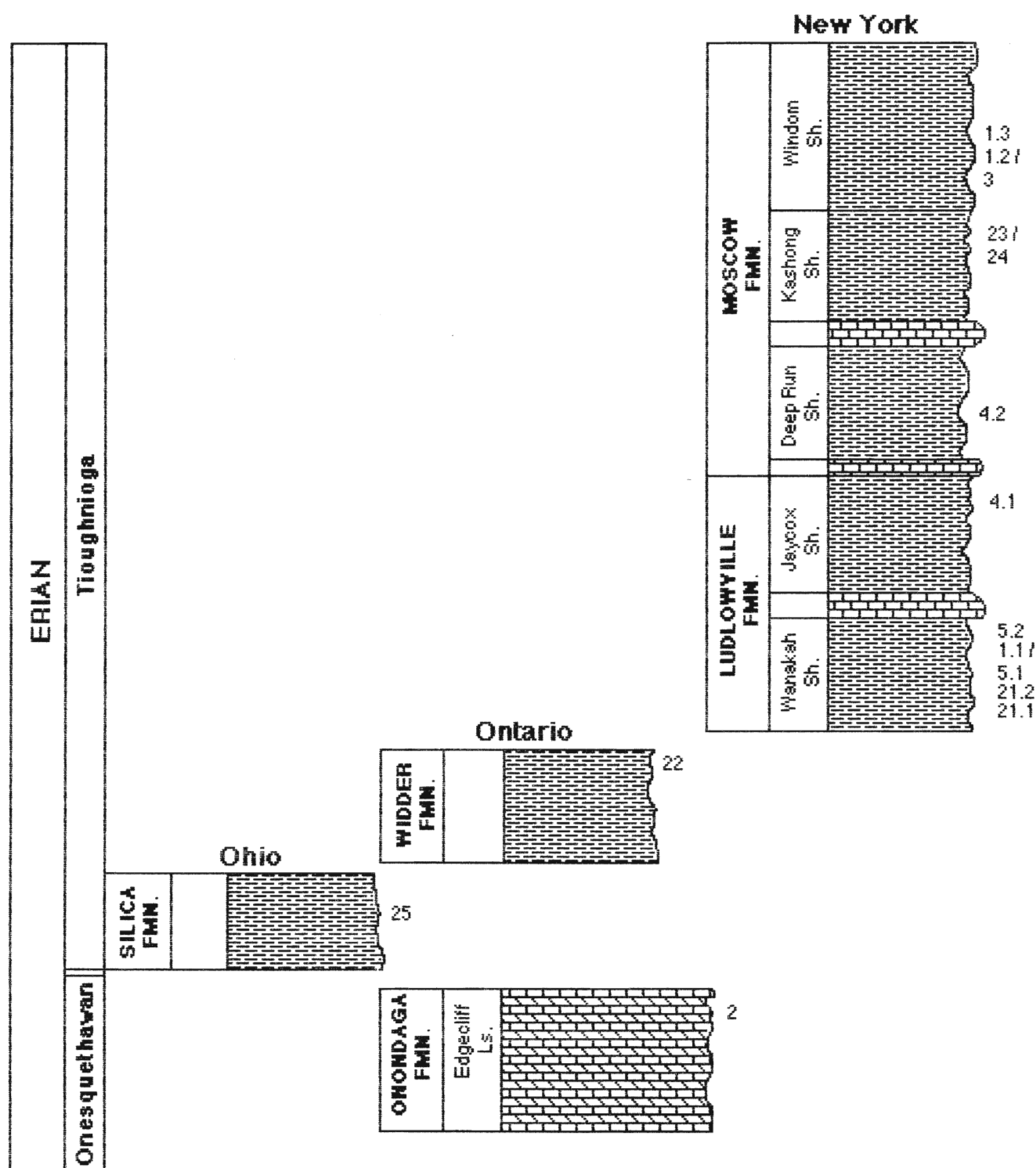


Figure 4: Idealized sections of Middle Devonian outcrops in Ohio, Ontario and New York State. Sections are not drawn to scale. Numbers to the right of the units are the localities from which material was obtained.

abandoned quarries in the Ipperwash-Thedford-Arkona region. It consists of highly fossiliferous shales and limestones, and overlies the Arkona Shale and the Hungry Hollow Formation of the Middle Devonian Hamilton Group (Wright and Wright, 1961). Specimens of *Greenops boothi* were obtained from the lowermost shales.

Ohio

The Silica Formation exposed in the Medusa Portland Cement Co. Quarry near Sylvania (loc. 25, Fig. 2) was one of the most popular Devonian collecting units in North America until the closing of the quarry in the late 1970's. This formation consists of argillaceous and fossiliferous fine- to coarse-grained gray-brown limestone interbedded with varying amounts of fossiliferous and calcareous bluish- to brownish-gray shale (Janssens, 1970). The Silica Formation is early Tioughiogon in age (Fig. 4) and has been correlated with the Hungry Hollow Formation of Ontario by Mitchell (1967). Deposition of this unit occurred on the west side of the Findlay Arch (Mitchell, 1967), within the wave zone (Driscoll et al., 1965), and in water of normal salinity and oxygen content (Nussmann, 1975). As in most Devonian shale units of North America, evidence indicating episodic sedimentation by storms exists in the Silica Formation (e.g. Nussmann, 1975).

New York

Composed predominantly of clastic rocks (Baird, 1979), the Middle Devonian of New York State is best known for its highly fossiliferous units. The Hamilton Group, which is divided into the Marcellus, Skaneateles, Ludlowville and Moscow Formations, comprises one of the most complete sequences of Middle Devonian strata in the world (Broughton et al., 1973; Brett, 1986), and serves as a major reference sequence for paleontologic and stratigraphic studies (Baird, 1979). During the Devonian, hurricane dominated storms occurring between 8° and 30° paleolatitude (Marsaglia and Klein,

1983) acted on the Acadian Orogenic Belt. Combined with pulses of tectonic uplift in the east and southeast, these storms contributed to abundant material being discharged westerly into the eperic sea (Brett and Baird, 1982; Miller et al., 1988). Severe storms are indicated by the presence of large amounts of fine-grained material reaching the then far-shore region of present day Erie County. This discharge was laterally extensive enough to suffocate a widespread benthic community (Speyer and Brett, 1984; Brett et al., 1986).

The oldest units of the Hamilton Group examined in this study are the Wanakah and Jaycox Members of the Ludlowville Formation (Figs. 4 and 5), which consist of fossiliferous shales interbedded with unfossiliferous material. During deposition of these units, the substrate was probably bioturbated and relatively fluid, with little in the way of stable platforms for the growth of sessile organisms (Bray, 1972). Several individual beds within the Wanakah, such as the Demissa (Fig. 5) and Murder Creek beds, have been recognized for their abundant and diverse faunas. The Wanakah through Jaycox sequence has been interpreted by Brett and Baird (1981) as a shallowing upward or regressive hemicycle.

The peak of the regression, with deposition in a high energy setting above wave base, is recorded by the Tichenor Limestone of the overlying Moscow Formation (Brett and Baird, 1981). The return to deeper water conditions is represented by the sediments of the Deep Run Shale Member (Moscow Formation), and indicates active, localized subsidence in the region (Brett and Baird, 1981). The presence of current structures within the Deep Run indicates that although this unit was deposited in deeper water below normal wave base, it was still within reach of storm waves (Brett and Baird, 1981). Overlying the Deep Run, is the Kashong Shale Member (Moscow Formation—Figs. 4, 5), which is faunally and lithologically similar to parts of the Deep Run Shale (Brett and Baird, 1981). The Deep Run-Kashong interval has been interpreted by Brett and Baird (1981) as a regressive sequence.

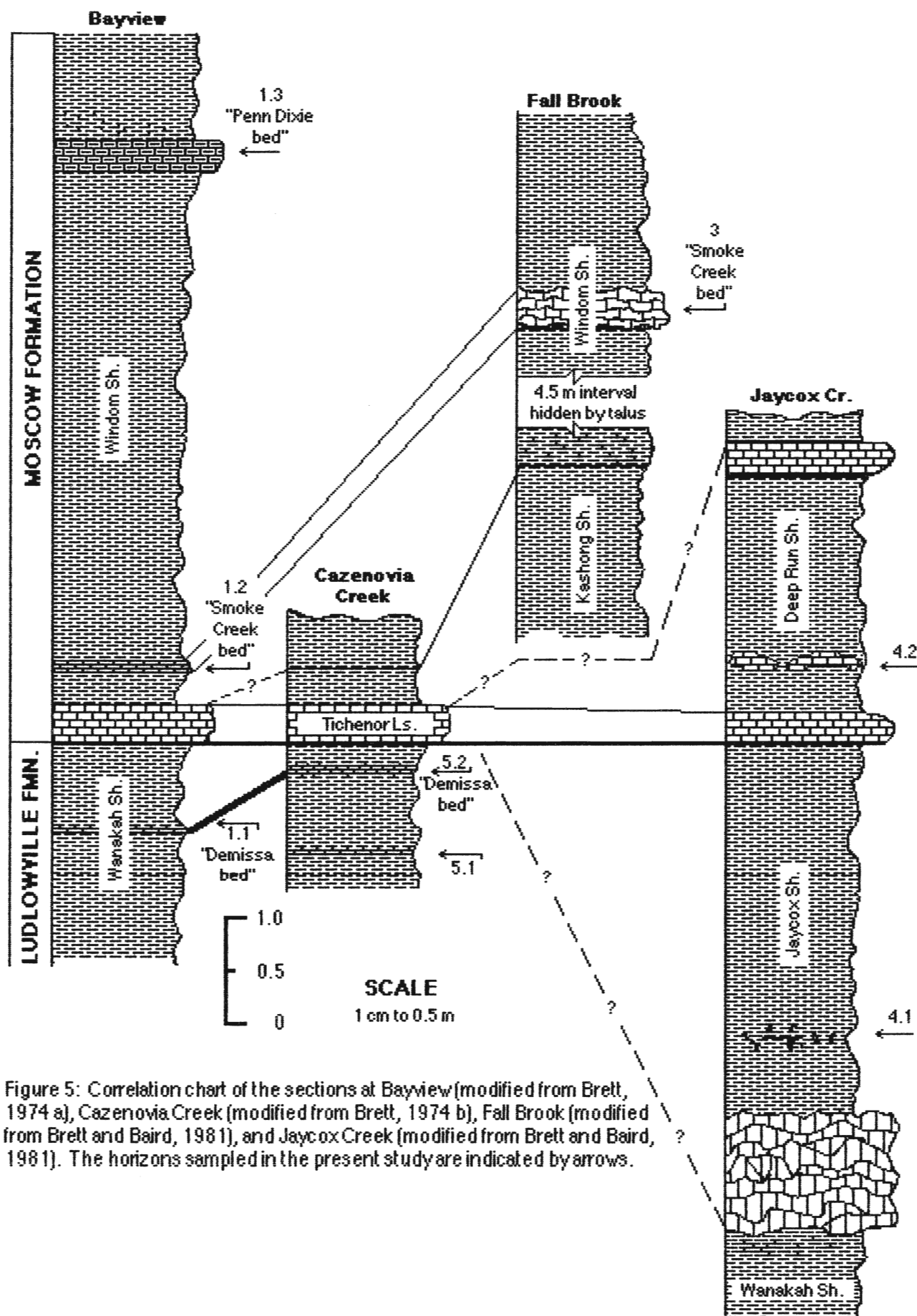


Figure 5: Correlation chart of the sections at Bayview(modified from Brett, 1974 a), Cazenovia Creek(modified from Brett, 1974 b), Fall Brook(modified from Brett and Baird, 1981), and Jaycox Creek(modified from Brett and Baird, 1981). The horizons sampled in the present study are indicated by arrows.

Overlying the Kashong Shale Member (Moscow Formation) is the Windom Shale Member (Figs. 4, 5). Exposed from Lake Erie through Genesee and Wyoming valleys, the Windom Shale is an unusually fossiliferous unit consisting of thin, grey marine shales and limestones in the west and sandstones, siltstones, and silty shales in the east (Baird, 1979; Brett, 1986). The Windom thins westward under Lake Erie and is not present in Ohio or Ontario. Within the Windom, the basal Smoke Creek bed can be traced from its type locality at Smoke Creek near Windom, Erie County, N. Y. 90 km east to Fall Brook (loc. 3, Fig. 2) and over 320 km east to Skaneateles Lake, where it becomes sandy and interfingers with the shales and sandstones of the Cooperstown Member (Brett, 1974b). In Erie County, the unit ranges in thickness from 3 to 15 m, with fossil bearing layers at the top (Penn Dixie bed—loc. 1.3, Fig. 5) and bottom (Smoke Creek bed—loc. 1.2, Fig. 5) of the unit (Brett, 1974b). The intervening 1 to 10 m of strata consist of barren, structureless shale (Brett, 1974b). Enrollment is a general response to adverse conditions in trilobites (Speyer, 1985), and an abundance of such trilobites preserved at several horizons within the Windom indicate that sudden and catastrophic events occurred immediately prior to their deaths. In addition, their intact preservation implies that they were subject to deep and rapid burial (Speyer and Brett, 1984; Speyer, 1988).

Life Mode of Devonian Trilobites

Covered in spines and ornaments, *Terataspis grandis* is the largest of the trilobites studied (exceeding 20 inches in length; Reimann, 1940) and was obtained as fragments from only one unit (Edgecliff Member, Onondaga Formation—loc. 2, Fig. 2). Although very little study has been undertaken on this trilobite, its size and ornamentation suggests that although benthic, *Terataspis* was most likely not a prolific burrower.

The phacopidacean trilobites *Phacops rana* and *Greenops boothi* inhabited shallow, tropical to subtropical, waters (Chlupáč, 1975). Stürmer and Bergström (1973) suggest that the species of *Phacops* that they examined was a benthic dweller, was capable of walking on and swimming above the bottom, and not adept at burrowing. Stürmer and Bergström (1973) also suggest that although able to prey on large animals, feeding was generally limited to other methods in the phacopids. Campbell (1975; in Stockton and Cowen, 1976) interpreted that some phacopids were epifaunal carnivores. Eldredge (1974) suggested that while phacopids were generally benthic, their larvae were most likely planktonic. These trilobites therefore must be assumed to have had several feeding options, and were capable of inhabiting a variety of mediums, with little emphasis on burrowing.

ORDOVICIAN

Trilobites were obtained from limestone and shale outcrops in south-central Ontario (loc. 6 - 13 and 20, Fig. 6), south-western Ohio (loc. 14 - 16, Fig. 6), south-eastern Indiana (loc. 17 and 18, Fig. 6), and Oklahoma (loc. 19, Figs. 1, 7). For a complete listing and description of localities see Appendix I.II. During the Ordovician, the region was tropical to subtropical (Fig. 7; within 25° of the equator; Scotese and Dunham, 1988) with shallow, warm epeiric seas and westerly-moving trade winds (Frey, 1987).

Oklahoma

The oldest strata from which samples were analysed is the Pooleville Member of the Bromide Formation (Simpson Group), in the Arbuckle Mountains of Oklahoma (loc. 19, Figs. 1, 7, 8). It consists of fine-grained shallow-water clastic and carbonate material deposited into the subsiding Ardmore-Anadarko trough (Shaw, 1974). Due to the fine-grained texture of the sediment and lack of disarticulation of the trilobites (Schramm,

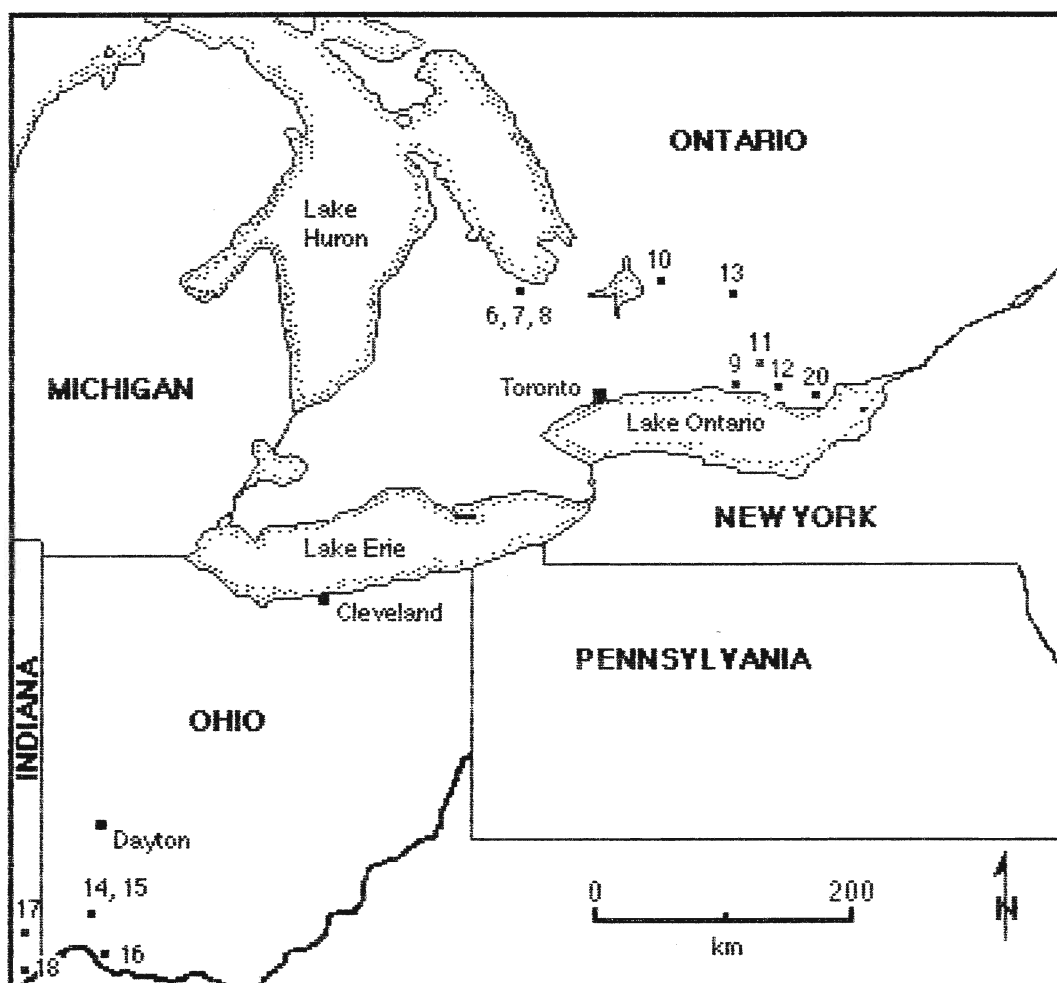


Figure 6: Diagram of sample localities for Ordovician trilobites in Ontario, Ohio and Indiana. Localities are: Trentonian Verulam Formation (9—Colbourne, ON; 10—Kirkfield, ON; 11—near Trenton, ON; 12—Belleville, ON; 13—Lakefield, ON); Trentonian-Edenian Cobourg Formation (7, 8—Collingwood, ON; 9—Colbourne, ON; 20—Bay of Quinte, ON); Maysvillian Whitby Formation (6—Craigleith, ON); Edenian Kope Formation (16—Ripley, OH); Maysvillian Fairview Formation (18—Aurora, IN); Richmondian Waynesville Formation (14—Caesar Cr., OH; 15—Waynesville, OH; 17—Brookville, IN); and Richmondian Liberty Formation (14—Caesar Cr.).

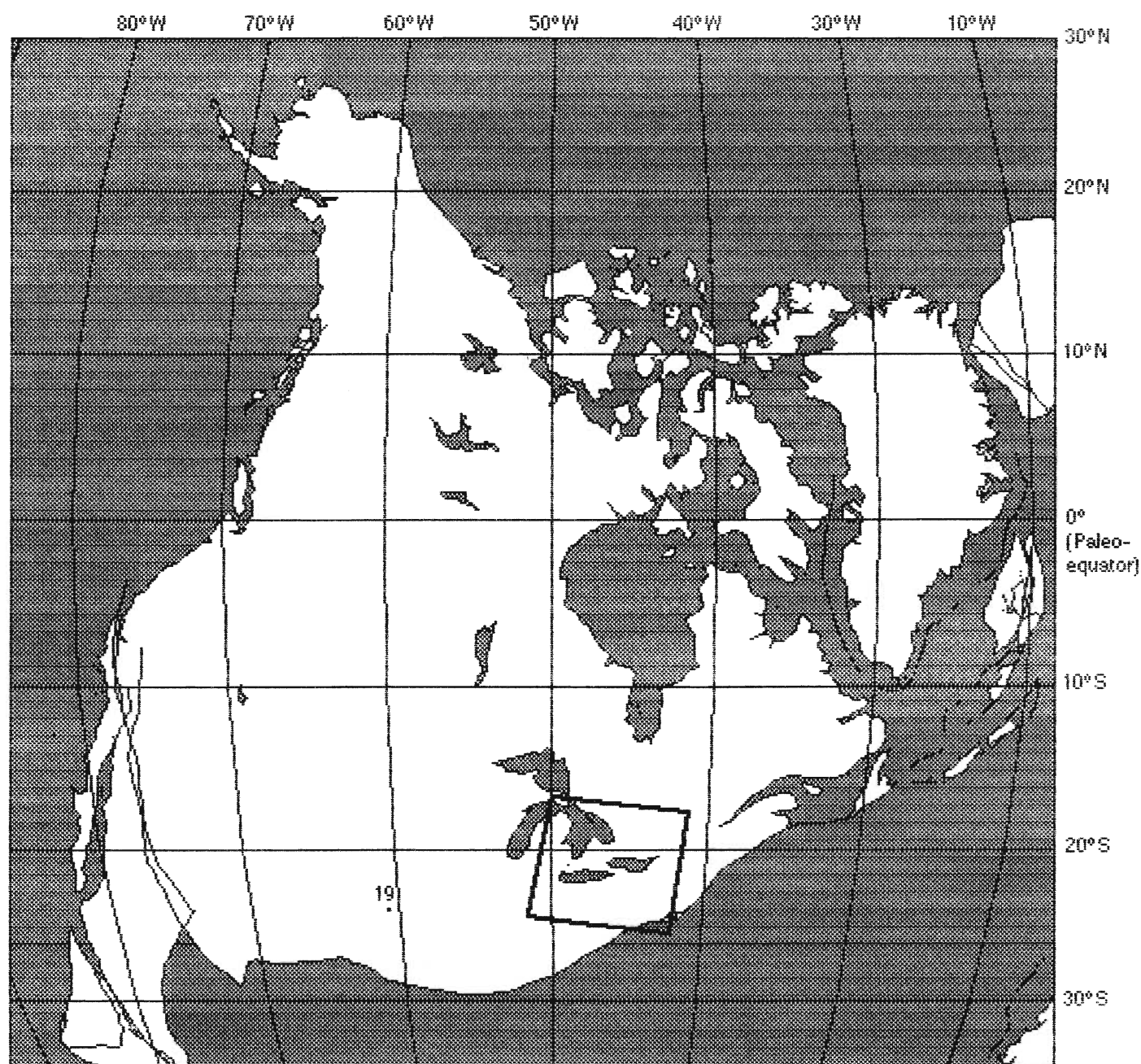


Figure 7: Orthographic projection of the relative continental plate positions (Scotese and Dunham, 1988) during the deposition of the Ordovician Formations of this study from approximately 457 to 443 Ma (Barnes et al., 1981; Harland et al., 1982). The area outlined is shown in more detail in figure 6. Paleoshorelines are not suggested by this diagram.

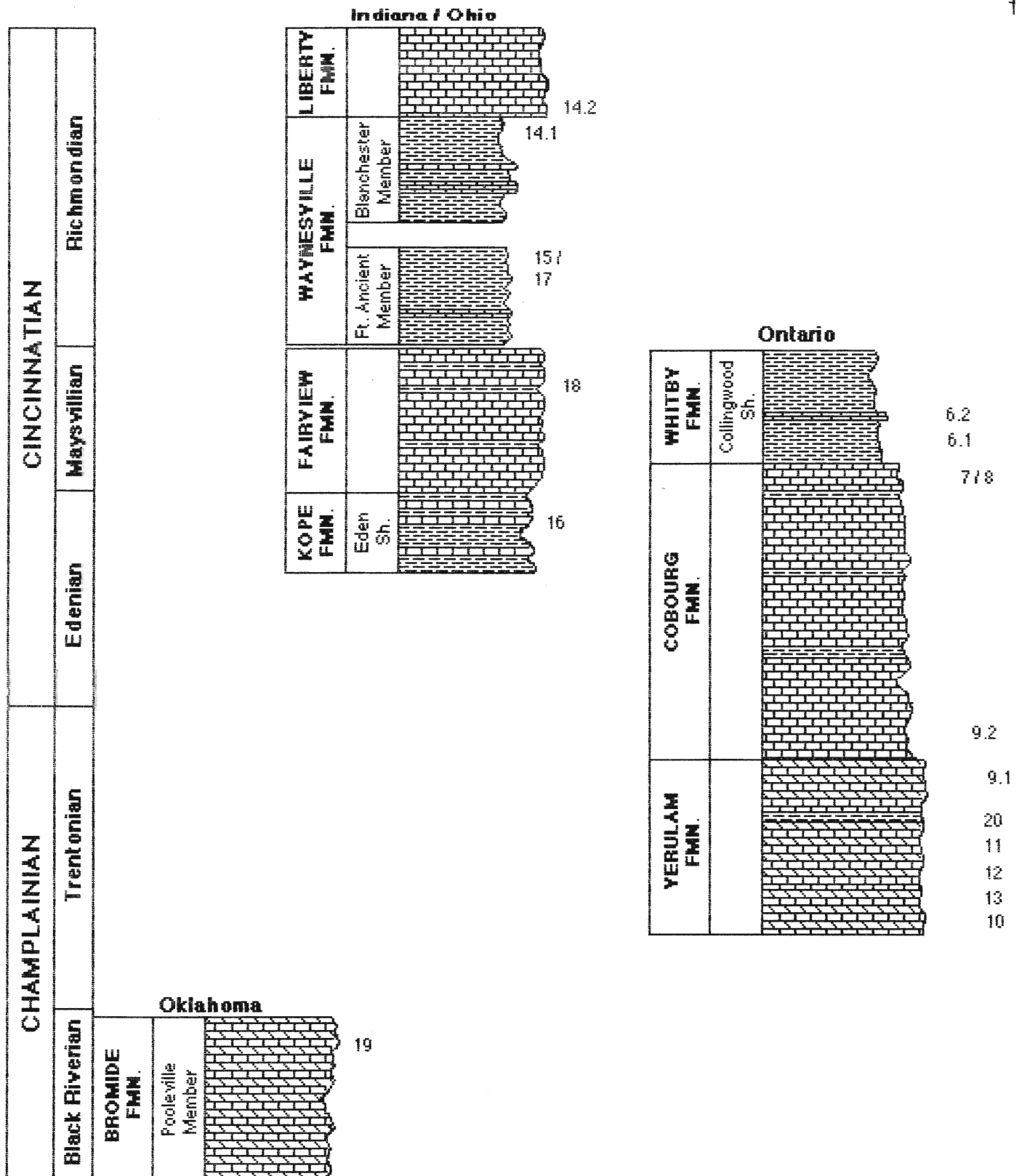


Figure 8: Idealized section of Middle (Black Riverian / Trentonian) and Upper (Edenian / Maysvillian / Richmondian) Ordovician outcrops in Oklahoma, Ohio, Indiana, and Ontario showing their relative correlations. Ontario correlations modified from Barnes et al., 1981. Sections are not drawn to scale, and are relative thicknesses. Numbers to the right of the units represent sample horizons.

1964; Shaw, 1974), the Bromide Formation is believed to have been deposited in a lower energy and deeper water environment than the super- and subjacent sediments. Shaw (1974) correlates the Bromide Formation with the Black River and Chazy Groups of the inner regions of the platform. The only trilobite collected from the Bromide was the *Isotelus* *Vogdesia bromidensis* (Esler; see Shaw, 1974 for discussion of taxonomy).

Ontario

In Ontario, outcrops of the Middle to Upper Ordovician Verulam, Cobourg and Whitby Formations (Fig. 8), were sampled from Trenton in the east, to Craigleith Station in the west (loc. 6 - 13 and 20, Fig. 6). According to Winder (1960), these units record a transgressive sequence, a hypothesis supported by data based on conodont assemblages (Barnes *et al.*, 1973; Barnes and Fahraeus, 1975). The oldest unit sampled, the Verulam Formation, consists of 80 m of cycles of limestone and shale (Liberty, 1967) and is fossiliferous throughout, with specimens of *Isotelus gigas* and *Isotelus* sp. Liberty (1969) suggested that sedimentation occurred in water of medial depth, a conclusion which he based on the presence of cross-bedding, para-ripples and slumping and channeling structures. Winder (1960) considered this formation (his Kirkfield and Sherman Fall Formations) an offshore, normal-marine limestone, with water depth increasing upward in the section. Brookfield (1988) and Brookfield and Brett (1988), however, have reclassified these units as being temperate or even cold shelf environments, based partly upon the geochemistries and mineralogies of bulk material. It should be noted that inaccuracies inherent to this type of analysis, such as failure to recognize the various chemistries and mineralogies of the different fossils contained in these samples, may bias the resulting conclusions and void interpretation (Brand, pers. comm., 1989). Based on the depositional rates, grain types, faunas, and erosional surfaces, Brookfield (1988) suggests a shelf environment indicative of temperate or cold conditions. This conclusion must be addressed with respect to trilobite mineralogy and

geochemistry, and must also be considered in the evaluation of not only the units in Ontario, but those in Ohio as well.

Overlying the Verulam Formation, the Cobourg Formation consists of a mixture of fossiliferous argillaceous limestone, crinoidal limestone, and shale. The unit is approximately 70 m thick, has a gradational lower contact and a sharp disconformable upper contact with the Whitby Formation (Liberty, 1969). Containing *Isotelus gigas*, *Isotelus* sp., and *Pseudogygites latimarginatus*, its environment of deposition is thought to have been slightly deeper and more stable than the conditions of deposition for the Verulam Formation (Liberty, 1969). Fluctuations in sea level and sedimentation, likely due to storm and glacio-eustatic influences (Brookfield and Brett, 1988), are indicated by the shale partings, and by lenses of breccia and conglomerates derived from underlying Ordovician and Precambrian sediments.

The lower Whitby Formation consists of 10 m of alternating black and gray fossiliferous shales and is best exposed at Craigeleith, Ontario (Fig. 6). Similar in lithology and fauna to the Utica Shale of New York (Sanford, 1978), it yielded occasionally pyritized specimens of *Isotelus maximus* and *Pseudogygites latimarginatus* (Liberty, 1969). Water conditions during deposition of the black shales were believed by Liberty (1969) and Copper (1978) to have been anoxic. Johnson and Rong (1989) have indicated that this unit marks a transgression that can be equated with a major rise in sea level seen elsewhere in North America and Scandinavia. Brookfield and Brett (1988) likewise suggest that the depositional environment for the shales was on a deep shelf, with the intercalated 'limestone' beds likely being storm reworked deposits. Such storm action would winnow out the clay fraction of the unit, leaving only the fossil material behind. This would support Liberty's (1969) observation of the interbedded limestone and black shale at Craigeleith (Fig. 9).

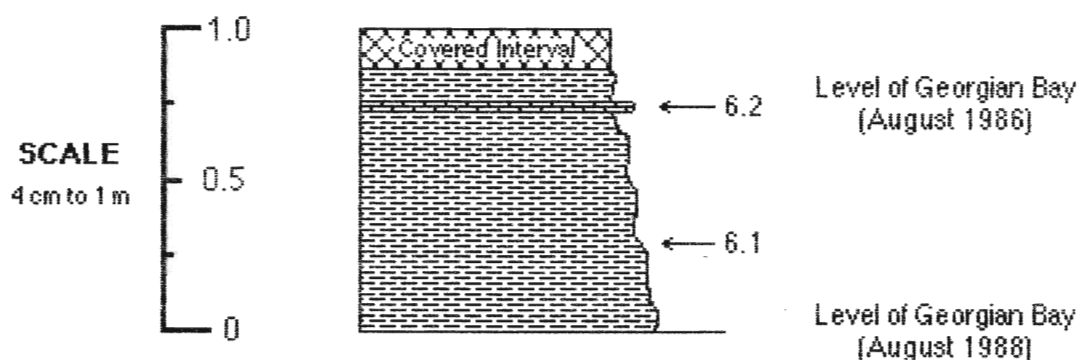


Figure 9: The 'Collingwood' bed of the Whitby Formation (Upper Ordovician) is exposed 0.5 km south of Craigleith Provincial Park. Measurements were made in the summer of 1988 when the level of Georgian Bay had dropped approximately 0.75 m from the level reported by McAllister (1987a), during the summer of 1986.

Ohio

The oldest specimens from the Ordovician of Ohio were collected from the Edenian Eden Shale of the Kope Formation (loc. 16, Figs. 6, 8), which is the basal unit of the Cincinnati Group. The Eden Shale consists of blue-gray clay shale alternating with micritic limestone (Brown and Lineback, 1966; Anstey and Fowler, 1969). The shale was deposited in relatively deep (≥ 20 m) and quiet water, and periodic storms blanketed the floor with lime mud transported from a carbonate bank to the south (Anstey and Fowler, 1969). The shale is time transgressive at its upper boundary, and is difficult to correlate and define (Ford, 1967). It is thought that the Eden Shale shallows upward into the Fairview Formation, as suggested by a decreasing wavelength of megaripples, and increasing limestone content and faunal abundance and diversity (Anstey and Fowler, 1969).

The Dillsboro Formation encompasses many of the previously unique units overlying the Kope Formation into one formation with few subdivisions, and therefore much of the resolution of the previous stratigraphic work is lost. For this reason, a combination of the divisions proposed by Caster *et al.* (1955) and Brown and Lineback (1966, as interpreted in Hay, 1977) will be used in this study to provide more detailed stratigraphic sampling information (Fig. 8). The Fairview Formation (loc. 18, Fig. 8) overlies the Eden shale of the Kope Formation. The basal terrigenous portion is a shallow water sequence, as indicated by the presence of mud cracks (Anstey and Fowler, 1969). The Fairview Formation then increases sharply in limestone content (Brown and Lineback, 1966), generally consisting of alternating limestone and minor terrigenous sediments deposited in deepening water.

Stratigraphically above the Fairview are the repetitious, even-bedded limestones and shales of the Waynesville Formation (Davis, 1981) (loc. 14.1, 15, 17, Fig. 8), which were deposited on a deep, open, stable shelf at the time of peak transgression (Hay, 1977). Of interest in the Waynesville is Frey's (1987) *Treptoceras duseri* (loc. 15, Fig. 6)

dominated unit and its Trilobite Shale equivalent (loc. 17, Fig. 6). These units represent coeval deposits in water depths similar to those of the Kope Formation, and under normal salinities (Frey, 1987). At the time of deposition this region of Ohio was subject to storms, which reworked sediments of the *Treptoceras duseri* unit (Frey, 1987). Frey (1987) suggests that storms originating in the east would lose energy passing over the Cincinnati shelf, and thus had little energy left to rework the sediments of the more westerly Trilobite Shale. Since they are correlative, these units should provide an excellent lateral datum.

Similar to the Waynesville Formation, the overlying Liberty Formation was deposited on an open stable shelf into deep water during a period of peak transgression (Hay, 1977). Deposition took place before the Late Ordovician regression (Hay, 1977), which was likely produced by the glaciation of Gondwanaland (Sheehan, 1973). This unit consists of essentially the same type of sediments encountered in the Waynesville Formation, although the frequency of limestone beds has substantially increased.

The only trilobite obtained from Ohio was *Isotelus maximus*.

Life Mode of Ordovician Trilobites

Detailed studies on the life modes of the *Isotelus* species and *Pseudogygites latimarginatus* of this study are rare and highly speculative. Based on their morphology, these trilobites are considered to have been benthic, producing mesophyciform burrows in the course of feeding (Westrop, pers. comm., 1989). They are also unlikely to have been permanent burrowers, as in some illaenids (Westrop, pers. comm., 1989).

Chapter 2

Methods of Analysis

INTRODUCTION

All specimens were separated and cleaned of the surrounding sediment to prevent intermaterial geochemical contamination (cf. Brand and Veizer, 1980). The matrix adhering to trilobite cuticle, and the tissue adhering to Recent specimens, was removed using dental tools and a razor blade. Recent specimens were also placed in a bath of distilled-deionized water to attempt to remove adhering salts. This was followed by a period of drying in an oven at approximately 75°C. The drying process led to separation of several Recent cuticles into two mineralized layers (Fig. 10). The red/pink pigmented outer epicuticle was relatively thin and fragile, whereas the inner endocuticle was white and relatively thick.

Cuticular fragments of trilobites and Recent arthropods were retained for SEM examination and the remainder powdered using a mortar and pestle for elemental, isotopic, and x-ray analyses.

Scanning Electron Microscopy (SEM)

Fracture fragments of selected cuticles were examined on an International Scientific Instrument (ISI) Super MINI-SEM. Samples were chosen to cover the full range of facies, ages and species, and to ensure a complete microstructural analysis, surface and cross-sectional examinations were performed on the majority of specimens. All fragments were washed for approximately 5 min. in an ultrasonic bath of doubly-deionized water and then dried in an oven at 35°C for approximately 12 h. After cooling in a desiccator, the samples were fractured, mounted on aluminium stages, and then sputter coated with gold-palladium.

A total of sixty-one specimens were examined by scanning electron microscopy. Modern specimens included two *Orconectes* sp., two *Callinectes* sp., and one *Limulus polyphemus*. Ordovician specimens included seven *Isotelus* sp., twelve *Isotelus maximus*, eight *Isotelus gigas*, two *Pseudogygites latimarginatus*, and two *Vogdesia*

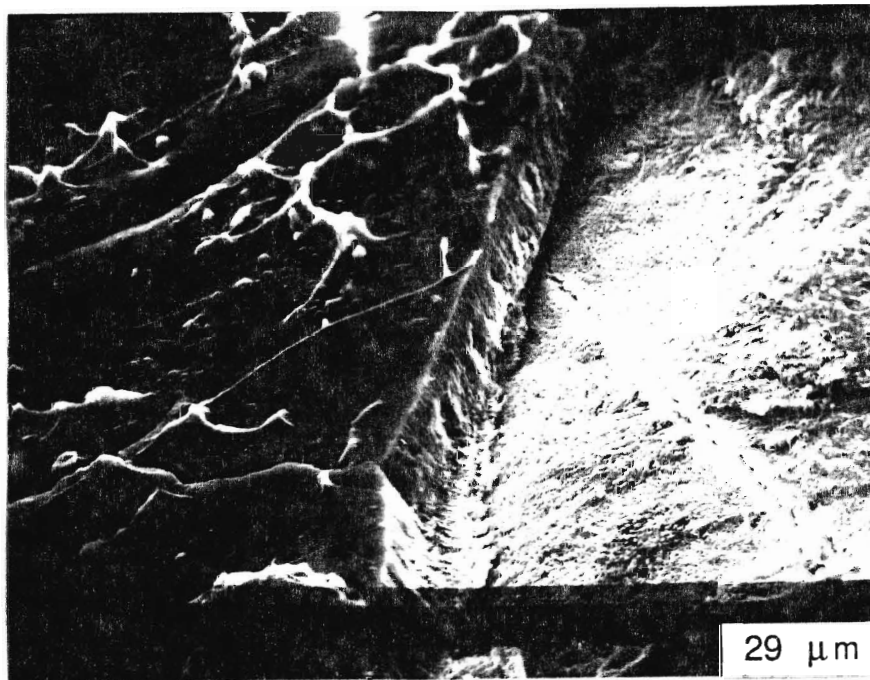


Figure 10: This molt of *Cirronectes* sp. demonstrates the apparent separation of the epi- and exocuticles from the underlying endocuticle due to desiccation. (11 254)

bromidensis. Devonian specimens included sixteen *Phacops rana*, three *Greenops boothi*, and six *Terataspis grandis* fragments.

Atomic Absorption Spectrophotometry (AAS)

Trilobites

The powdered cuticles were dried in an oven at approximately 75 °C for 24 h, allowed to cool, and then weighed out in fractions of either 0.5, 0.25, or 0.1 g. Powders were then dissolved in 18, 9, or 4.5 mL of 5 % (v/v) HCl with 5000 ppm K corresponding to the weight initially assigned to the sample. The powders were then left to digest for approximately 2 h, after which the solutions were filtered through ashless filter paper (Whatman #40). After a deionized-distilled water rinse of the digestion beaker into the funnel, and subsequent filtering into a volumetric flask, the collected solution was then topped up with DDI water to its working volume of 50, 25, or 10 mL. Insoluble Residue (I.R.) of the sample was determined by incinerating the filter paper at 800 °C for 1 h and recording the remaining acid non-soluble mass.

A total of 155 Ordovician and 117 Devonian trilobite samples were prepared and analyzed on a Varian AA-1475/Hewlett-Packard 85 atomic absorption spectrophotometer (AAS) for major (Ca), minor (Mg and Sr) and trace elements (Mn, Na, Fe, and Al). In addition, 10 Ordovician and 11 Devonian matrix samples were analyzed, and all geochemical data are presented in Appendix III. Precision of values was better than 8% based on duplicate analyses. Accuracy of data with respect to that of National Bureau Standards (NBS) 634 and 636 was better than 5 to 10 relative percent for all elements except Al, for which accuracy was better than 10 to 15 relative percent. The solutions were subject to various dilutions to bring their respective concentrations within the linear working range. Dilutions are given in Table 2.1. All elemental concentrations

were recalculated to an insoluble residue free, 100% carbonate basis (cf. Brand & Veizer, 1980).

Table 2.1: Dilutions required to bring the solutions of marine and fresh water crustacea, and trilobites within the range of the atomic absorption spectrophotometer. The high value given for sodium (Na) in crustaceans is due in part to fluid inclusions within the cuticle of the marine specimens. Values in parenthesis indicate the maximum dilutions required.

Element	Dilution Factor		
	Trilobites	Marine Crustacea	Fresh Water Crustacea
Ca	100	100	100
Mg	100	100	100
Sr	10	10	10
Mn	10	0	0
Na	10	50 (100)	25
Fe	10	0 (5)	0 (5)
Al	0	0	0
Cu	0	N/A	N/A
Zn	0	N/A	N/A

Recent Arthropods

The processing of powdered Recent arthropod cuticle for analysis was similar to that outlined for trilobites, with several necessary variations. I. R. for Recent arthropod samples was calculated by comparing the previously recorded weight of empty filter paper to that containing the undissolved material. Filter papers were dried at 75°C overnight and then put into a desiccator to remove any moisture prior to final weighing. The resulting difference in weight of the filter paper is the I. R., or the organic fraction of the organism which failed to dissolve in HCl. The prepared solutions were analysed for major (Ca), minor (Mg and Sr) and trace elements (Mn, Na, and Fe) on the Varian AA-1475. The dilutions applied in this analysis differed from trilobites, and, indeed, between some species of decapod. The respective dilutions are given in Table 2.1.

X-Ray Diffractometry (XRD)

The mineralogy of a representative group of samples was determined using a Picker 6238 diffractometer, the results are contained in Appendix V. Forty-five samples were prepared by applying a thin coat of vacuum grease to a clear glass slide, and then powdered cuticle was sprinkled onto the greased portion of the slide. The slide was then placed into the XRD, with the powdered side facing into the x-rays. Potassium radiation of the samples occurred with a copper target, and was measured in 2 θ . An aragonite standard was analysed with each batch of samples to calibrate the XRD. For more detailed information on the diffraction technique, and peaks for calcite and aragonite and errors involved in this work see Milliman (1974; pp. 22-29).

Stable Isotopes

Trikobites

Samples were analyzed for oxygen and carbon isotopes on a V.G. Micromass® 903 mass spectrometer at the University of Waterloo's isotope lab. The method of analysis requires 5 mg of powdered sample, which is reacted with 100 % phosphoric acid at 50 °C for 30 min. The isotopic ratios are expressed in the usual and corrected (δ) notation relative to PDB in permil (‰), unless otherwise indicated. Average accuracy and reproducibility compared to recommended values for N.B.S. 20 (Solnhofen Limestone) were better than 0.2 ‰, with all samples being corrected for ^{17}O .

A total of seventy-five isotopic analyses were performed, of which there were three *Vogdesia bromidensis*, eight *Isotelus* sp., eleven *Isotelus gigas*, twenty *Isotelus maximus*, three *Pseudogygites latimarginatus*, twenty-three *Phacops rana*, five *Greenops boothi*, and two *Terataspis grandis*.

Statistical Analysis

All data compilation and statistical analysis (student t-test and factor analysis where necessary) were performed with an Apple® Macintosh™ Plus computer using Cricket Graph™ version 1.2, StatWorks™, and Statview 512+ software. Tables containing statistical data may be found in Appendix IV.

Chapter 3

Recent Arthropods

INTRODUCTION

Several studies (Towe 1973; Teigler and Towe 1975; Dalingwater and Miller 1977) determined that trilobite cuticles are more heavily calcified than those of most extant arthropods. Varying amounts of chitin (polyacetyl-glucosamin) act as architectural reinforcement (Teigler and Towe, 1975). Although chitin consists of complex biopolymers that have a certain degree of resistance to decay (Allison, 1988a), it is subject to many natural paths of destruction, particularly the action of chitinovorous bacteria. Bacteria feed on the tissues and chitin of the arthropod carcass, and are a major cause of the exoskeletal decomposition of modern arthropods (Johnson, 1932; Benton, 1935; Campbell and Williams, 1951; Plotnick, 1986), and contribute to early diagenetic pyritization (Allison, 1988b). The one physical limiting factor on the activity of the bacteria appears to be the proportion of calcite in the cuticle, with heavily calcified cuticles being more resistant to decomposition than those with a significantly lower calcite content (Plotnick, 1986; Allison, 1986). It was therefore decided at the outset that the best material for comparison with microstructures and geochemistry of trilobites would be heavily-calcified Recent arthropods.

MICROSTRUCTURES

By definition, a pristine microstructure must be an original microstructure in the organism and not the result of subsequent alteration. The most logical place to find pristine microstructures is obviously in freshly killed specimens. Examining pristine microstructures and their functions in Recent marine arthropods allows for the interpretation of their features and functions, and possible analogy to similar microstructures in trilobites.

Laminae

Examinations of modern arthropod cuticles (Rolfe, 1962; Neville *et al.*, 1969; Neville and Berg, 1971; Dalingwater, 1975a) have shown that layers and laminations, in general, are omnipresent and inherent to arthropods. However, laminae were not observed in the majority of the Recent cuticles; identifiable laminae were only observed in one specimen of competent non-molt *Panulirus argus* (Figs. 11 A and B). Close examination of the laminae reveal that the material composing this microstructure exhibits a woven texture, not previously noted by researchers.

Feldmann and Tshudy (1987) found that the presence of laminae in fossil crustacea depends on the molt phase of the cuticle, as well as the preservation of the cuticle. They suggested that molted cuticle is characterized by a deterioration of lamination in the inner endocuticle, with the intermolt exhibiting lamination throughout the endo- and exocuticles (Feldmann and Tshudy, 1987). In summary, while the laminations may be initially controlled by the genetic blueprint of the organism, diagenesis ultimately has the ability to destroy and/or significantly alter laminations.

Pore Canals and Tegumental Ducts

The majority of microstructures that were found are obviously related to the architecture of the cuticle. For example, specimens of modern *Limulus* display a variety of openings on the lower (Figs. 12, 13) and upper (Fig. 14) surfaces of their cuticle. Judging by their number and dimensions, these openings are probably tegumental gland ducts (which penetrate the cuticle and are used in the tanning and hardening of the cuticle) and smaller blood and nerve conduits. Penetration of the cuticle (Fig. 15) and structure (Figs. 16 and 17) of these features designates them as the tegumental gland ducts of Dennell (1960), because pore canals are of a much finer scale (Fig. 15). The larger tegumental ducts of modern *Limulus polyphemus* (Fig. 15) are similar in size to those illustrated by Neville and Berg (1971-Plate 30, Fig. 2) in the cuticle of a Jurassic

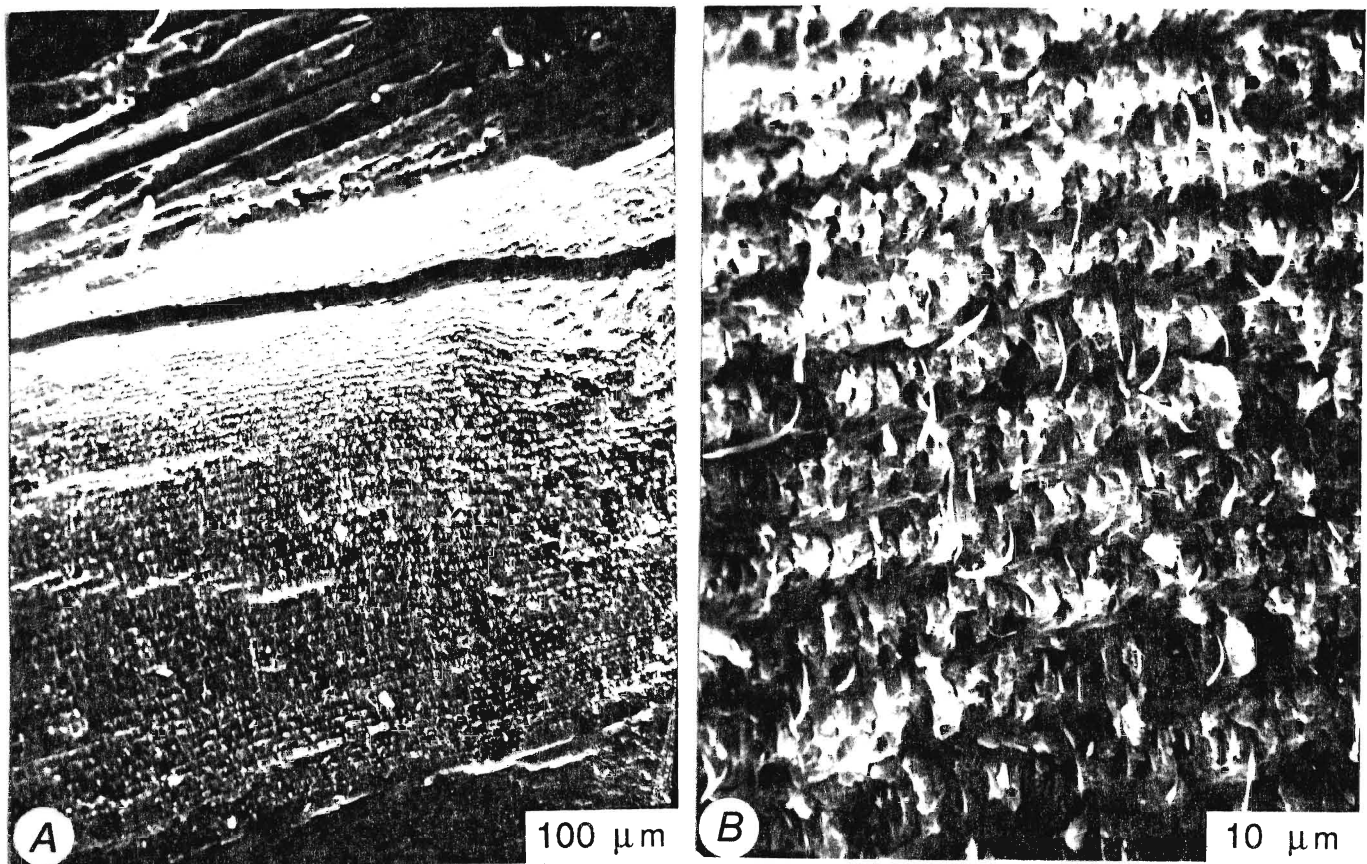


Figure 11: Laminae in the cuticle of a pristine specimen of the lobster *Paralithodes argus*. A. General view of laminae in the upper layers (epi- and exocuticles) becoming finer in texture with passage into the endocuticle. B. A woven texture characterizes the laminae. (11 300)

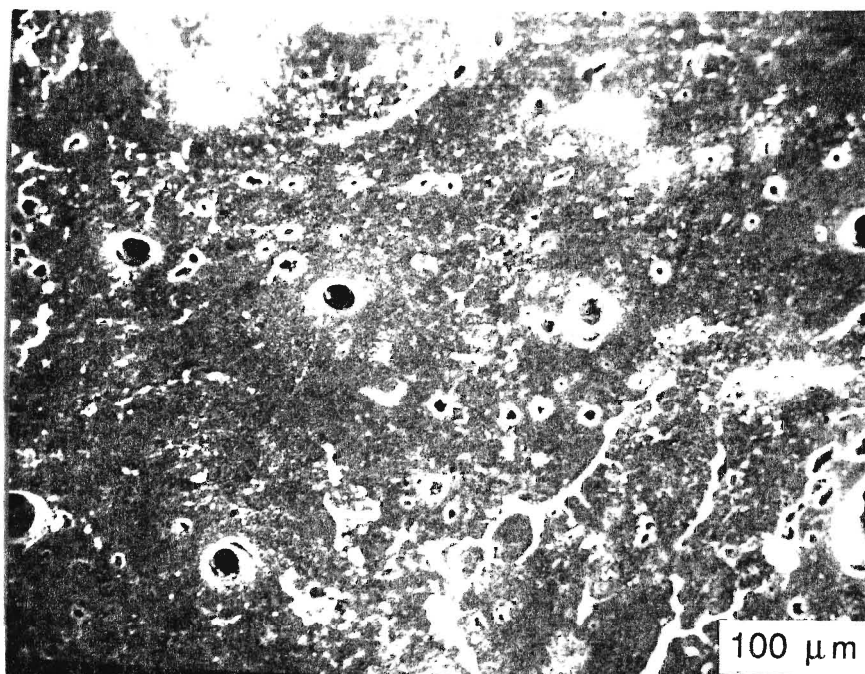


Figure 12: Tegumental gland ducts, and pore canals opening onto the inside cuticle of a specimen of *Limulus polyphemus*. Note the variety of sizes and shapes of the openings. (11 322)

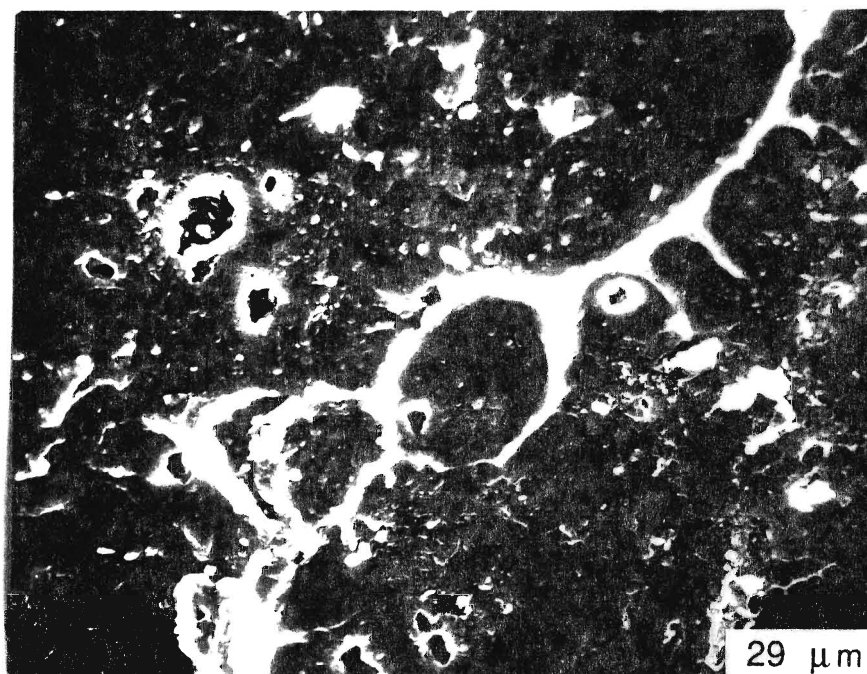


Figure 13: Close-up of the openings of Figure 12. Note the dendritic microstructure among the openings. (11 322)

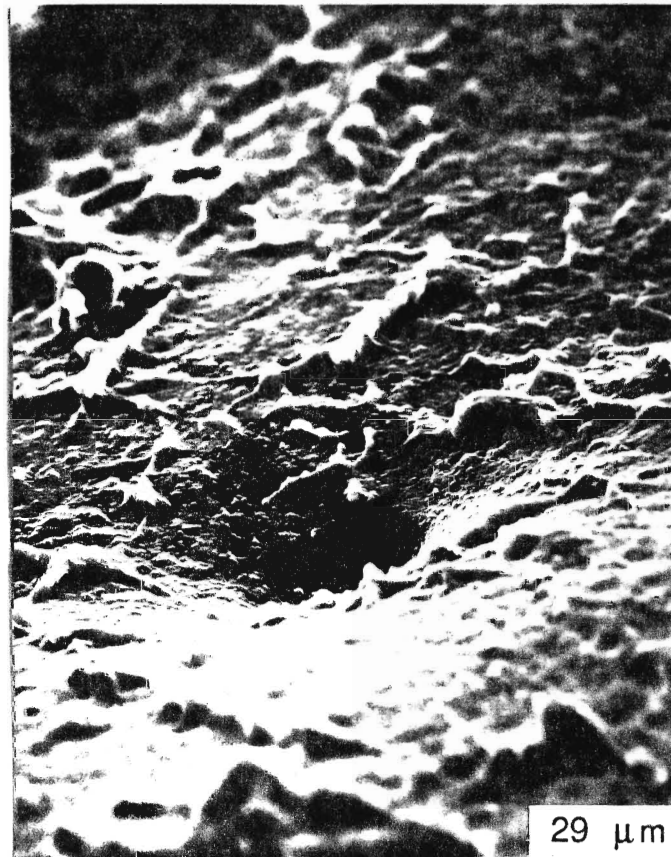


Figure 14: The 'dendritic' microstructure in a specimen of *Limulus polyphemus*. Note the surficial relief of the microstructure. Depression in centre of photograph is a tegumental duct opening. (11 322)

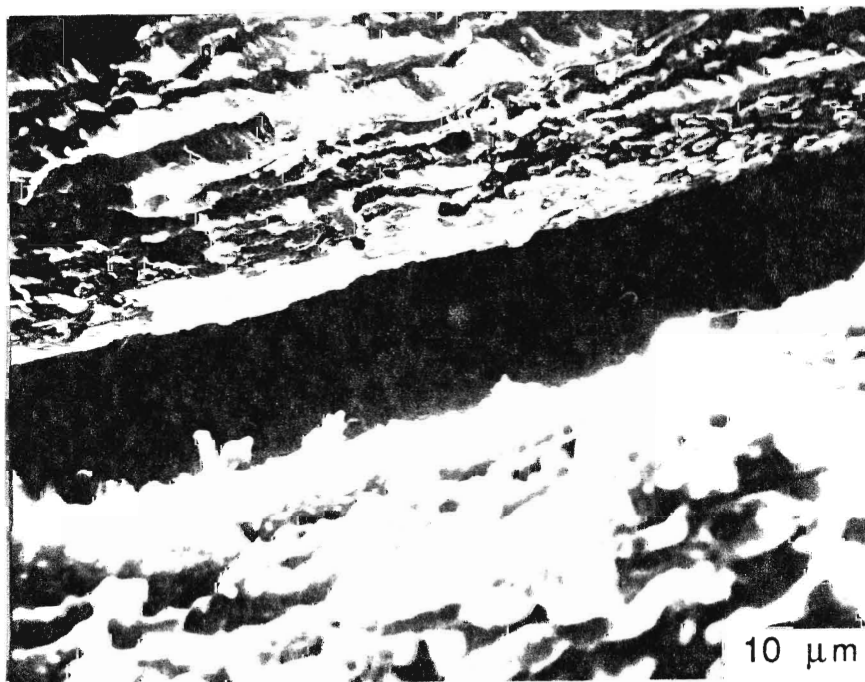


Figure 15: Tegumental gland duct passing through the cuticle of a specimen of *Limulus polyphemus*. The surfaces of the cuticle are to the left and right, with the smaller 'pore canals' (top) being parallel to the canal. (11 322)

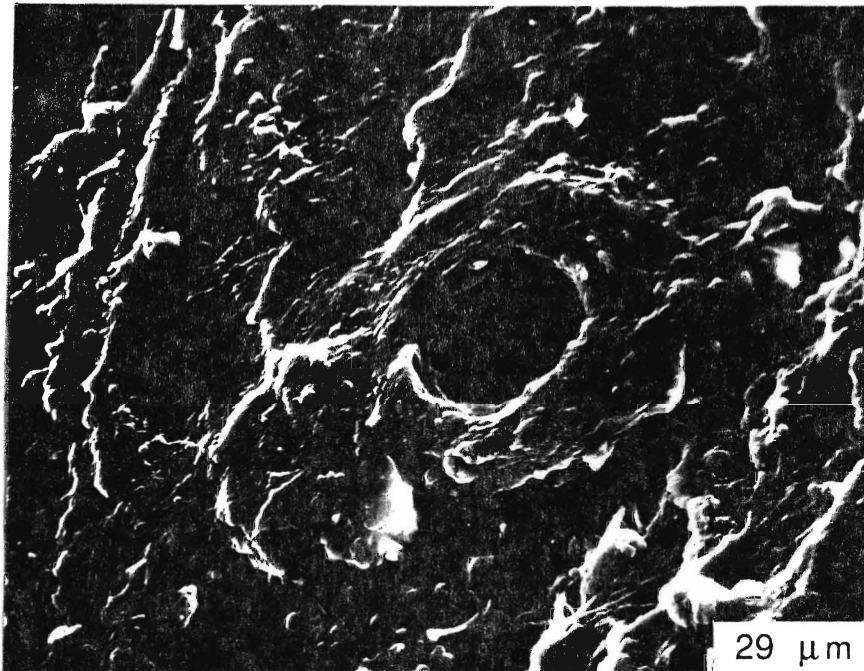


Figure 16: Tegumental duct opening on the dorsal cuticle surface of a specimen of *Limulus polyphemus*. The rough texture is as a result of the upper layer being sheered off. (11 322)

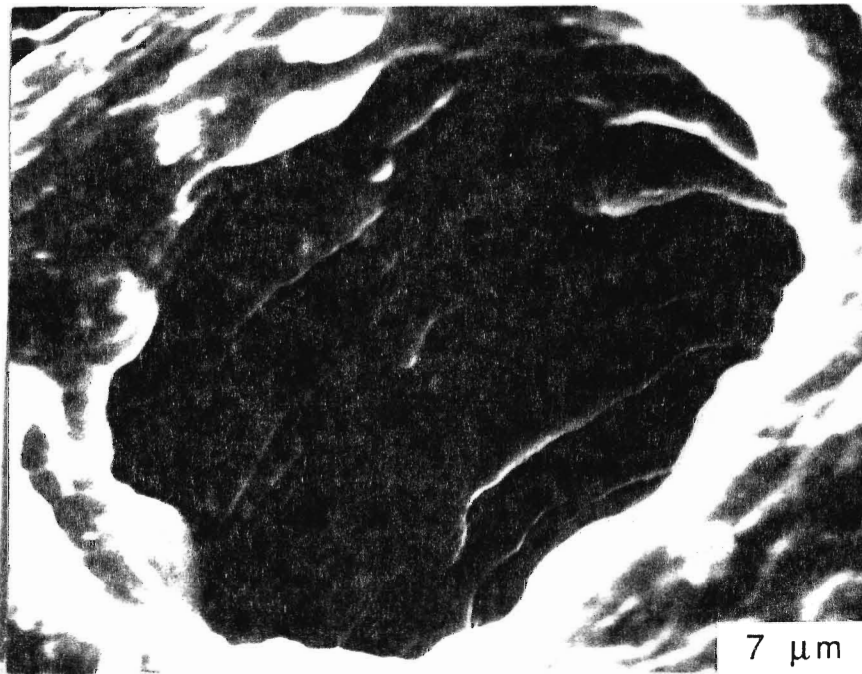


Figure 17: The detail of the opening of Figure 16. Note the 'ribbed' internal structure of the tegumental duct. (11 322)

crustacean. However, the helical nature of the 'pore canal' as reported by Neville *et al* (1969) in thin sections of *Limulus* were not visible in the present SEM examination. Neville and Berg (1971), Kennaugh (1965) and Neville and Luke (1969) reported helical pores in other species of arthropod, and there is no reason to doubt their findings. However, close examination of Neville *et al*'s (1969; Figs. 10 and 11) illustrations show an offsetting twist of the pore canals at the 'laminations'. This effect may have been produced by thin-section preparation, because the pore canals observed in cross-section (Fig. 15 - top) in the present SEM study are straight. The 'laminae' (Neville *et al*, 1969-Figs. 10 and 11) may also be an artifact of (tearing of the cuticle), because none were observed in SEM examination of this species. Pore canals were not found in any of the other specimens examined. The fact that they were not found in this examination should not discount the presence of helical pores in the cuticle of this or other species, as there may be, at least, intraspecific variability in pore morphology.

Setae

Dorsal setae, such as those found on *Limulus* (Figs. 18 and 19), are distributed around the margins of all arthropods, and act as fine mechanoreceptors, allowing the animal to evaluate its depth of burial. Setae may vary in size, being dependant on the size of the individual, the function that has been assigned the setae, and the locality of emplacement. For example, those found on the claw of *Orconectes* sp. vary in size from thick, resistant setae (Fig. 20) on the inside of the pincers, giving it a sense of when to close its pincers to capture or tear prey, to thinner ones on the outside of the claw (Fig. 21) used to detect obstacles. Size of the setae pit is important to note, as it is this feature rather than the setae itself that will be preserved in fossilized specimens

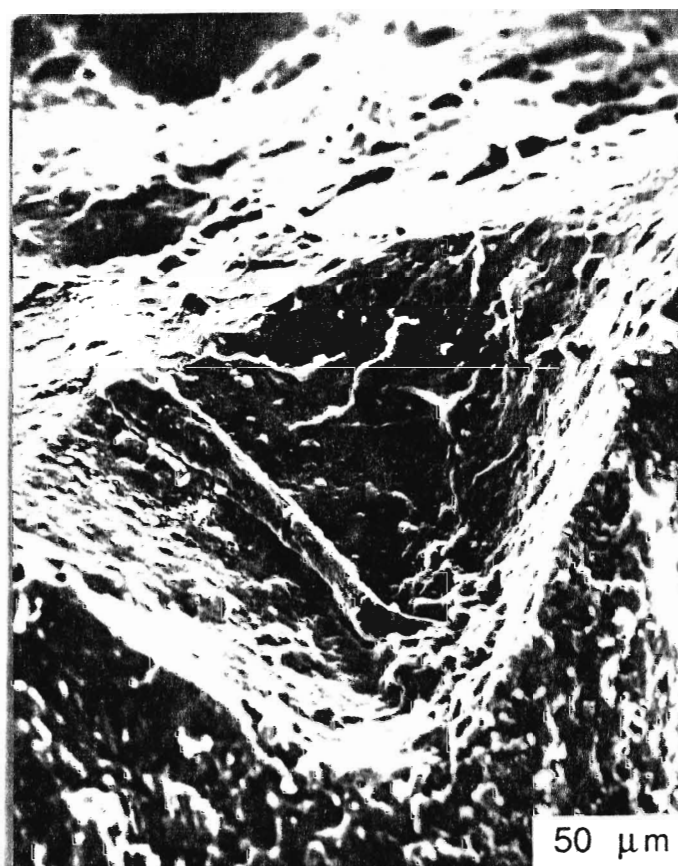


Figure 18: Setae in the cephalon of a specimen of *Limulus polyphemus*. (11322)

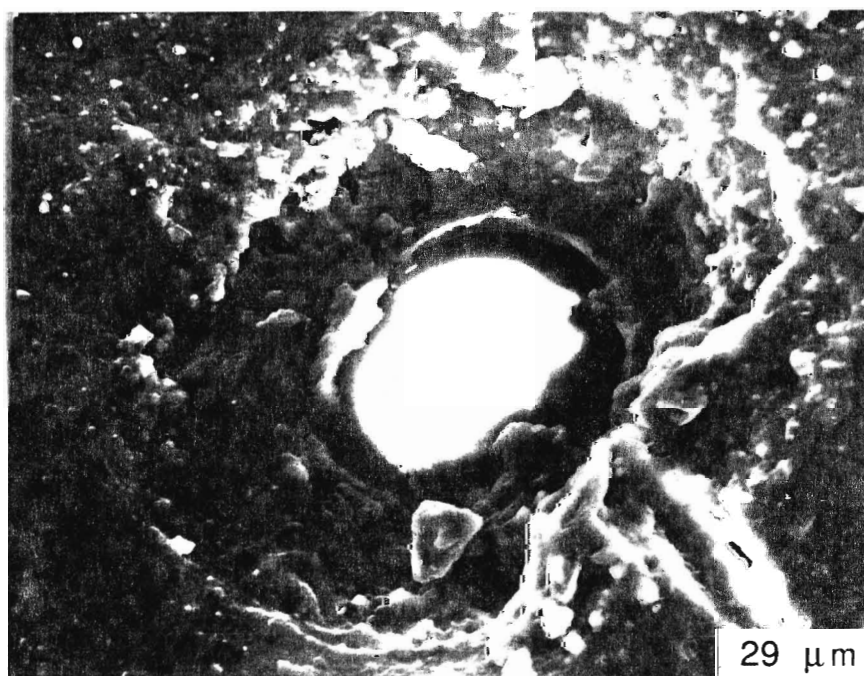


Figure 19: Setae on the cephalon of a specimen of *Limulus*. (11322)



Figure 20: Receptors in a claw specimen of *Cirronectes* sp. is shown. Note the scale of the basal opening. (18 265)

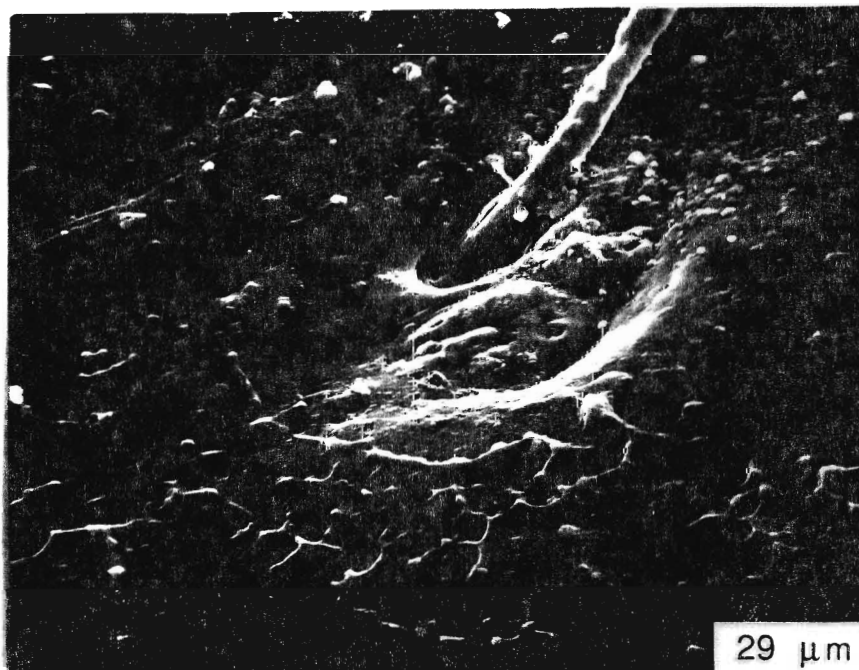


Figure 21: Setae in a claw specimen of *Cirronectes* sp. Note the scale of the basal opening. (18 265)

Dendritic Microstructures

McAllister and Brand (1989) described a 'dendritic' microstructure that they interpreted as a diagenetic feature, based on thirty-seven trilobite specimens and no Recent cuticles. At that time they noted that the knowledge of diagenetic microstructures was sparse. This microstructure has since been found in many Recent marine (*Limulus*, Fig. 14, 22; *Callinectes*, Fig. 23) and fresh water (*Orconectes*; Fig. 24) arthropods, and, therefore, it is likely an original or very early diagenetic microstructure.

In Recent specimens, the dendritic microstructure stands out in relief, and appears to have only shallow penetration of the cuticular material (Fig. 14), as the microstructure was not observed in cross-section. In studies of other material prepared and analysed using similar methods and equipment, 'dendritic' microstructures were only found on Recent and fossil arthropod cuticle. This excludes sample preparation error as a source for this microstructure. Further study of other arthropod species, and greater numbers of those already examined is therefore needed to reach a conclusion as to the function and/or formation of this microstructure.

General Surface Textures

The majority of the specimens lacked surface microstructures other than those already described, with a couple of exceptions. The surface of the modern lobster *Panulirus argus* (Fig. 25) was found to have an apparent primary proteinaceous layer veiling fine calcite rhombs. The ventral surface of a *Callinectes* sp. specimen had abrasion marks (Fig. 26), likely caused by the passage of the organism over coral as it scavenged for food.

TRACE ELEMENT GEOCHEMISTRY

The chemical contents of Recent arthropod cuticular calcite will be evaluated with emphasis on inferring pristine compositions, as well as early diagenetic effects, and the

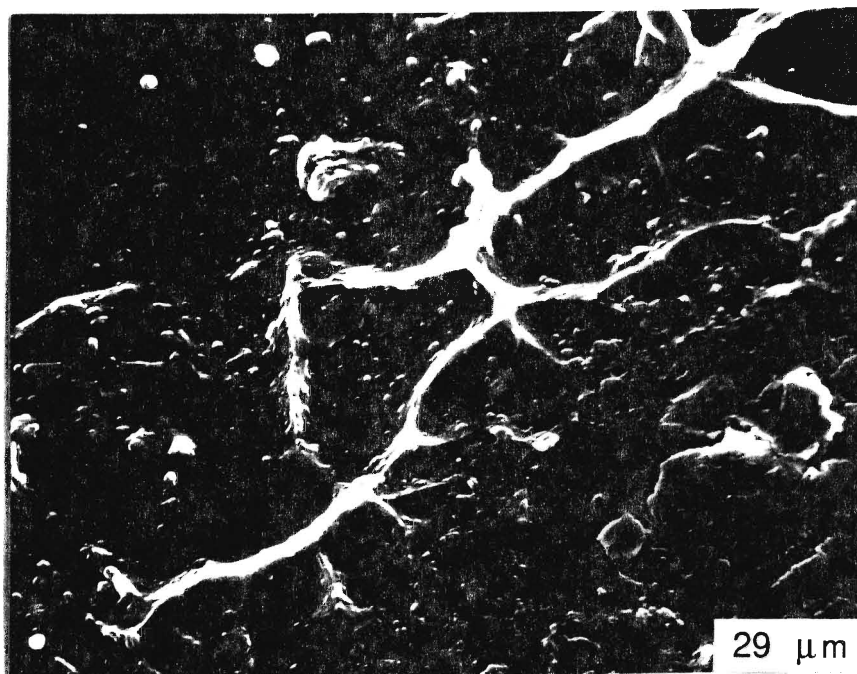


Figure 22: 'Dendritic' microstructure on a fragment of *Limulus*. Note the branching characteristic of the dendritic microstructure. (11322)

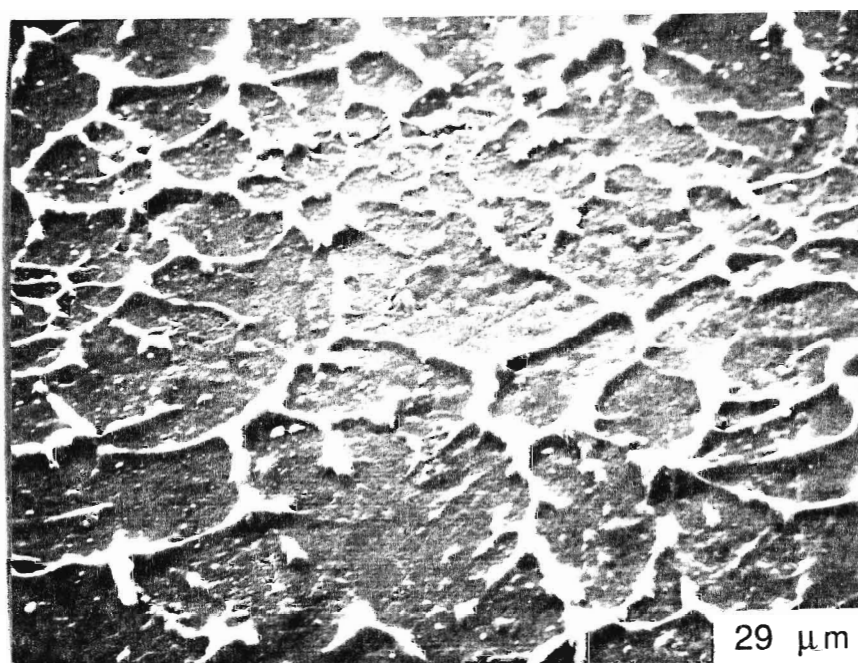


Figure 23: The 'dendritic' microstructure on the claw of a specimen of *Callinectes* sp. Note the relief of the microstructure and the texture of the cuticular surface. (17 207)

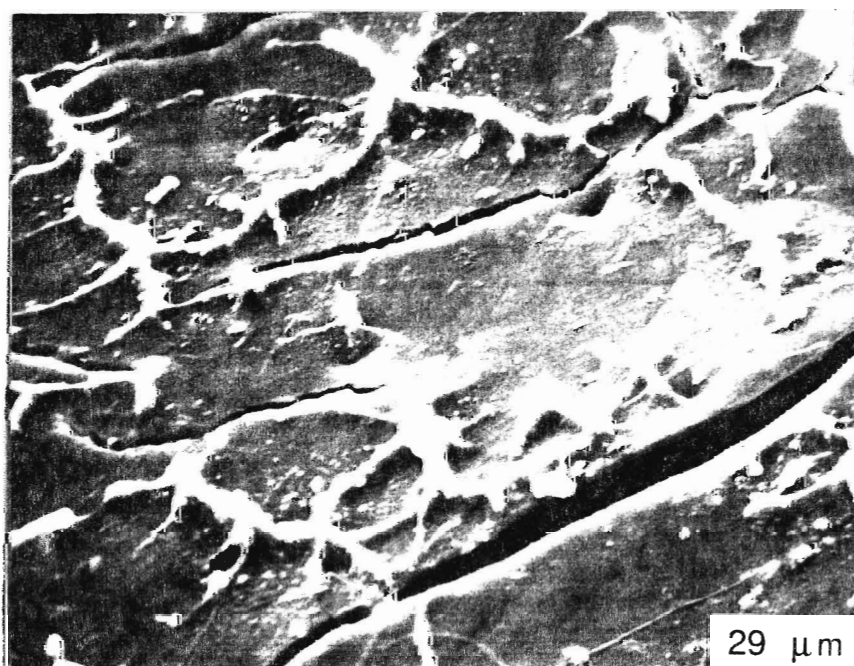


Figure 24: 'Dendritic' microstructure on the epicuticle of *Callinectes* sp. Note the fracturing in the cuticle caused by desiccation. (11 254)

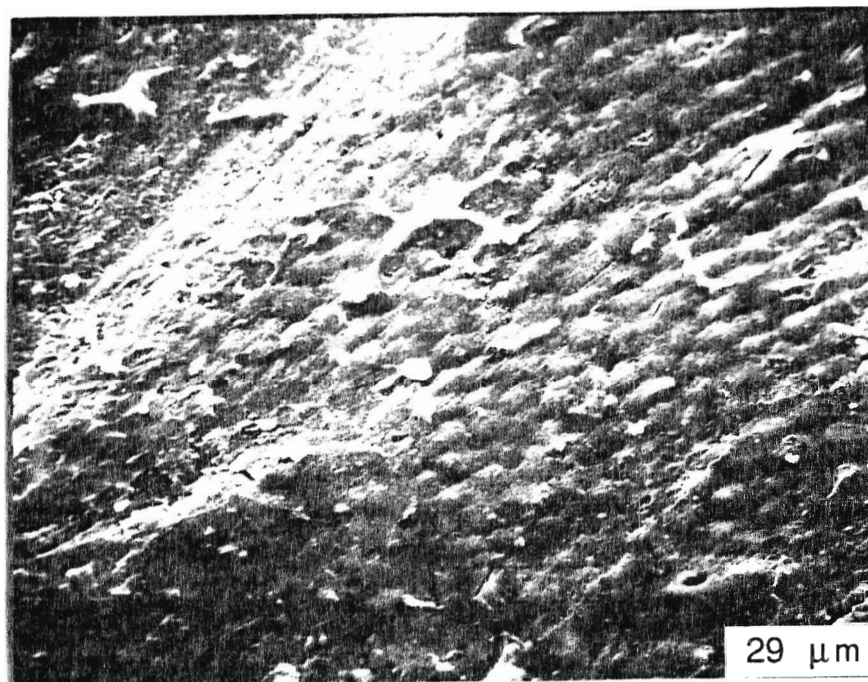


Figure 25: Surface texture of a *Parulirus argus* specimen from Long Key State Park, Fla. Note the proteinaceous layer covering the rounded calcite rhombs. [11 300]

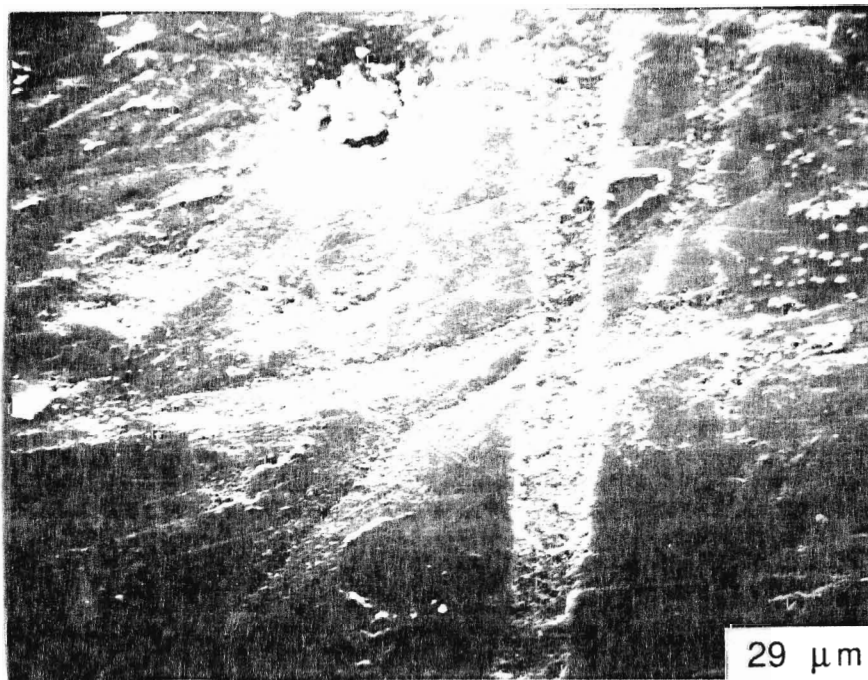


Figure 26: Abrasion marks on the ventral surface of a specimen of *Callinectes* sp. [22 210]

influence of environmental and depositional conditions on elemental distribution.

This study initially focused on *Limulus polyphemus*, a species suggested by previous workers (Eldredge, 1970; Bergström, 1975a,b; Thayer, 1979) to be ecologically similar to the trilobite. In the process of sample preparation, however, *Limulus polyphemus* was found to lack appreciable amounts of calcium carbonate in its cuticle, and for this reason, the majority of these specimens were discarded. The fact that this species lacks extensive biomineralization, suggests that the similarities between it and the heavily biomineralized trilobite are purely morphological. The specimens that were analysed (Appendix III) were found to be very high in I. R. (due to the presence of organics that failed to decompose). The specimens of *Limulus* will, therefore, not be considered further.

Pristine Composition

By using Recent arthropod cuticular calcite as a guide for pristine chemical compositions, it is hoped that a better understanding may be attained for trilobite cuticular calcite. Although, it is acknowledged that Recent arthropods are not directly related to trilobites, and that there are alternative interpretations to the proposed hypotheses, it is felt that the method of calcite emplacement in the cuticle may be sufficiently similar to justify such a comparison.

McAllister (1987a,b) and McAllister and Brand (1987; 1989; In press) established that, although, there is variation in chemical composition within the trilobite cuticle, this variation is small, and they concluded that fragments are representative of the entire specimen. This was also found to be the case with Recent arthropods.

Molting in Recent Arthropods

To understand the method of calcite emplacement and influences on the chemical compositions of cuticles, the molting process in Recent arthropods must be

examined. Molting in Recent arthropods is triggered by a number of natural conditions. For example, it is thought that lengthening of the photoperiod in spring initiates molting in crayfish (Stephens, 1955), whereas experiments on marine crustaceans have shown that higher temperatures cause the organisms to molt more frequently (Travis, 1954; Passano, 1960; Quackenbush and Herrnkind, 1983).

Molting affects the general chemistry of the organism, including that of the cuticle (Brannon and Rao, 1979; Huner *et al.*, 1979a and b; Vigh and Dendinger, 1982; Greenaway, 1983; Quackenbush and Herrnkind, 1983; Dendinger and Alterman, 1983; Engel, 1987). Biomineralization of the cuticle involves the secretion of material from the creatures' epidermis onto the exterior epicuticle. Initial hardening of the exoskeleton occurs rapidly after molting by the impregnation of calcium salts into the cuticle, with subsequent hardening aided by the tanning of the protein component in the procuticular layers (Russell-Hunter, 1969). In the epicuticle, iron is used in the formation of the pigment ferrin by most arthropods (Goodwin, 1960), with copper used in the pigment hemocyanin by arthropods such as *Limulus polyphemus* (Horseshoe crab) and *Homarus americanus* (Atlantic lobster). A significant difference in the cuticular iron (t-test -2.661, $p < 0.05$, $f = 12$; Appendix IV) and manganese (t-test -3.2, $p < 0.05$, $f = 12$; Appendix IV) contents between carcass and molt *Oreoneustes* sp. cuticles (Fig. 27) suggests that the iron locked in the pigments is not retrievable prior to ecdysis, and is lost with the molted cuticle. It is most likely that reabsorption of lower cuticle matter causes the high iron content of the epi- and exocuticles and leads to enrichment of the overall composition of the exuvia. The presence of higher concentrations of manganese in the exuvia as compared to non-molt cuticles (Fig. 27) confirms Rainbow's (1988) assertion that 98 % of body manganese is bound in the exoskeleton, and further suggests that the bulk of this manganese is in the outer layers of the cuticle. There the manganese is closely associated with calcium, and is likely laid down with calcium carbonate at appropriate stages of the molt cycle (Rainbow, 1988). A higher level of strontium (t-test -

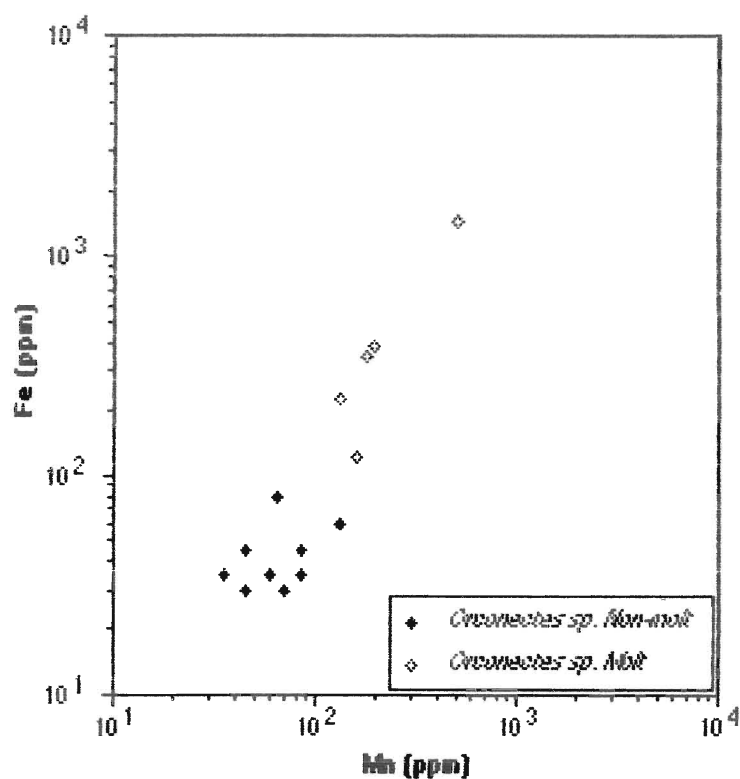


Figure 27: Scatter diagram of iron versus manganese concentrations in molt and carcass (non-molt) specimens of *Cronechetes* sp.

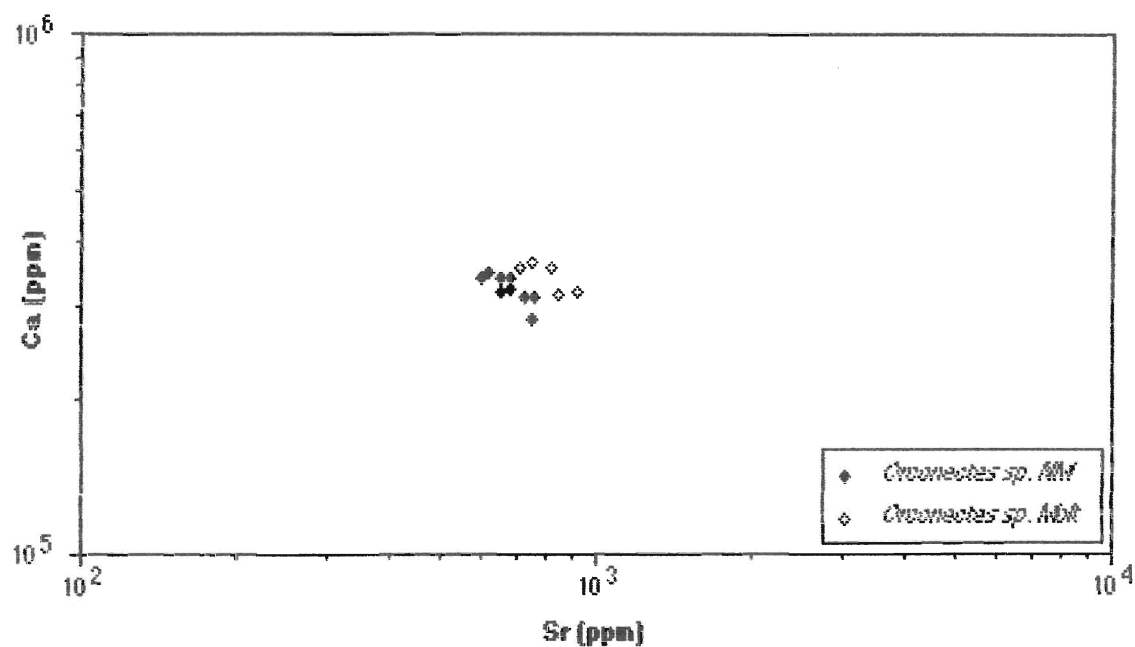


Figure 28: Scatter diagram of the calcium versus strontium concentrations in molt and carcass (NM) specimens of *Cronechetes* sp.

3.5, $p < 0.05$, $f = 12$; Appendix IV) in the exuvia (Fig. 28) suggests that this element is also concentrated in the outer calcified layers of the cuticle by a similar process.

Reabsorption of calcium salts from the old exoskeleton into the blood stream is common in most arthropods, it not only aids in the molting process, but also provides necessary material to form the new exoskeleton. Hoarding of material is characteristic of fresh-water species (Passano, 1960), and is likely due to low concentrations of certain elements in the surrounding medium. For example, the blood chemistries of fresh water and marine species are remarkably similar, except for higher calcium and lower magnesium concentrations in fresh water organisms (Florkin, 1960). In ocean water, sodium and chloride ions are the most abundant, whereas in fresh water calcium and carbonate ions are the most abundant (Kinne, 1964). The higher sodium concentrations of ocean water are not apparent in the blood of marine crustaceans (Florkin, 1960). However, significantly lower levels of sodium (t -test 2.421, $p < 0.05$, $f = 12$; Appendix IV) were observed in exuviae as compared to non-molts of *Oreonectes* sp. (Fig. 29) suggesting that it is reabsorbed into the blood stream prior to ecdysis. It is most likely that sodium is stored in the lower levels of the cuticle, where it may be required in molting-postmolt processes.

Leaching of sodium from non-molt cuticles is thought to represent a form of early diagenesis. Shown in Figure 29, carcass specimens with the lowest sodium concentrations, were collected along the shore of Severn River after an unknown period of exposure to water and weathering. These specimens, unlike those deemed pristine, lacked original pigmentation and were brittle due to advanced bacterial action. The samples with highest sodium concentrations collected soon after death were frozen immediately, thus loss of sodium by leaching was minimal, and specimens represent pristine chemistries. It is obvious that sodium may be a useful indicator of early leaching in Recent specimens and, due to its mobility, diagenesis in fossil arthropods. It will therefore be important in future geochemical studies to differentiate between molt and

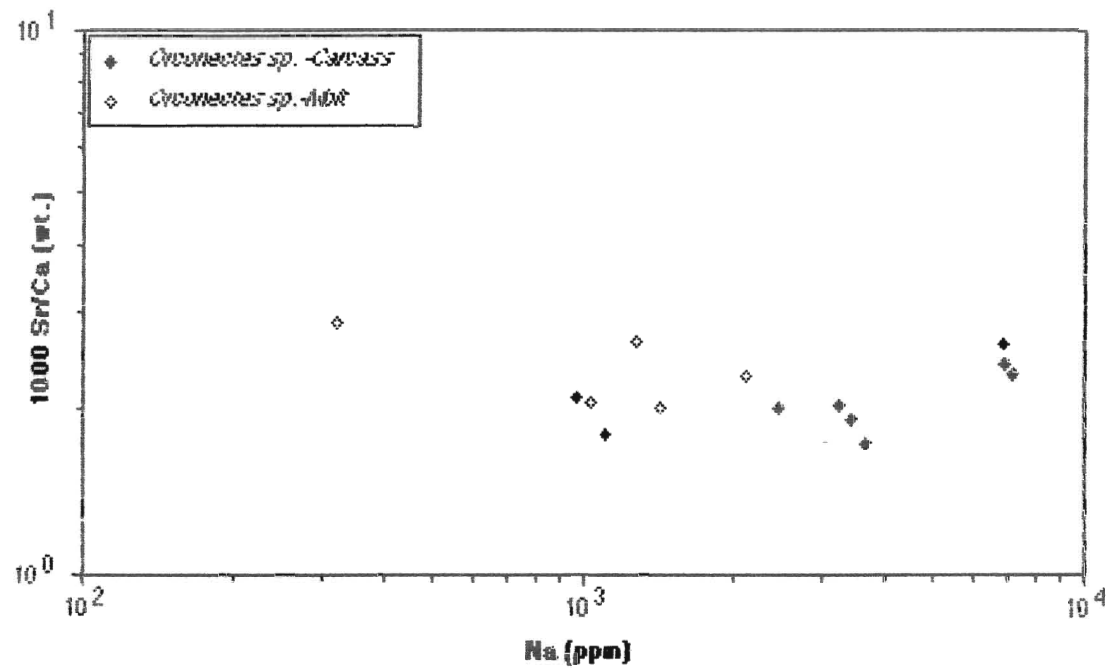


Figure 29: Scatter diagram of the 1000 strontium/calcium ratios versus the sodium concentrations in molt and carcass specimens of *Circonectes* sp.

non-molt cuticles (cf. Feldmann and Tshudy, 1987). Unfortunately, a comprehensive method for differentiating molt and non-molt trilobite cuticles has yet to be devised, therefore trilobite cuticles were not separated into these two groups.

Environmental Influences on Recent Arthropods

Salinity

Salinity has a restrictive influence on crustaceans, as well as most aquatic organisms. Organisms naturally attempt to escape, or compensate for the deviations in salinity by producing various biological responses to this stress (Kinne, 1964). Kinne (1964) reports various reactions from passive tolerance to adjustments of functional and structural properties. In crustaceans, a salinity of approximately 10 to 5 ‰ leads to a marked decline in the number of marine species, whereas an increase from 3 to 5 ‰ represents the highest tolerance limit for freshwater species (Abele, 1982). The salinity tolerance threshold separating marine and freshwater crustacea thus lies between 3 and 5 ‰. Response to an increase in salinity varies between species of arthropod, with most experiencing an increased metabolic rate and oxygen consumption (Shumway and Jones, 1981; Dalla Via, 1987a, b). Decreased salinities generally lead to production of copious amounts of isosmotic urine (Davenport and Wong, 1987), and increased protein and copper concentrations (Sabourin, 1984).

The influence of variable salinity on the cuticular magnesium concentration of invertebrates has been the subject of numerous studies. Magnesium concentrations in echinoids (Pilkey and Hower, 1960) and brachiopods (Lowenstam, 1961) have been positively correlated with salinity. This is also the case for Recent arthropods, because Price Sheets and Dendinger (1983) found that a substantial decrease in external salinity (from 30‰ to 10‰) caused *Callinectes sapidus* to discriminate for magnesium and against calcium in their cuticular calcite. Greenaway (1983) also found that salinity had

a similar effect in the crabs *Callinectes sapidus* and *Carcinus maenas*. The changes were more noticeable in post-molt cuticles, suggesting that levels of salinity and, possibly, other environmental parameters at the time of ecdysis may be reflected in new cuticular calcite.

During the spring molting period of *Orcinectes* sp., high concentrations of road salt in melt waters result in elevated salinities at the sample site of Washago, which should be reflected in higher than normal concentrations of magnesium in cuticular calcite. As predicted, chemical examination of *Orcinectes* sp. reveals that there is an apparent increase in magnesium with a corresponding decrease in calcium with elevated salinities; an observation that is also borne out by factor analysis (Appendix IV). Due to the flushing action of the river, individuals molting later in the year would be subject to less saline waters, and this would be reflected in their cuticular chemistries. The marine crab *Hemigrapsus nudis* from Cape Beale similarly shows an increase in magnesium with a decrease in calcium concentration (factor analysis, Appendix IV). This is likely caused by the movement of some individuals from normal subtidal marine waters into the brackish waters of the lagoon during the immediate post-molt period. Although speculative, this is a potentially testable hypothesis that could prove useful in paleontologic studies.

Sediment

The present study concentrated on the deposit-feeding crustaceans *Cancer* from Cape Beale and *Callinectes* from Florida. *Cancer* and *Callinectes* are exposed to elevated levels of the metals iron and manganese in the sediment slurry, which they ingest during feeding (Rainbow, 1988), and pass into their blood and cuticle. Most of the metal found in the cuticle is a fraction of the metal concentrations to which the organism is exposed (Rainbow, 1988), however the level of manganese in the surrounding medium (a mixture of sediment and water) will determine the concentration of

manganese in the cuticular calcite. Therefore, manganese content of cuticles may be largely dependant upon the life mode of the organism (see Appendix II) and the sediment in which it feeds. In *Hemigrapsus nuxlis*, *Cancer productus* and *Cancer magister* from Cape Beale, this relationship is reflected in statistically similar concentrations of manganese (see Appendix IV) in their cuticles (Fig. 30). Differences in sediment/water composition, and thus the concentration of manganese in the cuticle, is apparent in a comparison of the burrowing crabs of Cape Beale and Florida. If the environmental control hypothesis is correct, significantly lower manganese (t-test -3.903, $p < 0.05$, $f = 50$) and higher iron concentrations (t-test 3.723, $p < 0.05$, $f = 50$) in the cuticular calcite of *Cancer* as compared to *Callinectes* may be interpreted as indicating that the sediment/water of Cape Beale is enriched in iron, while that of the Florida Keys is enriched in manganese (Fig. 31; Appendix IV). The geochemistries of the sediments of Cape Beale (known to be igneous derived; Brand pers. comm., 1989) and the Florida Keys have not been studied so that a direct test of the hypothesis cannot be made at present. However, Brand *et al.* (1986) reported concentrations of iron in the seawater at Cape Beale at 0.16 ppm, compared to 0.002 ppm of iron in average seawater. This may therefore be indicative of overall higher iron concentrations in the sediment/water at Cape Beale.

Strontium did not appear to change in concentration in the cuticular calcite of crabs between marine carbonate and detrital environments (see Appendix IV), indicating that strontium is not influenced by temperature of ambient seawater, but may reflect a general salinity stability (cf. Brand *et al.*, 1986). This hypothesis may be supported by differences in the strontium concentrations of the fresh-water crayfish *Orconectes* sp. and the marine lobster *Panulirus argus* (t-test -15.779, $p < 0.05$, $f = 25$; Appendix IV), unfortunately there is no corresponding data on water/sediment chemistries. In molluscs, strontium concentration in surrounding waters has been found to biologically influence aragonite precipitation and test construction (Buchardt and Fritz, 1978; Bidwell

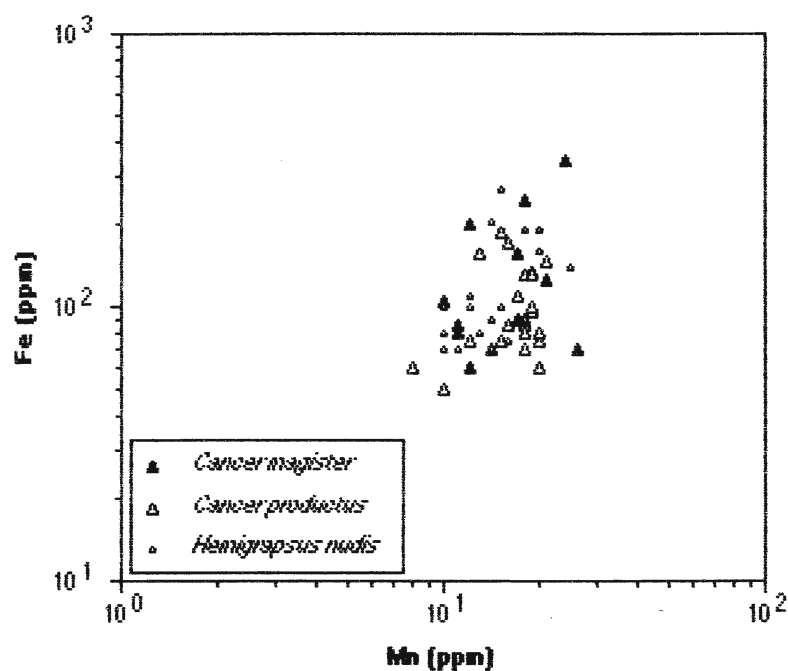


Figure 30: Scatter diagram of iron versus manganese concentrations in marine crabs from Cape Beale, B. C. Note the similar concentrations of iron and manganese for these specimens.

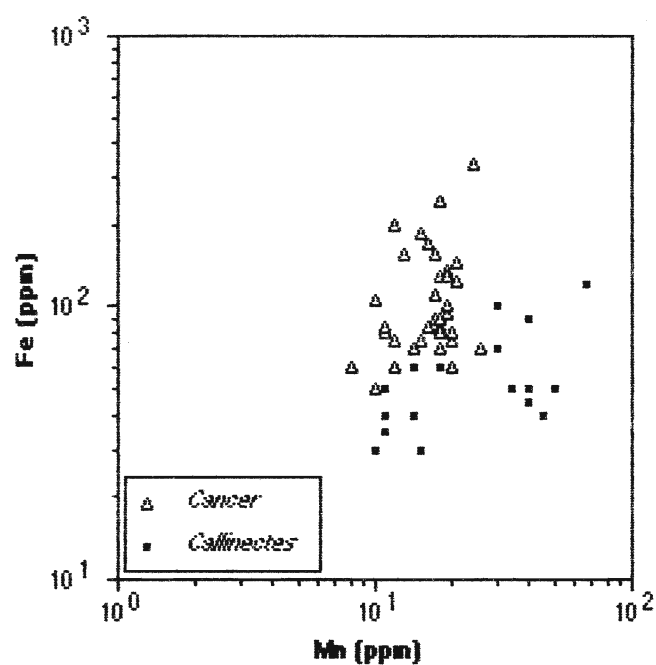


Figure 31: Scatter diagram for iron versus manganese for the crabs *Cancer* from Cape Beale, and *Callinectes* from the Florida Keys.

et al., 1986), however it is unknown what effect strontium fluctuations would have on the cuticular calcite of arthropods.

MINERALOGY

A calcite mineralogy with 6 and 14 mole % MgCO_3 has been suggested for Recent marine arthropod cuticles (Lowenstam, 1963). It was found that the mineralogy of the studied marine arthropod cuticle is between 4.43 and 12.1 mole % MgCO_3 , and 0.96 and 1.82 mole % MgCO_3 for fresh water species. In the same locality, the mineralogies appear to vary between genera, but are similar between individuals of the same species. For example at Cape Beale, *Hemigrapsus nudis* has an average mineralogy of 5.28 mole % MgCO_3 (15215 ppm), whereas *Cancer productus* and *Cancer magister* have similar average mineralogies of 6.18 (17821 ppm) and 6.02 (17355 ppm) mole % MgCO_3 , respectively (see Appendix IV). When plotted together with data of other Recent arthropods (Fig. 32), the separation becomes obvious, and although the data are limited, it is possible to suggest at least two explanations for differences in mineralogy between these arthropods. Firstly, ecophenotypic variations may occur in response to salinity or other environmental factor. This may be the case where *Hemigrapsus nudis* has statistically lower magnesium (t-test -5.004, $p < 0.05$, $f = 39$; Appendix IV), and statistically higher calcium (t-test 2.661, $p < 0.05$, $f = 39$; Appendix IV) concentrations than those in *Cancer productus* (Fig. 33). *Hemigrapsus* inhabits near shore brackish mudflats and lagoons, while *Cancer* is a burrower of the subtidal zone and, as previously explained, the concentration of magnesium in the cuticular calcite may be influenced by the salinity of the surrounding medium. As in *Cancer* from Cape Beale, specimens of *Callinectes sapidus* and *Callinectes* sp. from Florida have similar concentrations of magnesium in their cuticular calcite (Fig. 34). These organisms most likely occupy similar ecological niches, and are highly influenced by salinity changes (Price Sheets and Dendinger, 1983). The less saline waters off Cape Beale (see

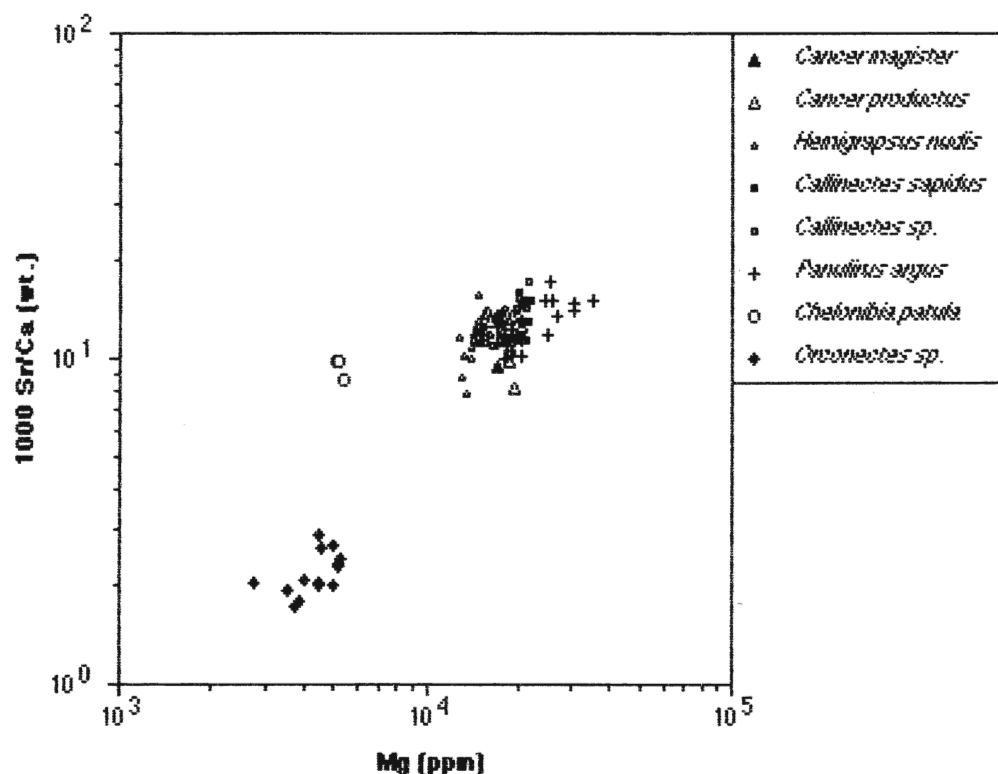


Figure 32: Scatter diagram of 1000 strontium/calcium versus magnesium concentrations for all of the Recent specimens analysed.

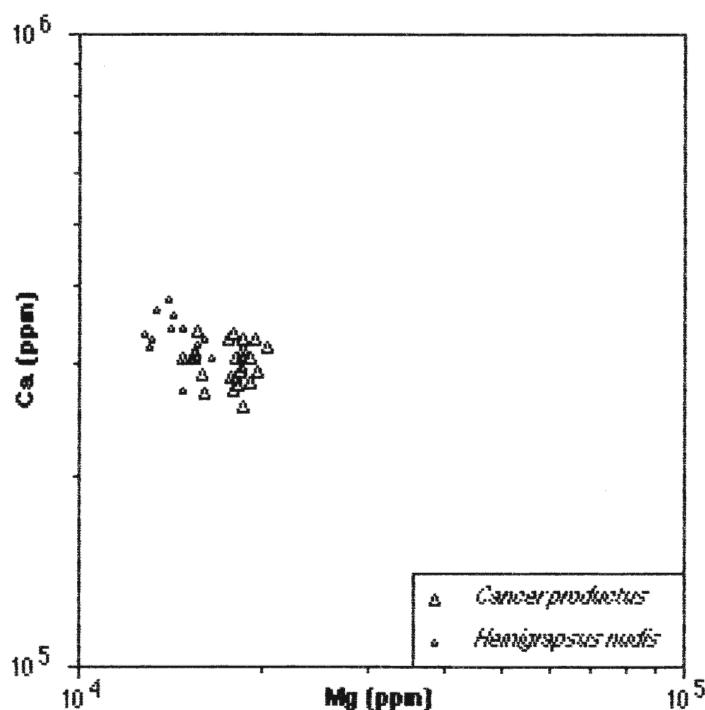


Figure 33: Scatter diagram of calcium versus magnesium concentrations in *Cancer productus* and *Hemigrapsus nudis* from Cape Beale, B.C. Note the separation of the data, most likely due to the influence of salinity on the formation of their respective cuticular calcites.

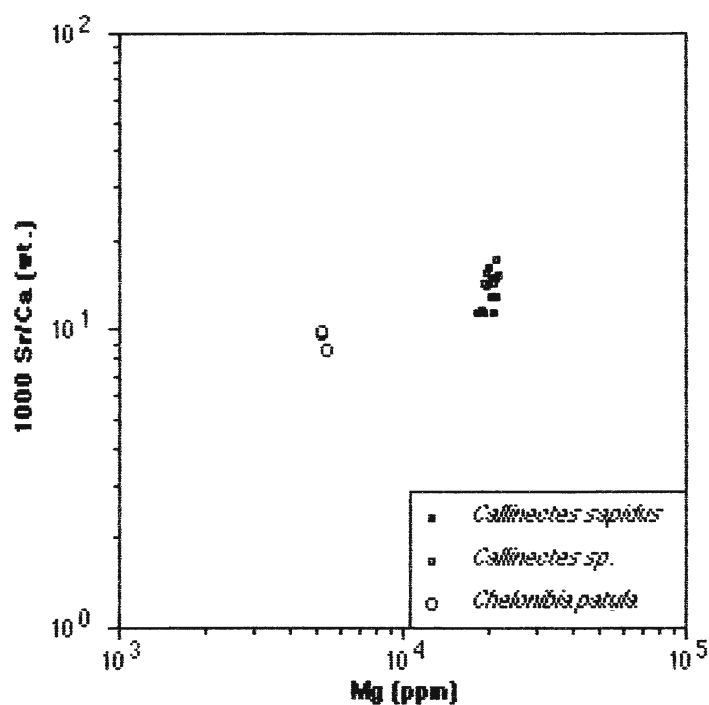


Figure 34: Scatter diagram of 1000 strontium/calcium versus magnesium concentrations for Recent arthropods from the Florida Keys. Note the similar magnesium concentrations for the species of *Callinectes* and their difference from *Chelonia*.

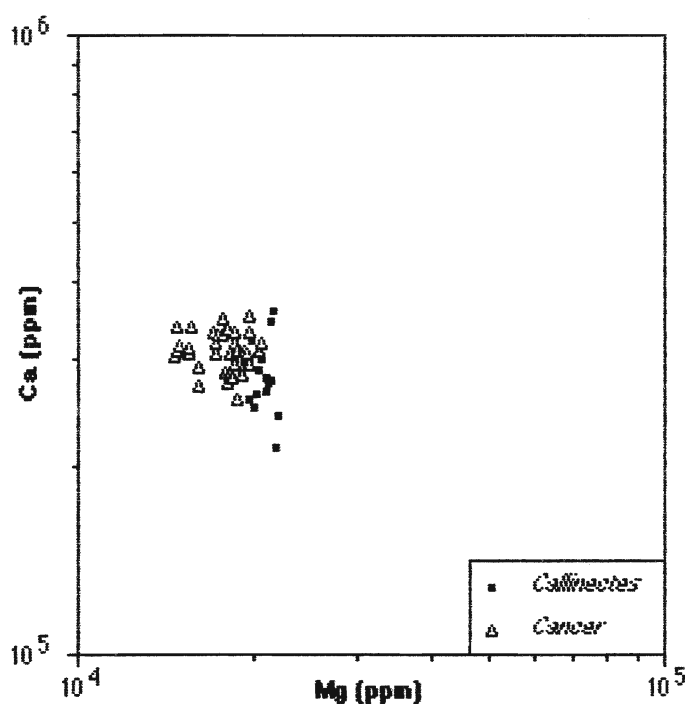


Figure 35: Scatter diagram of the calcium and magnesium concentrations in the crabs *Callinectes* from Florida and *Cancer* from Cape Beale, B. C.

Chapter 1) therefore appear to have affected the cuticular compositions of *Cancer*, as *Callinectes* had statistically higher concentrations of magnesium (t-test -6.379, $p < 0.05$, $f = 50$; Appendix IV) and lower concentrations of calcium (t-test 3.099, $p < 0.05$, $f = 50$; Appendix IV) in its cuticular calcite (Fig. 35). This hypothesis is also supported by overall variations in magnesium with calcium between fresh, brackish and marine arthropods (Figs. 32 and 36).

The second hypothesis for variable mineralogies in Recent arthropods would be that differences between taxa influence the incorporation of magnesium into the cuticular calcite. This assumption is supported by the fact that other marine arthropods, such as the crab barnacle *Chekonibia patula*, have lower magnesium concentrations from those of *Callinectes* (Fig. 32). In this case, the habitat of *Chekonibia* is identical to that of *Callinectes* because it adhered to *Callinectes*' carapace. These organisms may possess distinct mineralogies at some level above genera. It is therefore possible that further study may reveal that variable mineralogy is also true at lower levels. The most likely hypothesis for this phenomena, however, is a combination of the two postulated hypotheses.

Five Recent arthropods (two *Cancer productus*, one *Cancer magister*, and two *Orconectes* sp.) were analysed using XRD in an attempt to further determine their mineralogy, the results of which are contained in Appendix V. Due to the relatively large amounts of organic material in the powders used in this experiment, the machine was not able to resolve peaks for two of the five analysed, and was weak in two others. Those that did register peaks, did so at a level consistent with low to intermediate magnesium calcite (29.6 to 29.8; Appendix V). This only serves to confirm the presence of calcite, however, for interpretations as to the level of magnesium calcite should not be made from the readings obtained as the machine is not accurate enough to detect such subtle differences.

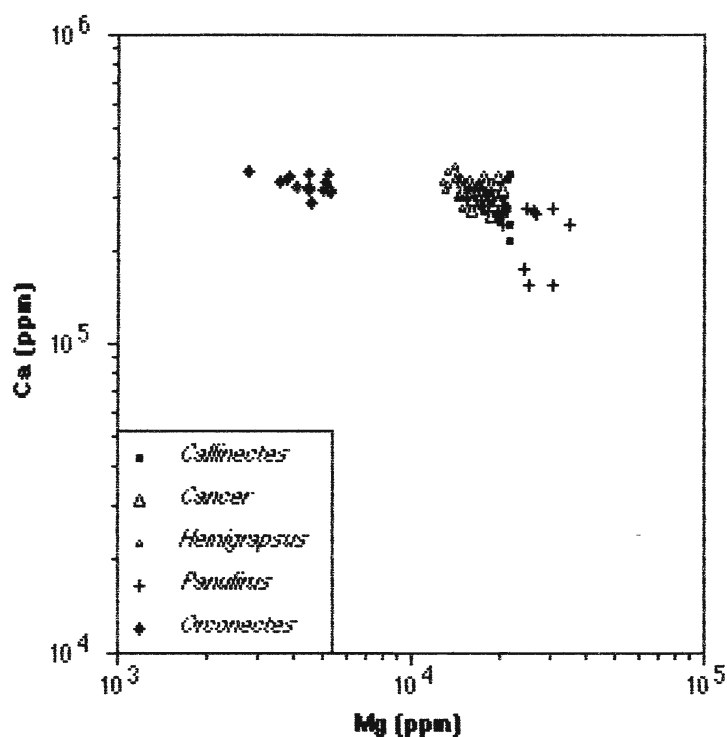


Figure 36: Scatter diagram of the calcium and magnesium concentrations in Recent arthropods. Note the statistical differences in magnesium concentrations (t-test - 14.261, $p < 0.05$, $f = 25$) between fresh water (*Orconectes* sp.) and marine (*Panulirus argus*) species.

Chapter 4

Trilobites

INTRODUCTION

Speculation as to the physical and chemical composition of trilobite cuticles, and environmental and diagenetic influences on them, has not been supported by detailed study. In order to establish a basis for further speculation, trilobites must be examined for pristine and diagenetic microstructures and analysed for trace element and isotopic compositions. Using Recent arthropods (see Chapter 3) as models for calcite emplacement, hypotheses of the effects of sea-water and sediment chemistry, as well as diagenetic fluids, may be applied to trilobites. Størmer (1980), however, advised caution in comparing trilobites to Recent arthropods since similar structures might develop independently in different groups (e. g. Gould and Lewontin, 1979). Gould and Lewontin (1979) have also suggested that many similarities may be due to constructional constraints imposed on the organisms, such as molting, as opposed to whether there are true phylogenetic similarities (that is, they are homologous structures which trilobites and Recent arthropods inherited from a common ancestor). However, Størmer (1980) also stated that analogous structures might be important in understanding the functions of the organs in the fossil forms. Therefore a comparative study of modern arthropod to trilobite cuticle, under similar conditions and magnifications, with emphasis on other functions for the microstructures, may aid in identifying pristine microstructures and geochemistries.

MICROSTRUCTURES

Trilobite microstructures are described using the terminology of Størmer (1980), who divided the cuticle into an outer prismatic layer, an outer laminate zone, a prominent central laminate zone, and a relatively thin, inner laminate zone. The prismatic layer and the outer laminate zone are considered to be equivalent to the epi- and exocuticle of Recent arthropods, whereas the central laminate zone is equivalent to the principal zone (Dalingwater and Miller, 1977).

Several microstructures noted by Teigler and Towe (1975) differ greatly, in large part due to the SEM magnifications used, from those noted in this and other studies. Teigler and Towe 's (1975-Plate 2) photographs were made at magnifications far exceeding those used in this study. It is not surprising that there is a lack of corresponding microstructures between earlier studies using high magnifications (e.g. Neville and Luke, 1969; Halcrow, 1978), and recent work employing lower magnifications (e.g. Feldmann and Tshudy, 1987; McAllister and Brand, 1989).

Pristine Microstructures

Preservation criteria are absolutely essential in identifying primary material, and in doing so one must be familiar with the physical and chemical characteristics of original cuticle material. The purpose of identifying pristine and diagenetic microstructures is to define degrees of morphological alteration. In conjunction with geochemical data, these provide a means of accurately characterizing the diagenetic state of fossil specimens.

Surface Features

The outer prismatic layer was only occasionally present, a finding similar to that of Størmer (1980). When found, the layer was thin and had a distinctly striated surface (Figs. 37 A and B). Variation in orientation on such a fine scale (Fig. 37 A) indicates that the striations are not the result of errors in sample preparation, but represent primary microstructural features. The possibility of the striations being a remnant of paleoabrasion is debatable. The lack of relief to the *Phacops rana* microstructure, and a lack of similarity to abrasions noted on specimens of the crustacean *Callinectes* sp. (Fig. 26), casts doubt on this interpretation.

General surface microstructures were found to vary in size and texture, and are largely dependant on the species of the organism. For example, the majority of well preserved *Phacops* specimens exhibit small, rounded rhombs of calcite (Figs. 38, 39).

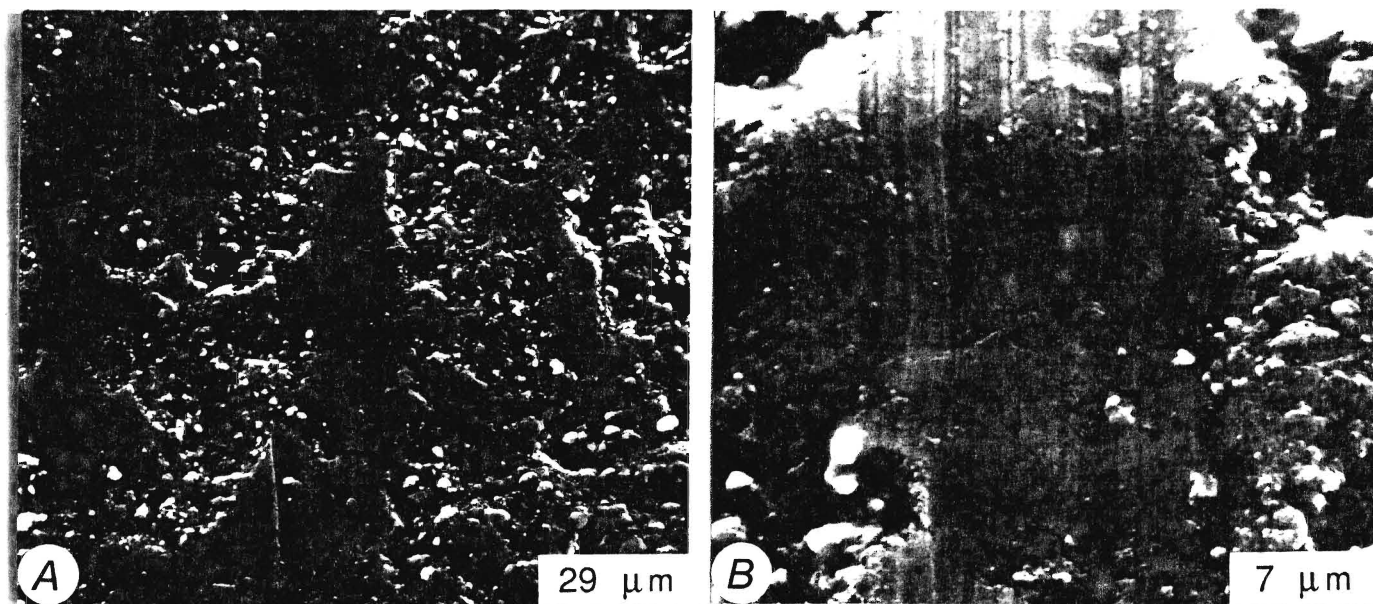


Figure 37: Striated primary prismatic layer in *Phacops rana*. A. Shown are the striations of the prismatic layer having a number of orientation. Osmólska cavities can be seen below. B. Detail of the prismatic striations. (17 91)

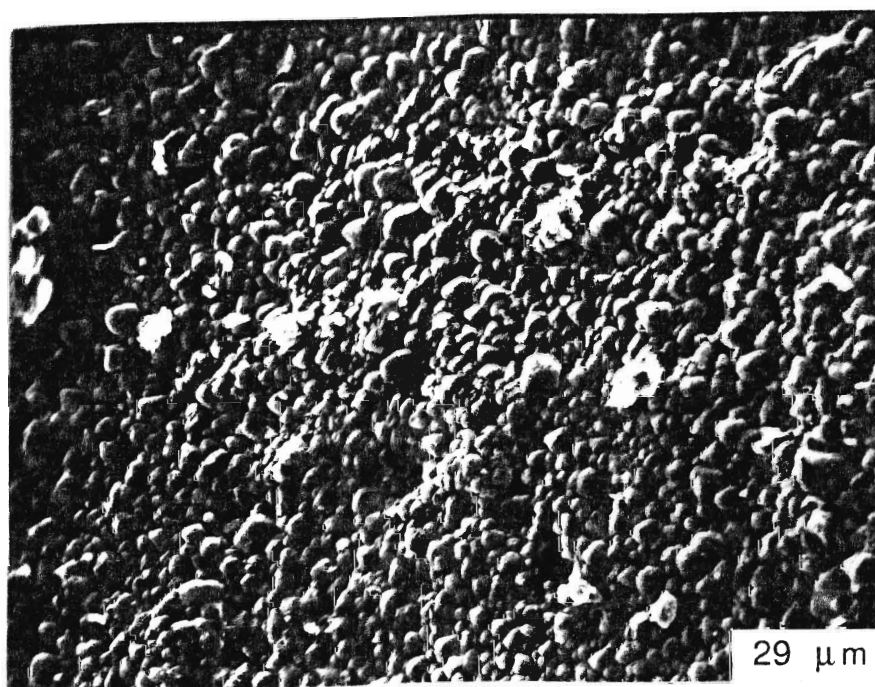


Figure 38: Surface texture of a *Phacops rana* specimen from the Ludlowville Formation of New York. Note the size and shape of the rounded calcite rhombs. [21 229]

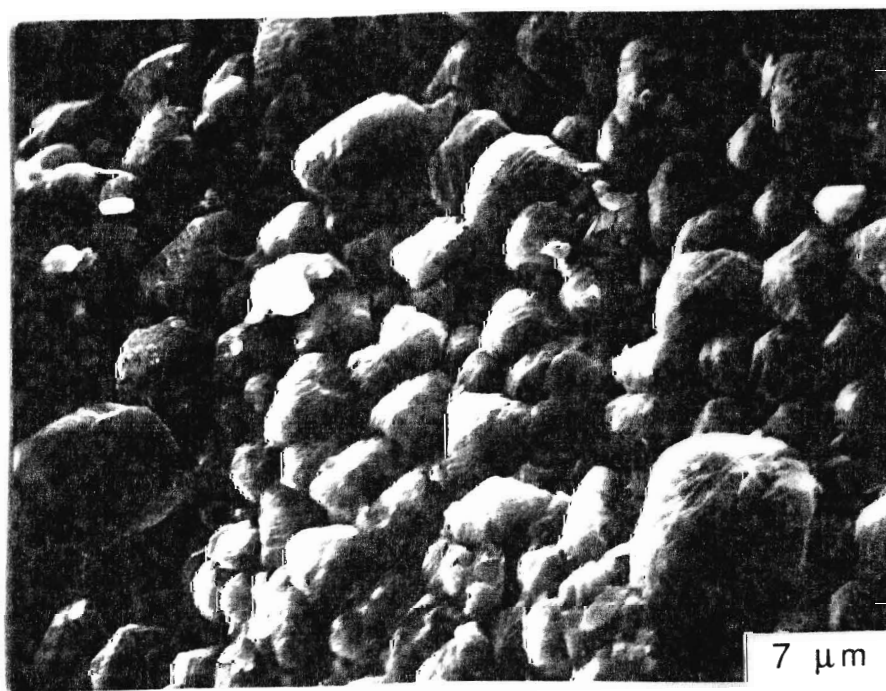


Figure 39: Detail of the surface texture of the above *Phacops rana* specimen. Note the distinct rounded calcite rhombs. [21 229]

Crystals vary from approximately 1 μm (Fig. 37 B), to 4 μm (Fig. 39). These rhombs are probably the surface 'calcite prisms' noted by Dalingwater (1973-Plate 107, Fig. 1). In specimens of *Isotelus* a larger trilobite than *Phacops* the surface was found to be composed of much larger, more angular, crystals of calcite (Figs. 40 and 41), indicating possible dependence of microstructure size on the species and ontogeny of the trilobite.

Osmólska Cavities

Osmólska cavities (Osmólska, 1975; Størmer, 1980) were observed by SEM below the thin outer prismatic layer (Figs. 42, 43) of *Phacops rana*. Similar to the problems encountered by Størmer (1980), limitations of SEM resolution made it impossible to discern whether or not the area directly below the cavities is penetrated by minute canals. The Osmólska cavities of this study have dimensions of 10 to 15 μm (Fig. 43), which correspond to those reported by Størmer (1980) and Dalingwater (1973). The findings of this study agree with Størmer's conclusion of a primary origin for these cavities, as the regular arrangement and spacing of the Osmólska cavities precludes formation due to acts of abrasion or boring algae. Furthering this postulation, it is suggested that this is a genetic biomineralization signature of the trilobite, and is indicative of the excellent preservation of cuticular calcite.

Pore Canals and Setae

The terms 'pore' and 'pore canal' used in extant arthropods and their application to primary microstructures found in trilobites has lead to some confusion. Dalingwater and Miller (1977) advised caution in the use of Teigler and Towe's (1975) term 'pore canal' for all categories of primary ducts dissecting trilobite cuticles, because they are not necessarily true pores. McAllister and Brand (1989) proposed the terms of 'hexagonal surface openings' and 'biomineralization microstructures' for primary microstructures that fit the 'pore' and 'pore canal' description in trilobites. This terminology was employed to

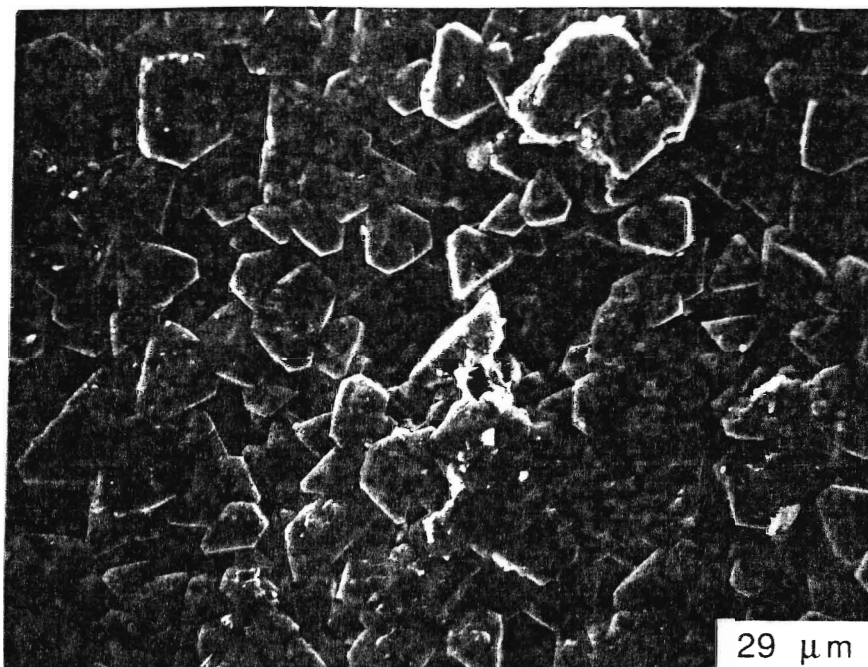


Figure 40: Surface texture of an *Isotelus maximus* specimen from the Waynesville Formation of Ohio. Note the size and shape of the angular calcite crystals. (19 536)



Figure 41: Detail of the surface texture of the above *Isotelus maximus* specimen. Note the distinct angular calcite rhombs. (19 536)

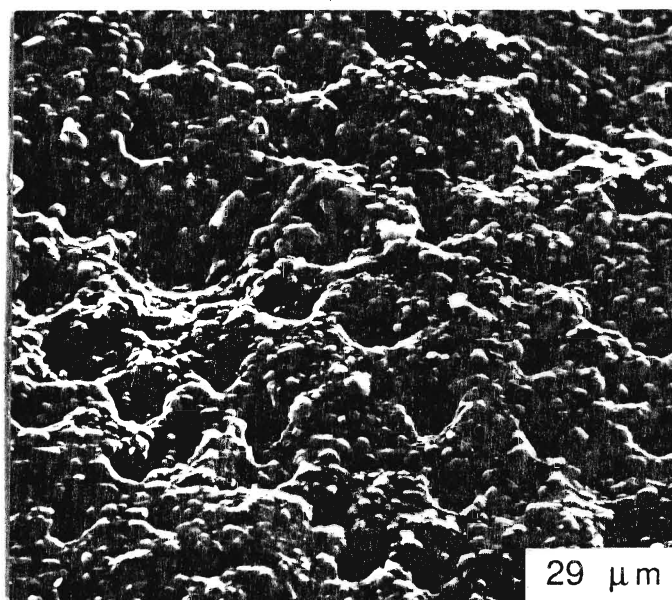


Figure 42: Osmólska cavities in the upper cuticular layer of a specimen of *Phacops rana*. Note the regular spacing of the cavities. (17 91)

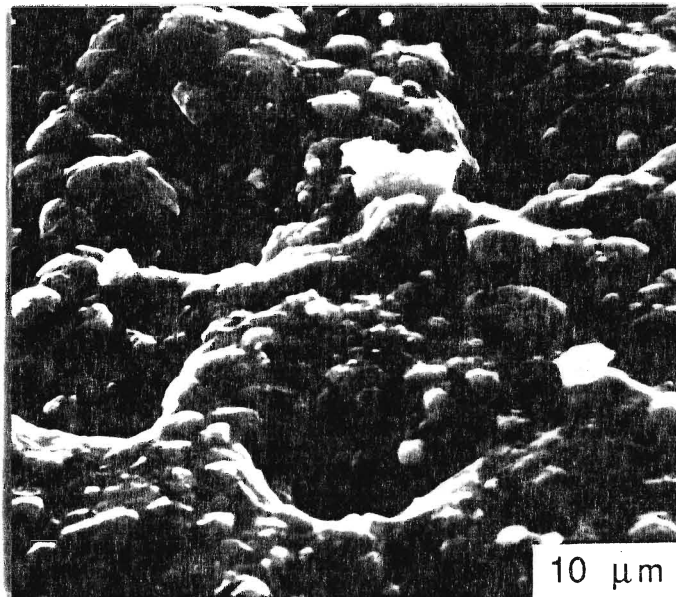


Figure 43: Close up of Osmólska cavities seen above. Note the rounded calcite rhombs. (17 91)

avoid the confusion pertaining to the true function and genetic importance of these structures. In many instances, the openings observed on the cuticle of trilobites do not penetrate the cuticle, and a decision as to the function of the feature has yet to be addressed.

In order to avoid ontogenetic variabilities, the trilobites *Isotelus* and *Phacops* were chosen to be compared microstructurally to the similarly sized Recent arthropod *Limulus*. The conclusion of Rolfe (1962) that smaller canals in trilobites are genuine pore canals and larger ones setal and tegumental gland ducts is supported by structures observed in *Limulus*. A comparison of the shape and size of tegumental gland ducts through the cuticle of *Limulus* (Figs. 15, 16, and 17) to surface openings in trilobites (Fig. 44) suggest a tegumental origin for some features in trilobites. Other 'hexagonal openings' (structures not penetrating the cuticle) on the cephalon of *Isotelus* (Fig. 45) are of the same size and shape as setae observed on *Limulus* (Fig. 18), although, as Størmer (1980) noted, setae themselves were not found on trilobites. In addition, clusters of surface openings found on the cephalon of *Phacops* (Figs. 46, 47) are identical in shape and scale to the openings observed on the dorsal cephalic surface of *Limulus* (Fig. 19). Taking into consideration species and ontogenetic differences, the smaller Devonian trilobite *Greenops boothi* from New York State shows probable setae openings on the tubercles of the pygidium (Figs. 48, 49), while *Phacops rana*, also from the Devonian of New York, has similar structures on the cephalon (Fig. 50). From this comparison it is apparent that there are several similarities in microstructures, although it is not known if this is indicative of common architectural or ancestral origins.

Dendritic Microstructures

As mentioned in Chapter Three, the 'dendritic' microstructure of McAllister and Brand (1989) is most likely an original or extremely early diagenetic microstructure. This new conclusion is supported by its presence on primary surface structures such as

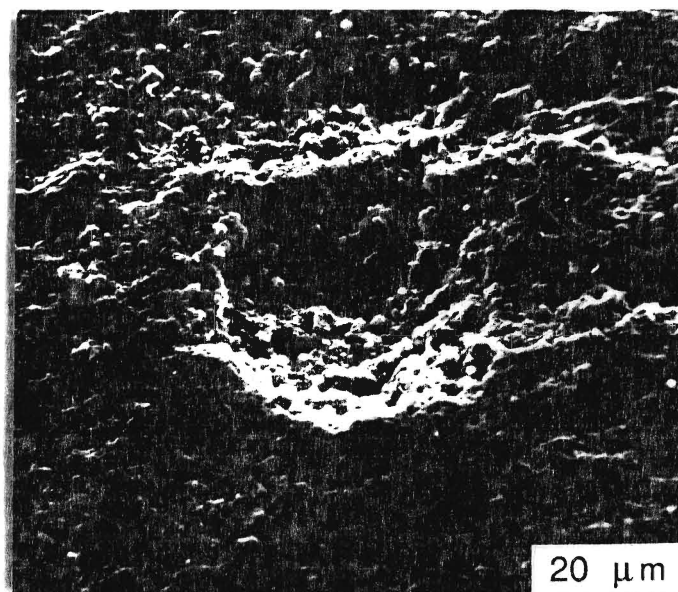


Figure 44: A hexagonal surface opening in a specimen of *Isotelus maximus* (Ordovician) is shown. Note the similarity in size to the tegumental gland ducts in Figures 15, 16, and 17. (11 23)

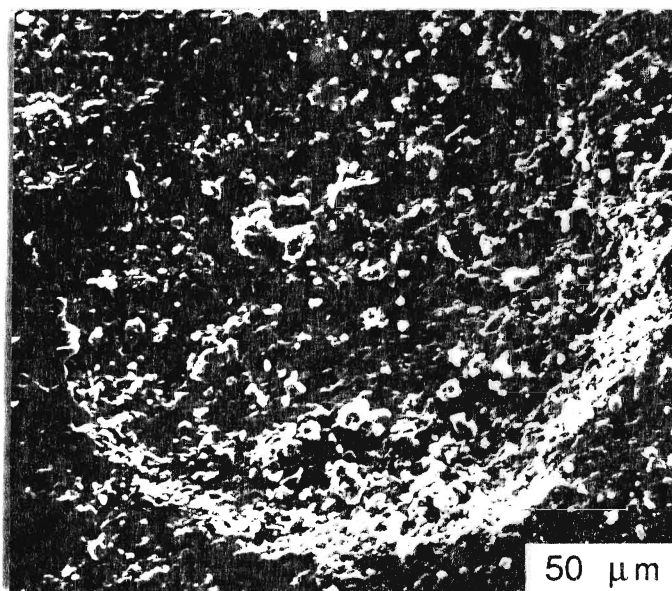


Figure 45: Opening on the cephalon of a specimen of *Isotelus gigas* from the Yerulam Formation (Ordovician). Note the hexagonal shape of the opening, and the large size of this microstructure. (11 129)

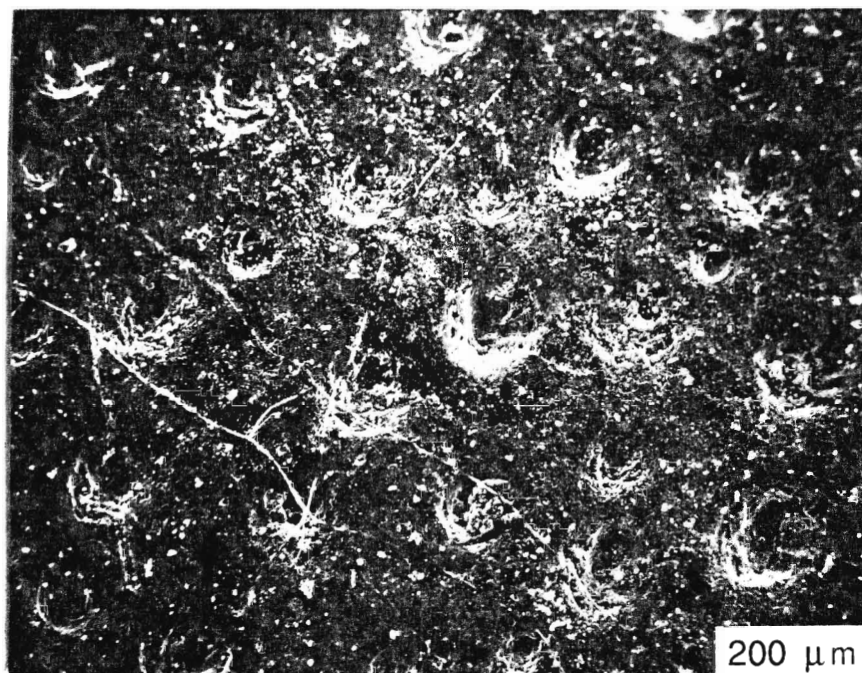


Figure 46: Cluster of possible setae openings on the cephalon of a specimen of *Vogdesia bromidensis* from the Bromide Formation (Ordovician). (11491)

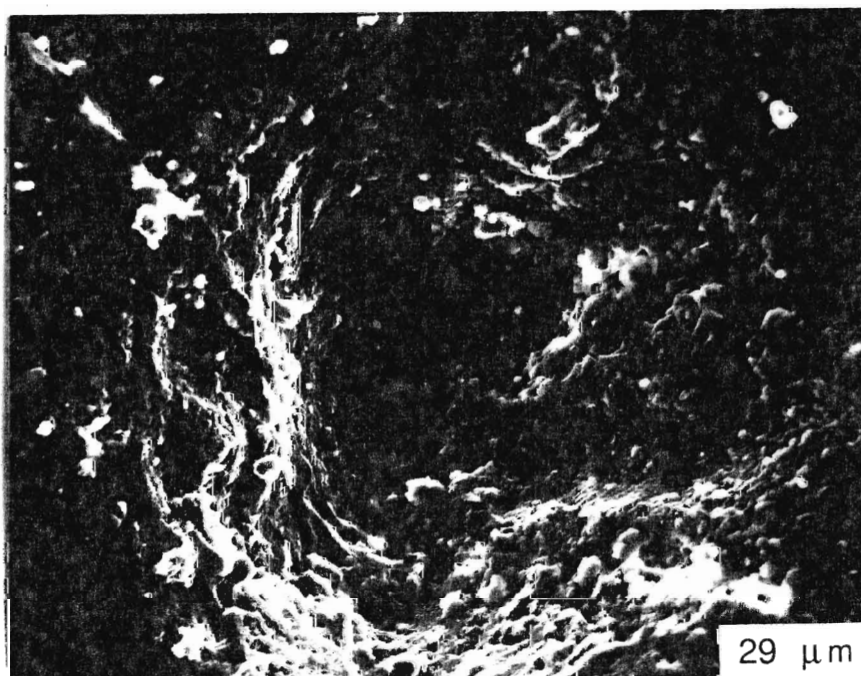


Figure 47: Possible setae in the *Vogdesia bromidensis*. (11491)

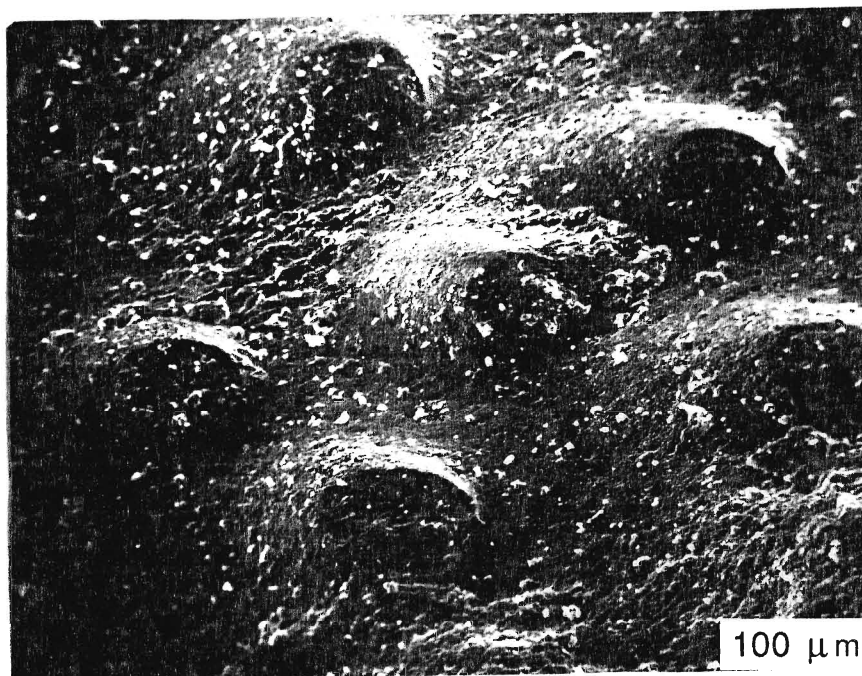


Figure 48: Numerous tubercles on the pygidial spines of a specimen of *Greenops boothi* from the Deep Run Shale Member of the Moscow Formation (Devonian). Many of the tubercles have had their peaks sheared during sample separation from the surrounding matrix. (13421)

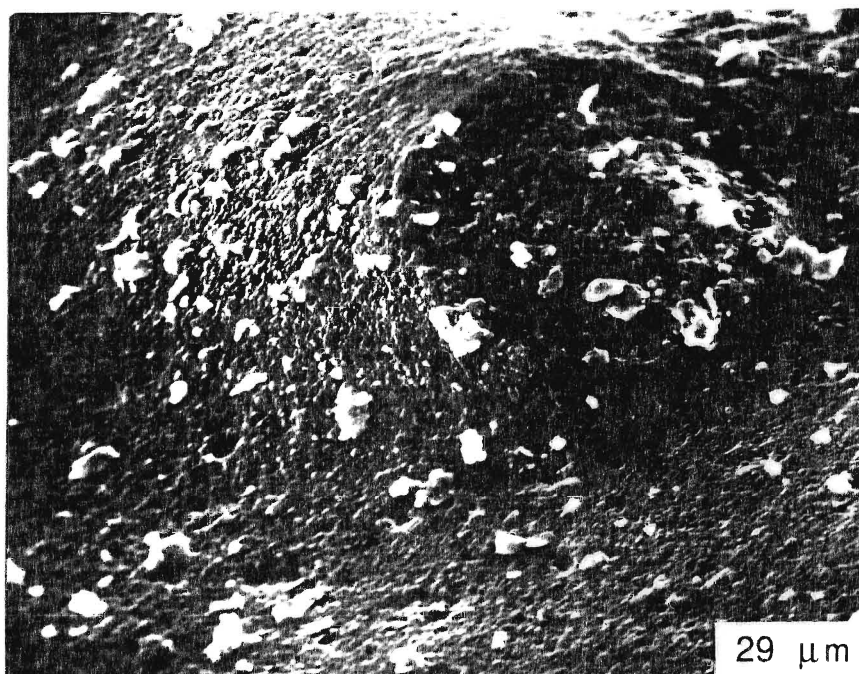


Figure 49: The tubercles noted in Figure 48 are shown in detail, with setae openings in the lower half of the picture. (13421)

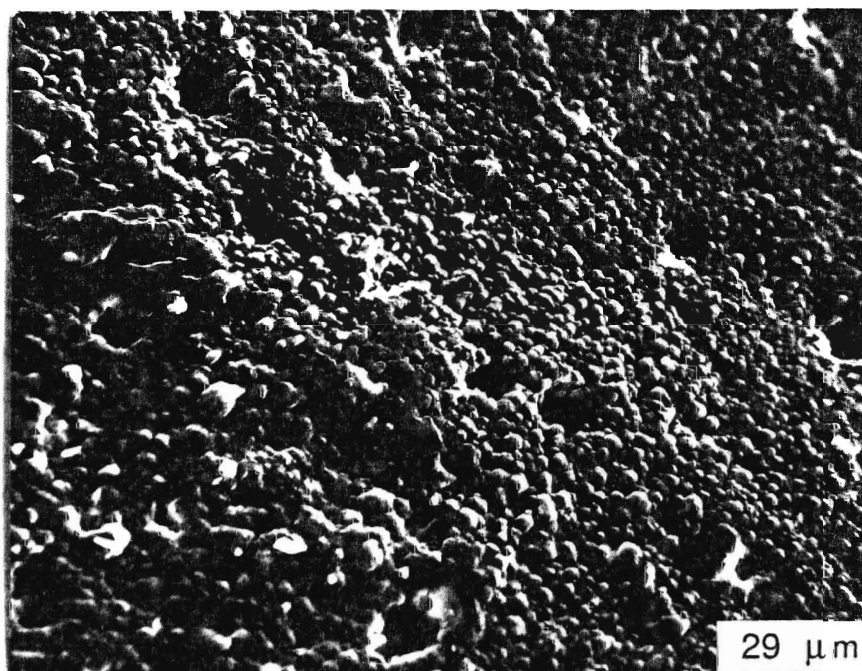


Figure 50: Numerous small openings (possible setae) on the cephalon of a specimen of *Phacops rana* from the Wanakah Shale Member, Ludlowville Formation (Devonian). (21 229)

terraces (Fig. 51 A). In trilobites, unlike Recent arthropods, this microstructure was not limited to just the horizontal surfaces of the cuticle, but appears to permeate the cuticle (Figs. 51 B, 52). If this microstructure was primary, one would expect them to disappear with extensive diagenetic alteration of the cuticular calcite. These microstructures are present in not only pristine but also on altered specimens. It is possible that preservation of this microstructure is indicative of a delicate diagenetic process, but there is no information as to its function and formation in trilobite and Recent arthropod cuticles. Their presence in both trilobite and Recent arthropod cuticles is intriguing; this similarity may infer a possible common ancestor, or simply refer to architectural similarities.

Laminae

Laminae in trilobites have been more consistently found in thin section examinations (e.g., Towe, 1975; Teigler and Towe, 1975; Dalingwater and Miller, 1977; Towe, pers. comm., 1987) than SEM. This is no more obvious than in a comparison of the Devonian trilobite *Phacops rana* from the Windom Member of the Moscow Formation. In the thin section examination by Teigler and Towe (1975), they observed laminae in all of their specimens, while specimens in SEM examination of this study do not exhibit laminae. Other than the laminae noted in Chapter 3 to have occurred in *Panulirus*, no laminae were observed in the present study.

Rolfe (1962) suggested preparation errors for the lack of laminae in several thin sections of his Silurian crustacea specimens, and Dalingwater and Miller (1977) concluded that specimen preparation and/or diagenesis are the controlling factors in detecting laminae in trilobites. Feldmann and Tshudy (1987) in their SEM study found the presence of laminae in fossil lobster to depend on the molt phase of the cuticle, as well as the preservation of the cuticle. In the present study, since laminae were absent from all but the lobster *Panulirus* (Fig. 11), it is possible that there is a genetic control at the family level. This supports Towe's (1975) assertion that some trilobite cuticles

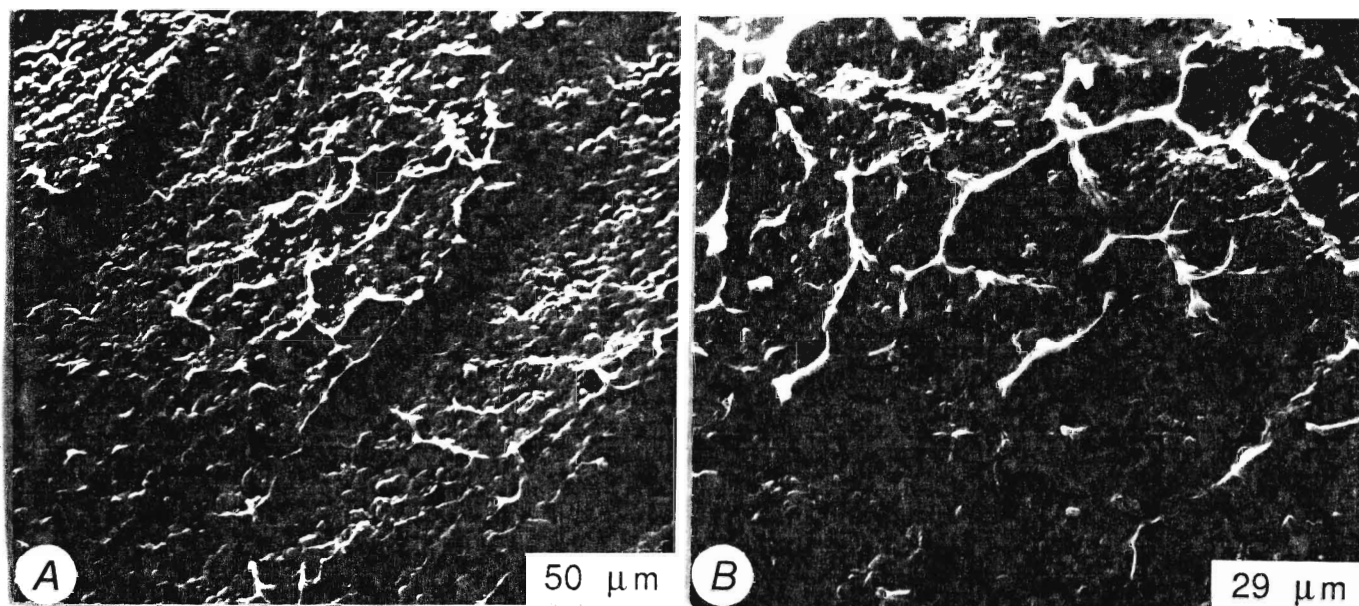


Figure 51: The 'dendritic' microstructures in specimens of the Devonian trilobite *Phacops rana* is shown. A. The microstructure on primary surface terrace structures of a relatively unaltered specimen (16 13—Jaycox Shale Member, Ludlowville Formation). B. Cross-sectional view of a fractured cuticle with the microstructure appearing to permeate through the cuticle (From McAllister, 1987—13 81)

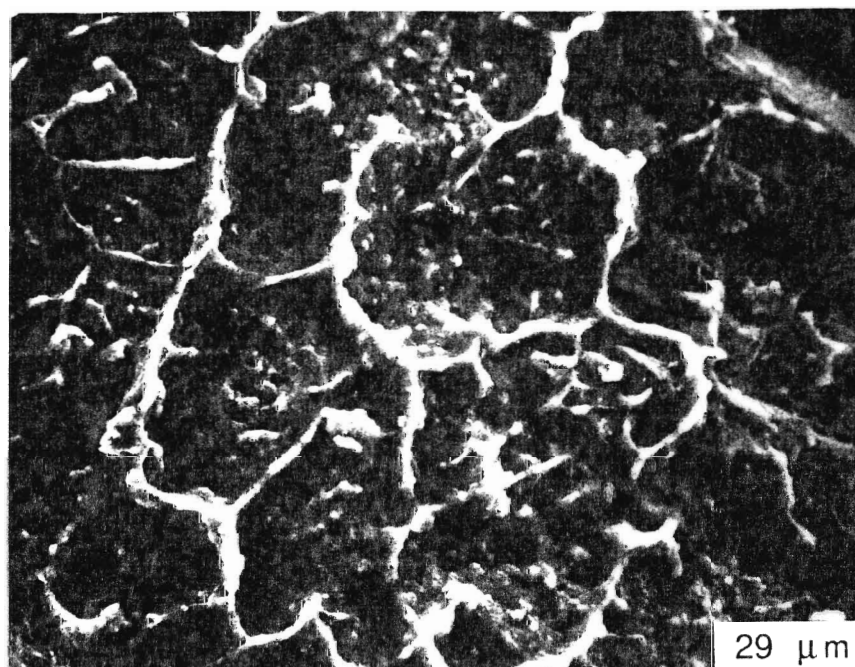


Figure 52: 'Dendritic' microstructure in a cross-section of *Isotelus maximus* (Waynesville Formation). (19 536)

contain laminations and others do not. It is therefore likely that the main determining factors as to the presence of laminae in trilobites are preservation, sample preparation, and the heredity of the specimen.

Biomineralization Structures

In Towe's (1973) examination of the eyes of various trilobites, he paid close attention to their calcitic lenses and state of preservation. Biomineralized calcite lenses in trilobite eyes (e.g., phacopids) were oriented in such a way that vision was free of the birefringence inherent to calcite. The fact that lens calcite has crystallographic properties comparable to other primary calcites, indicates that it represents pristine material and conditions. Therefore, other biomineralization microstructures can and should be preserved in trilobite cuticles, a conclusion substantiated by the studies of Dalingwater (1975b) and Størmer (1980).

'Biomineralization structures' (McAllister and Brand, 1987) found in cross-sections of *Asote/us* fragments consist of narrow (approximately 5-20 μm wide) calcite needles aligned perpendicular to the surface of the cuticle (Figs. 53, 54, 55, and 56). Emplacement of these microstructures in trilobites likely occurred immediately post-molt, when the calcification process is most rapid in Recent arthropods. The absence of these microstructures in many trilobites is most likely a reflection of diagenetic obliteration (cf. Teigler and Towe, 1975; Brand, 1987a). It is interesting to note that needle-shaped biomineralized microstructures were observed only in species of *Asote/us*, but it is not known if they are unique to this genus.

Diagenetic Microstructures

With extensive diagenetic alteration of the cuticle, one would expect significant changes in the microstructures of trilobites. Alteration has been found to have various degrees of intensity, largely due to the surrounding matrix. For example, Miller (1975)

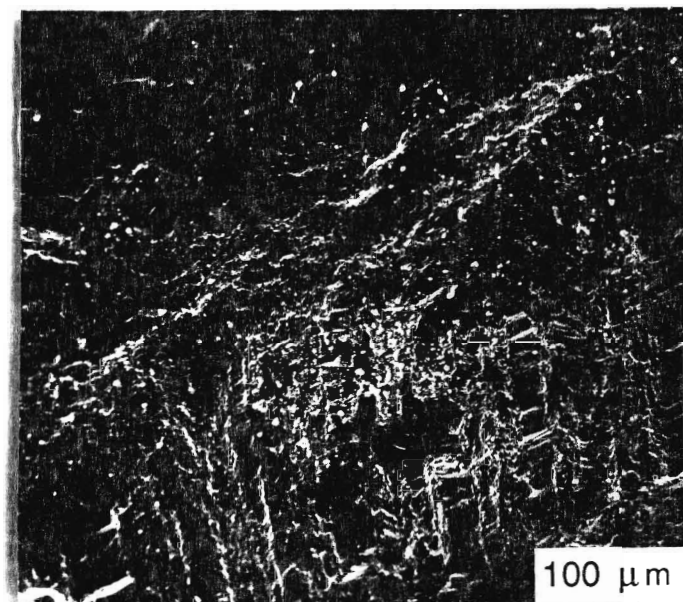


Figure 53: Biomineralization structures in a cephalon fragment of the Ordovician trilobite *Isotelus maximus* (Whitby Formation) are shown to trend perpendicular to the surface of the cuticle (upper left). (From McAllister, 1987—11 22)

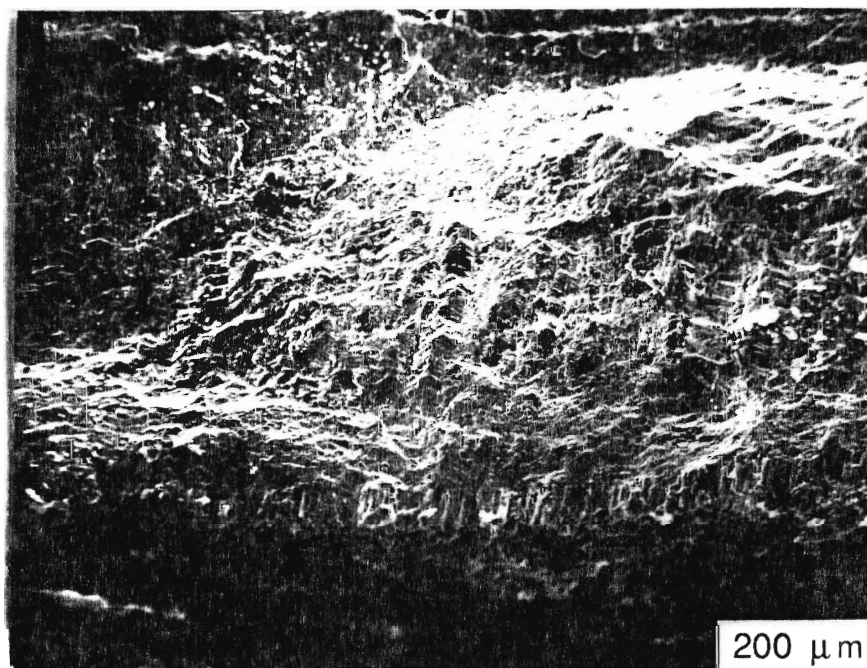


Figure 54: Biomineralization microstructures in a thorax fragment of *Isotelus maximus* (Waynesville Formation) are shown. Note the upper surface (top) and lower surface (bottom) with the biomineralization in the midsection of the cuticle. (12 526)

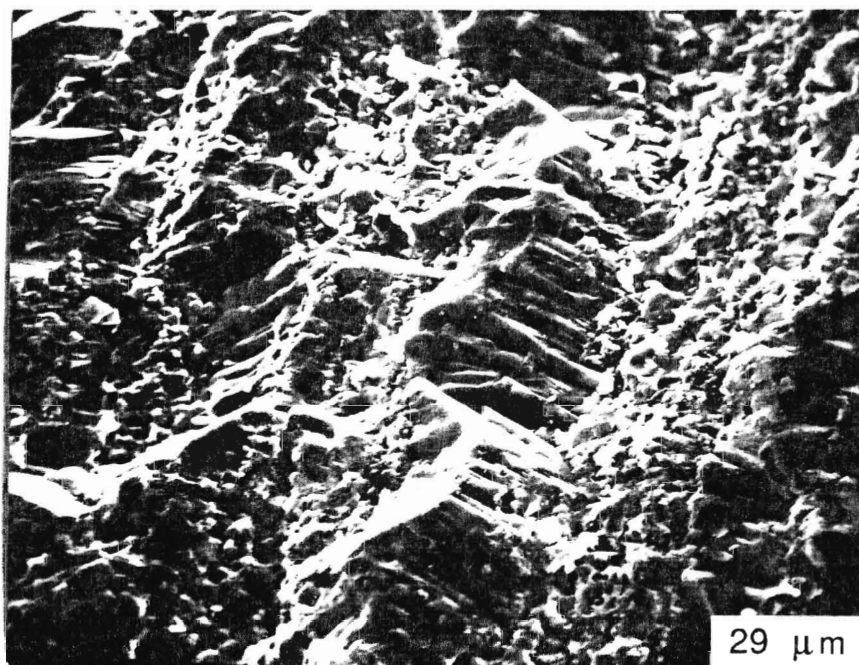


Figure 55: Detail of the the biomineralization structures in Figure 54 are shown. (12 526)

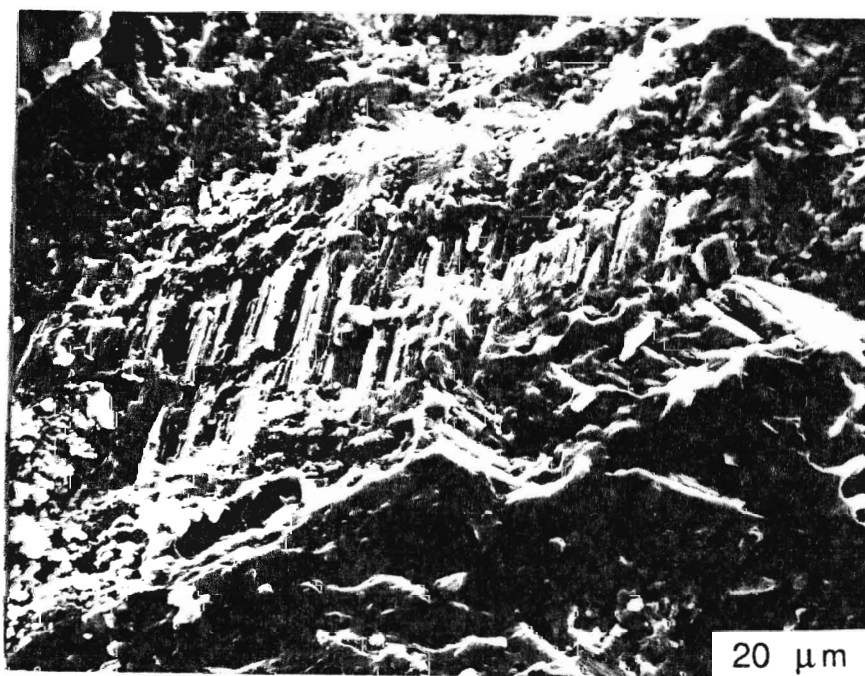


Figure 56: Biomineralization microstructure in a fragment of *Isotelus* sp. (Cobourg Formation) is shown. (19 114)

and McAllister and Brand (1989) noted localized occurrences of physical alteration on a very fine scale in specimens from shale. Størmer (1980) found that specimens from shales exhibit good surface structures, whereas those from limestones generally lack fine internal structures and are more heavily recrystallized. Miller (1975) suggested that biological and mechanical recrystallization, solution and replacement all have to be considered factors in the alteration of cuticular calcite.

The higher degree of calcification in trilobite cuticles than in most crustaceans is a major control on the extent and preservation potential of their primary microstructures. Diagenesis of the cuticular calcite hinders the detection of many original microstructures and creates new features, which may be mistaken for primary exoskeletal microstructures. For example, Rolfe (1962) stated that many of the proposed subdivisions made for fossil cuticular microstructures are really diagenetic products. Diagenetic alteration of cuticles must also be considered a major factor for the apparent lack of primary microstructures in some trilobites, particularly those from limestones.

Replacement and Pyritization Microstructures

In the course of this study, several apparent diagenetic microstructures were noted, with the most obvious diagenetic changes having occurred in the general surface structures and textures of the cuticle. The most apparent form of diagenetic alteration is not what microstructure has been left behind, rather what microstructures are no longer present. Replacement of the original cuticular calcite generally obliterates all traces of primary microstructures, while initial forms of diagenesis generally lead to a 'fusing' of the cuticular calcite present, a process first noted by McAllister and Brand (1989). For example, progressive diagenesis of *Phacops* cuticle results in the primary small sub-rounded rhombs of calcite (Fig. 38 and 39) changing to fused cuticular calcite (Fig. 57). This 'fusing' was observed in the present study and by McAllister and Brand (1989) to

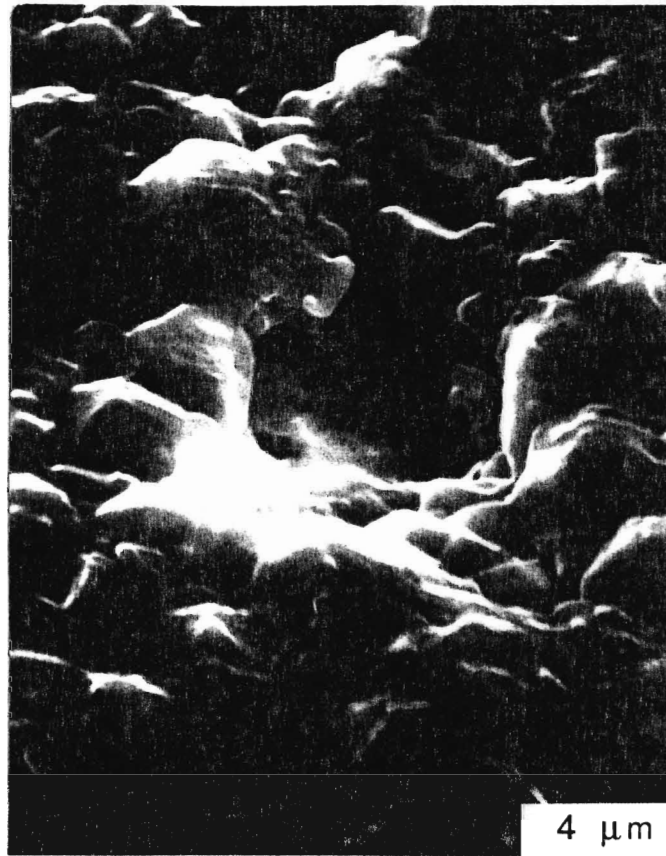


Figure 57: Fusing of cuticle calcite rhombs in a specimen of *Phacops rana*. (21 229)

also occur in *Isotelus* (McAllister and Brand, 1989—Fig. 6) and *Terataspis* (McAllister and Brand, 1989—Fig. 7) specimens.

The replacement of cuticular calcite with secondary minerals was also observed in specimens of the present study. Cuticles of *Phacops rana* (Fig. 58) and *Isotelus maximus* (Fig. 59) displaying characteristic diploidal cubic and pyritohedron pyrite were found in shale units known to represent reducing environments, and that also yielded specimens with pristine microstructures. The emplacement of pyrite into the cuticle has been noted previously by Rolfe (1962), Osmólska (1975), Teigler and Towe (1975), and Babcock (1982), however, it is believed that this is the first SEM evidence of pyritized trilobite cuticle. Babcock (1982) has suggested that pyrite growth into Osmólska cavities is due to the composition of the reducing sediment or diagenetic waters, and Allison (1988b) has found that the action of bacteria will cause pyrite growth on Recent cuticles under anoxic conditions (Allison, 1988b). It is therefore likely that initial pyrite growth is linked to water/sediment conditions and the presence of appropriate bacteria on the cuticle.

TRACE ELEMENT GEOCHEMISTRY

Trilobites are thought to have been more heavily calcified than Recent arthropods (Towe 1973; Teigler and Towe 1975; Dalingwater and Miller 1977), and to have required a minimal amount of chitin in their cuticles (Dalingwater and Miller 1977). The chitin was not found preserved by Teigler and Towe (1975) in their examination of cuticles, although they emphasized that this need not mean that chitin was lacking in trilobites. Similarly, Sohn (1958) and Rolfe (1962) identified little or no organic framework in the poorly mineralized cuticles of fossil crustacea. The organic fraction of the trilobite cuticle therefore appears to be of little consequence to their present geochemical composition, and will not be considered further.

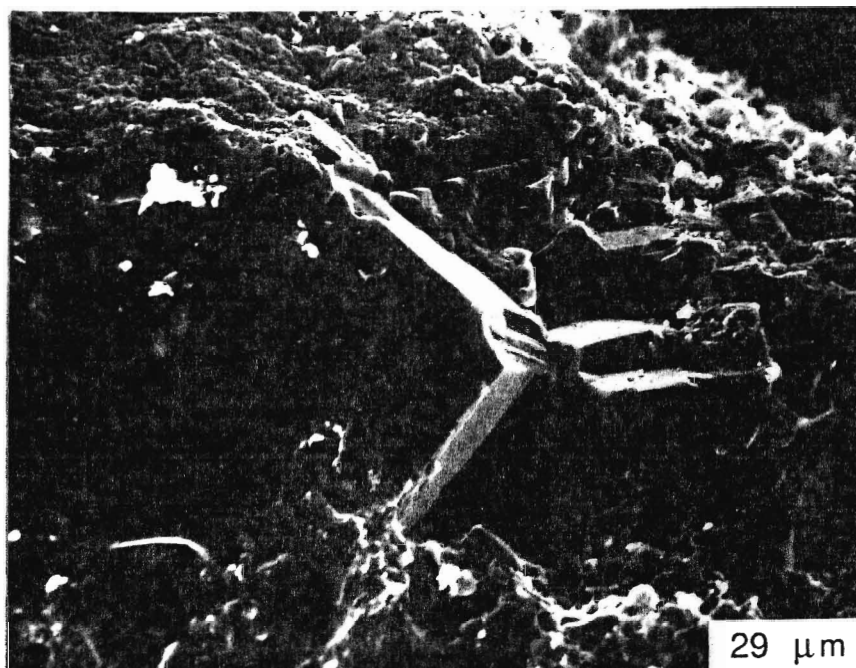


Figure 58: Large cubic pyrite crystals in the cuticle (cephalon) of a specimen of *Phacops rana* from the Penn Dixie Bed, Windom Shale Member, Moscow Formation. (21461)

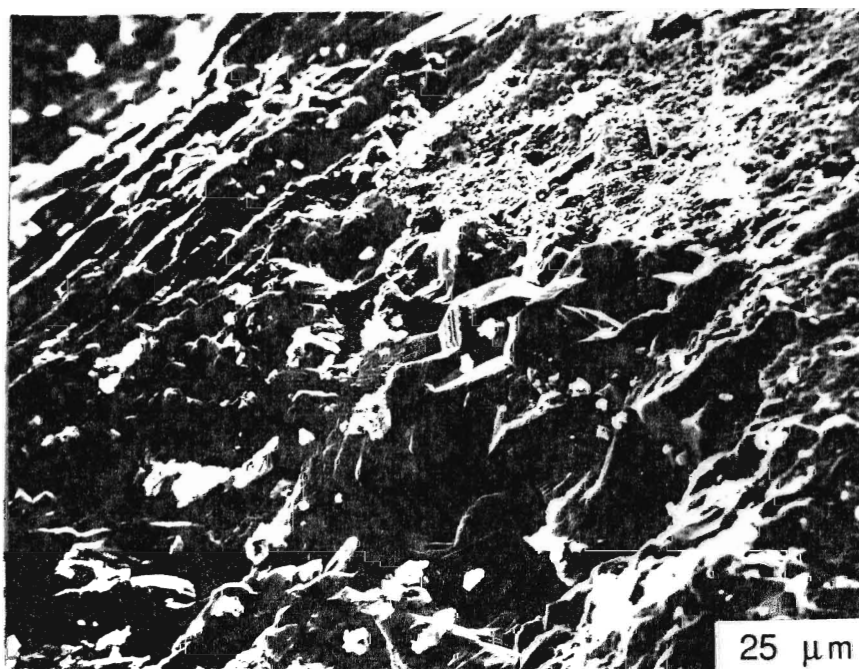


Figure 59: A cluster of pyritohedron pyrite crystals in the cuticle of *Isotelus maximus* from the Whitby Formation (Ordovician). (1127)

Geochemical studies of fossil material have proven useful in determining not only the degree of diagenetic alteration but also the original mineralogy of the test (e.g., Lowenstam, 1961; Brand and Veizer, 1980). In addition, the studies of Veizer and Demovic (1974), Veizer *et al* (1978), Brand (1987a, 1989), and Popp (1981) among others have developed hypotheses about the paleosalinity, paleotemperature and other ambient environmental conditions in which a particular organism lived. However, the results of these studies are based mostly on the shell chemistries of well-preserved brachiopods and molluscs, and not those of trilobites. Comparing the compositions of trilobites with those of Recent arthropod cuticles (Chapter 3) will aid in removing the diagenetic imprint on trilobites, suggest an original chemistry and mineralogy, and infer environmental influences.

Diagenesis in Trilobites

Discrimination of altered and pristine material is imperative in determining an original composition for trilobites. McAllister (1987) concluded that most trilobites lose sodium, strontium and magnesium with diagenesis (cf. Brand and Veizer, 1980), an observation expanded upon in the present study. The majority of trilobites in the present study have undergone some degree of geochemical alteration from their pristine composition, and most likely the degree of alteration is in large part due to the influence of the surrounding facies. Pristine microstructures, although not exclusive to shales, generally are more abundant in this lithofacies. McAllister and Brand (1989) found that the influence of facies (lithology) on the geochemical contents of cuticular calcite can be inferred from differences in manganese concentrations between pristine specimens obtained from shales and limestones. This is interpreted as reflecting differences in the redox potential of the two environments in which the studied trilobites lived, and supports Rainbows' (1988) observations, and those of the present study, of metal uptake in Recent arthropods. Although there are differences in the manganese contents, the

strontium/calcium ratios in trilobites from shales and limestones were found to be similar. This is a clear indication of the redox-independent behaviour of strontium in calcium carbonate, and the high mobility of the strontium ion in diagenesis, with a high strontium/calcium ratio reflecting a lesser degree of diagenesis. Pristine specimens should therefore possess high concentrations of strontium and sodium, similar to Recent arthropods, and manganese and iron being facies and diagenetically controlled. The fact that diagenetic fluids are able to pass through porous limestones in greater volumes than through shales is the obvious cause of this preservation phenomenon.

Devonian Trilobites

The majority of Devonian trilobites were obtained from shale facies (Fig. 60, 61), and most of those studied by SEM possessed pristine microstructures (e.g. Figs. 37, 38, and 42). High concentrations of manganese (Fig. 60) and strontium and sodium (Fig. 61) in trilobite cuticles from the shale units emphasize the facies influence and better preservation usually inherent to this lithology. Apparent alteration of specimens in shale was observed (e.g. - *G. boothi*-Widder Fmn., Fig. 61), and therefore analysis is focused on both shale diagenesis, and the influence of the depositional environment on the chemistries of the trilobite cuticular calcite.

The strontium, manganese and sodium concentrations in trilobites from shales show a high degree of variability and may change laterally from locality to locality within the same bed, as in *Phacops rana* from the Demissa bed of the Ludlowville Formation (Figs. 62 and 63). *Phacops* specimens from the Demissa Bed at Bayview and Spring Brook, N. Y. were found to be statistically different in magnesium (t-test -7.115, $p < 0.05$, $f=7$; Appendix IV), strontium (t-test -5.264, $p < 0.05$, $f=7$; Appendix IV), sodium (t-test -3.620, $p < 0.05$, $f=7$; Appendix IV), and manganese (t-test 6.267, $p < 0.05$, $f=7$; Appendix IV) concentrations. These elements are generally thought to be controlled by diagenesis (Brand and Yeizer, 1980), and suggest that *Phacops* from Spring Brook, N. Y. are less

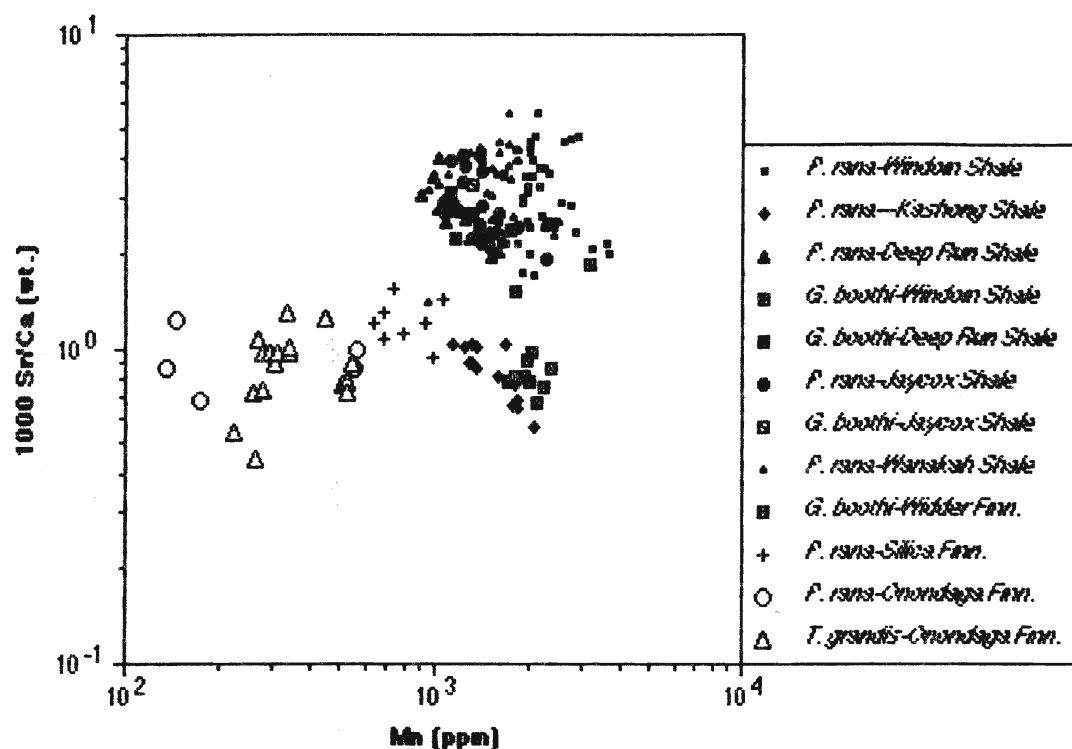


Figure 60: Differences in the manganese concentrations in Devonian trilobites from shale (solid symbols) and limestone (open symbols) facies. Due to low strontium/calcium ratios, all samples from limestone, and some from shale, are considered altered.

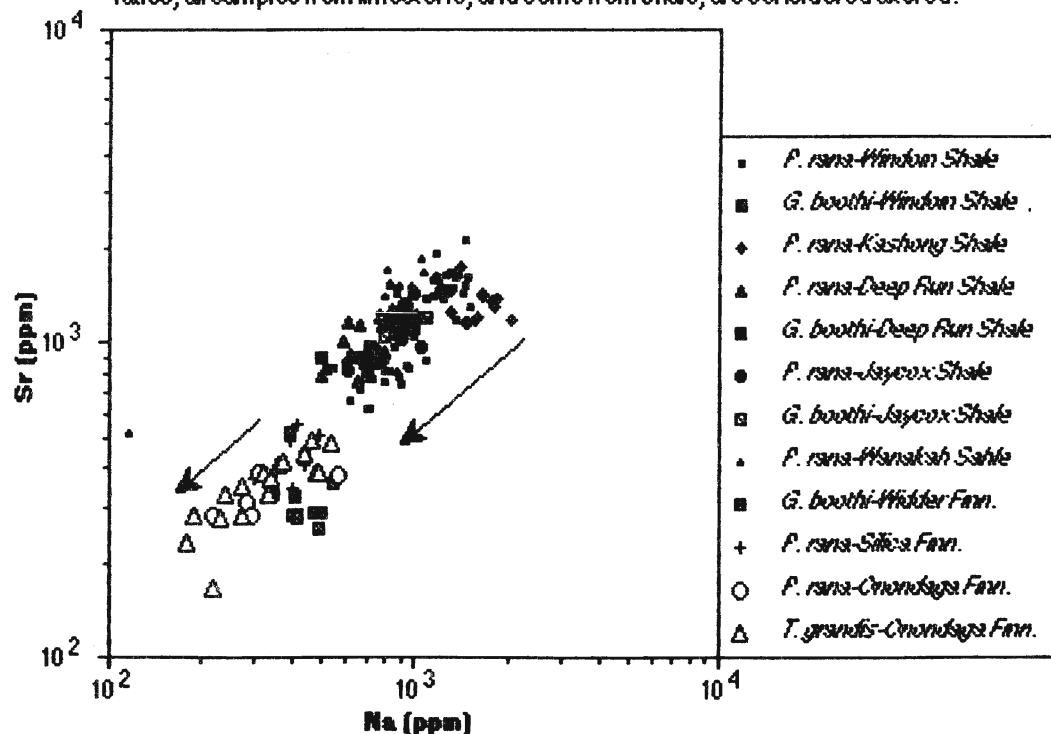


Figure 61: Differences in strontium and sodium concentrations in Devonian trilobites from shale (solid symbols) and limestone (open symbols) facies due to alteration. Arrows indicate direction of alteration.

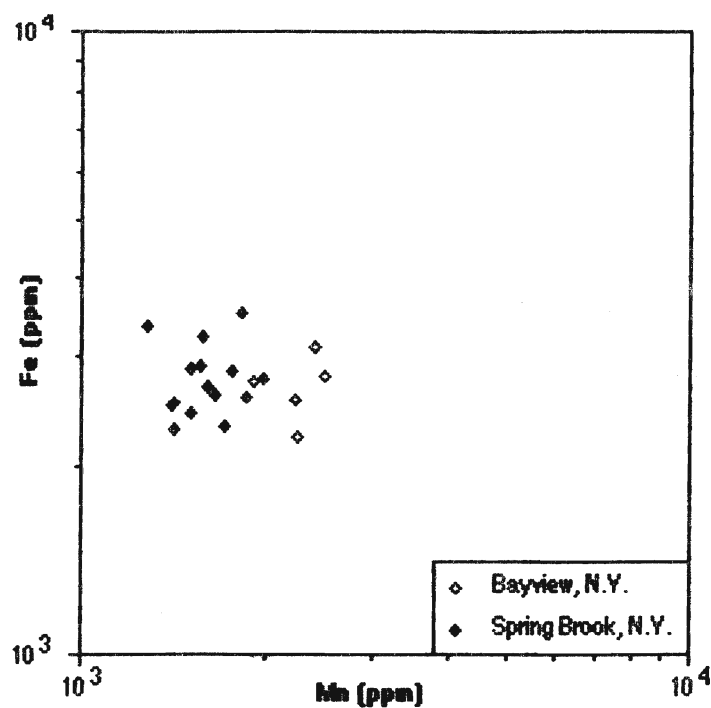


Figure 62: Lateral variation in iron and manganese composition of *Phacops rana* within the Demissa Bed (Ludlowville Formation) due to differences in alteration at Bayview (loc. 1.1) and Spring Brook (loc. 5.1) N. Y.

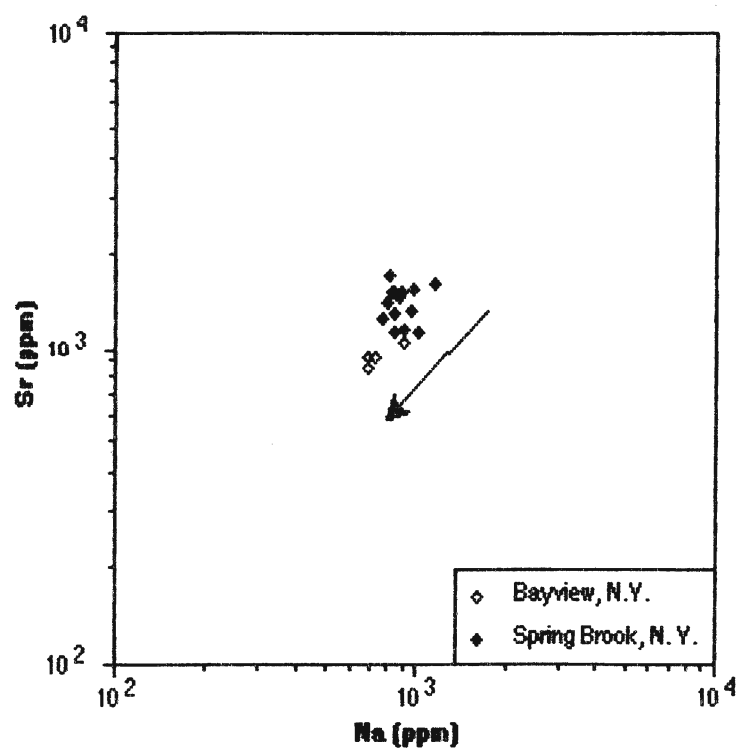


Figure 63: Variation in strontium and sodium concentrations in *Phacops rana* from the Demissa Bed (Ludlowville Formation) due to differential alteration at Bayview (loc. 1.1) and Spring Brook (loc. 5.1) N. Y. Arrow indicates direction of alteration.

altered than those from Bayview, N. Y., due to higher magnesium, strontium, and sodium concentrations with a decrease in manganese. It is therefore most likely that it is lateral differences in degree of alteration, and diagenetic fluids, within the unit that are observed. Lateral variance in preservation was also observed in specimens from the Smoke Creek Bed of the Moscow Formation. *Phacops* specimens from the Smoke Creek Bed at Bayview, N. Y. were found to possess statistically lower concentrations of magnesium (t-test -6.842, $p < 0.05$, $f = 25$; Appendix IV), strontium (t-test -5.674, $p < 0.05$, $f = 25$; Appendix IV), and sodium (t-test -3.349, $p < 0.05$, $f = 25$; Appendix IV) than those at Fall Brook, N. Y. (Figs. 64 and 65). Specimens from this unit have been found to contain pristine microstructures (Figs. 37 and 42) and are thought to be some of the least altered specimens from this study.

Alteration of cuticular calcite may also vary stratigraphically within a section. For example, the cuticular calcite of *Phacops rana* from the section at the Penn Dixie Quarry, Bayview N.Y. (Fig. 5) varies in iron and manganese (Fig. 66) and strontium and sodium (Fig. 67). Variation of these elements is most likely a reflection of differential alteration of the specimens due to the passage of diagenetic fluids. Concentrations of all elements investigated in specimens from the two lowermost beds, the Demissa Bed (loc. 1.1) of the Ludlowville Formation and the Smoke Creek Bed (loc. 1.2) of the Moscow Formation, were found to be statistically similar to one another (Appendix IV). This may suggest that either the two units were altered by the same diagenetic fluid, or that very similar conditions existed for both periods of deposition. Since the concentrations of the diagenetically controlled elements have followed an alteration trend (namely lowered concentrations of magnesium, strontium, and sodium from 'pristine' specimens at Fall Brook), the former appears to be indicated. The cuticular calcite chemistries of these units, and the stratigraphically superior Penn Dixie Bed of the Moscow Formation, are statistically different in calcium, magnesium, strontium, manganese, and iron (see Appendix IV), and suggest different diagenetic fluid chemistries. Compared to the Penn

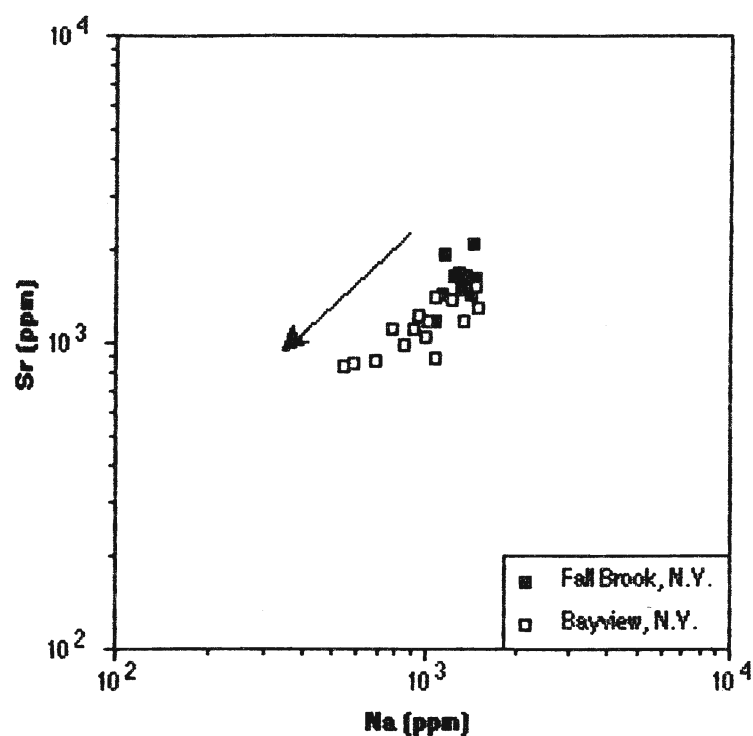


Figure 64: Differential alteration of the Devonian trilobite *Phacops rana* from exposures of the Smoke Creek Bed (Moscow Formation) at Fall Brook (loc. 3) and Bayview, N. Y. (loc. 1.2). The arrow indicates the direction of alteration, lower strontium and sodium concentrations.

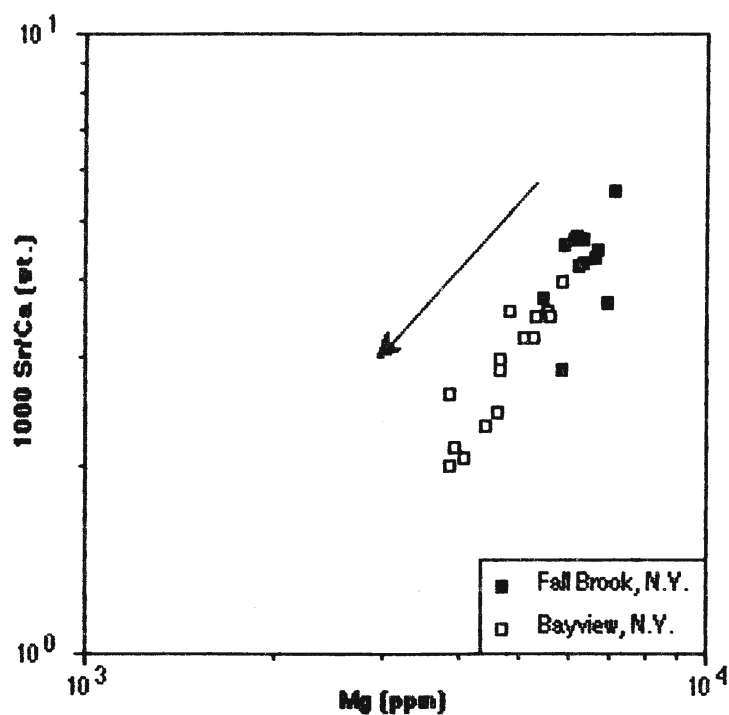


Figure 65: Lateral variation in preservation of *Phacops rana* from the Smoke Creek Bed at Fall Brook (loc. 3) and Bayview, N. Y. (loc. 1.2). Arrow indicates direction of diagenesis.

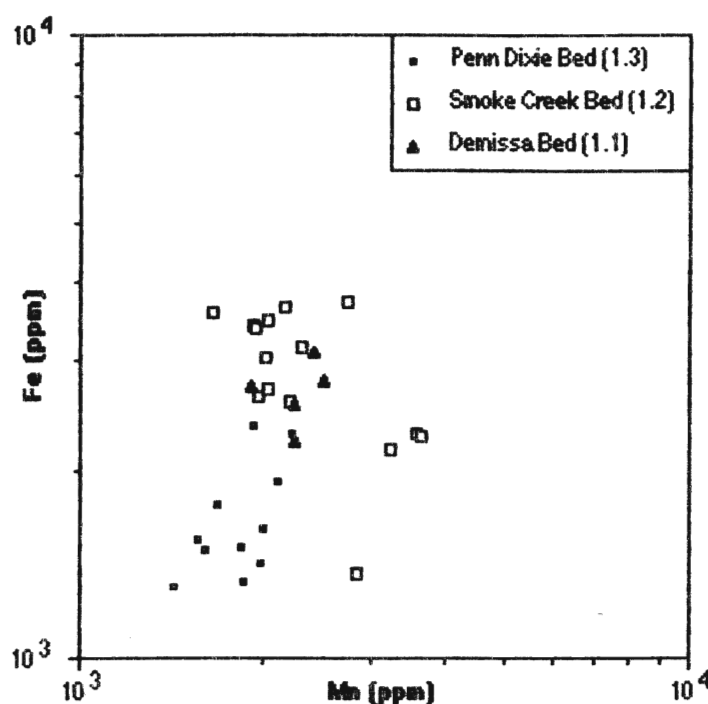


Figure 66: Stratigraphic variation in iron and manganese concentrations in *Phacops rana* from Bayview, N. Y. Specimens from the Penn Dixie Bed were found to be partially silicified in XRD analysis (Appendix Y), and pyritized in SEM examination (Fig. 58), and therefore are considered the most altered of this suite.

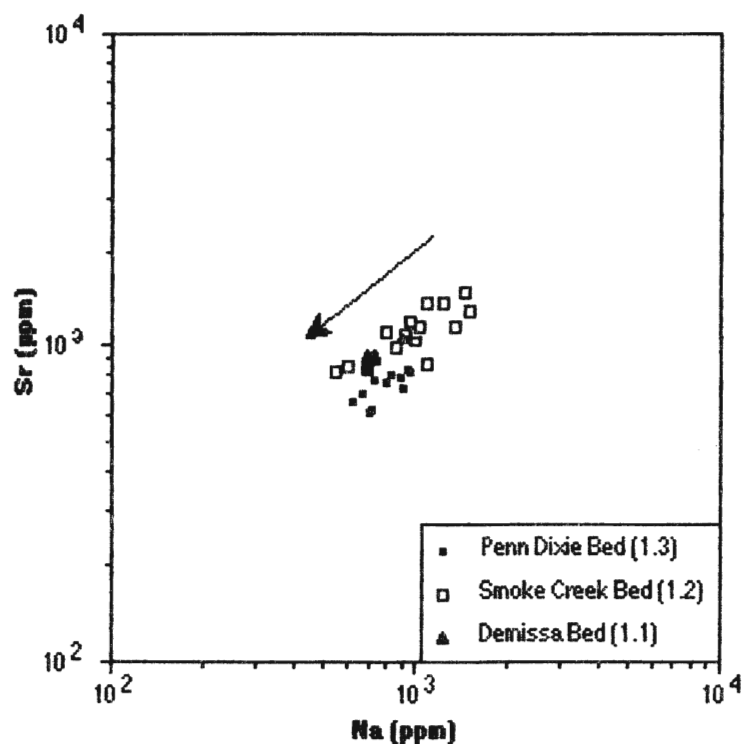


Figure 67: Stratigraphic variation in alteration is illustrated by *Phacops rana* having different levels of the diagenetically controlled elements strontium and sodium. The Penn Dixie Bed possesses the lowest concentrations of the beds at Bayview, N. Y., confirming observations made in Figure 66.

Dixie Bed, the Smoke Creek Bed was found to have statistically higher concentrations of strontium (t-test 5.596, $p < 0.05$, $f = 24$; Appendix IV) and sodium (t-test -2.251, $p < 0.05$, $f = 24$; Appendix IV) (Fig. 66), which suggests greater alteration of the Penn Dixie Bed than the underlying strata. The presence of abundant pyritized brachiopods (Brett, 1974b) and trilobites (Fig. 58), and XRD analysis (Appendix V) showing partial silicification of some trilobite specimens, serve to confirm this hypothesis.

Altered trilobites, and brachiopods (Brand and Veizer, 1980), generally show a decrease in magnesium and the ratio of strontium to calcium with diagenesis. Trilobite specimens from the lower shale of the Widder Formation, for example, possessed much lower concentrations of strontium (Fig. 61), magnesium, and strontium/calcium ratios (Fig. 68), than other specimens from shale units, and have previously been described as physically altered (Wright and Wright, 1961). Conversely, high concentrations of magnesium in cuticular material does not necessarily mean that the material is in a pristine state. For example, samples from the Edgecliff Member, Onondaga Formation, are considered microstructurally (McAllister and Brand, 1989) and geochemically altered, due to low strontium and sodium concentrations (Fig. 61). The high magnesium concentrations (Fig. 69) in this case reflect the partial dolomitization of the cuticular calcite, a process not limited to limestone facies. Trilobites from the Kashong shale are most likely dolomitized due to low strontium/calcium ratios (Figs. 60, and 68) with high concentrations of magnesium (Figs. 68, and 69). Pristine cuticular calcite should therefore have high strontium and sodium concentrations, with a high magnesium concentration and Sr/Ca ratio apparently being secondary consideration in some shale and limestone facies.

Strontium and sodium have been proven effective as sensitive indicators of diagenesis (Brand and Veizer, 1980). Unfortunately, these elements are not useful in determining all types of alteration. Silicification of trilobite cuticle can not be detected through trace elements, largely due to the recalculation back to a 100 % calcium

carbonate composition for the fossil. Representing the material that failed to dissolve, insoluble residue proves useful in detecting silicification. For example, the Deep Run and Jaycox shales yield specimens that can not be determined from strontium, sodium and magnesium concentrations to be highly altered (Figs. 61, and 68). High insoluble residues for specimens from these units (Appendix IV) suggest silicification, and this was confirmed by XRD analysis of the cuticular powders (Appendix V). Although insoluble residue may be indicative of other procedural errors (i. e. inclusion of matrix), high I. R.'s in trilobites should warrant further XRD examination.

Ordovician Trilobites

Unlike the Devonian specimens of this study, the majority of Ordovician trilobites were obtained from limestone facies (Figs. 5, 70, and 71). This has had the effect of weighing the Ordovician data in favour of limestone diagenesis, where preservation potential is low. This has proven beneficial to the present study as it allows examination of limestone diagenesis in trilobites and perhaps more definite determinations of pristine trilobites from this facies. Generally, in fossils obtained from limestone the ratio of strontium to calcium decreases while the manganese contents increase with progressive post-depositional alteration of metastable carbonate phases (Brand and Yeizer, 1980). This rationale of elemental re-distribution with diagenesis applies to the trilobite material from limestones (Fig. 71), where the most altered specimens from limestones have the lowest strontium/calcium ratios and the highest manganese contents, whereas unaltered and slightly altered samples contain less than 200 ppm manganese and have strontium/calcium ratios greater than 1.5.

Alteration of trilobites obtained from limestone varied stratigraphically, and was indicated by significantly lower concentrations of sodium, strontium and magnesium, and increases in manganese (Figs. 72, 73), all of which are diagenetic indicators in this facies. *Isotelus* from the Yerulam Formation at Ogden Point (loc. 9.1) were observed to

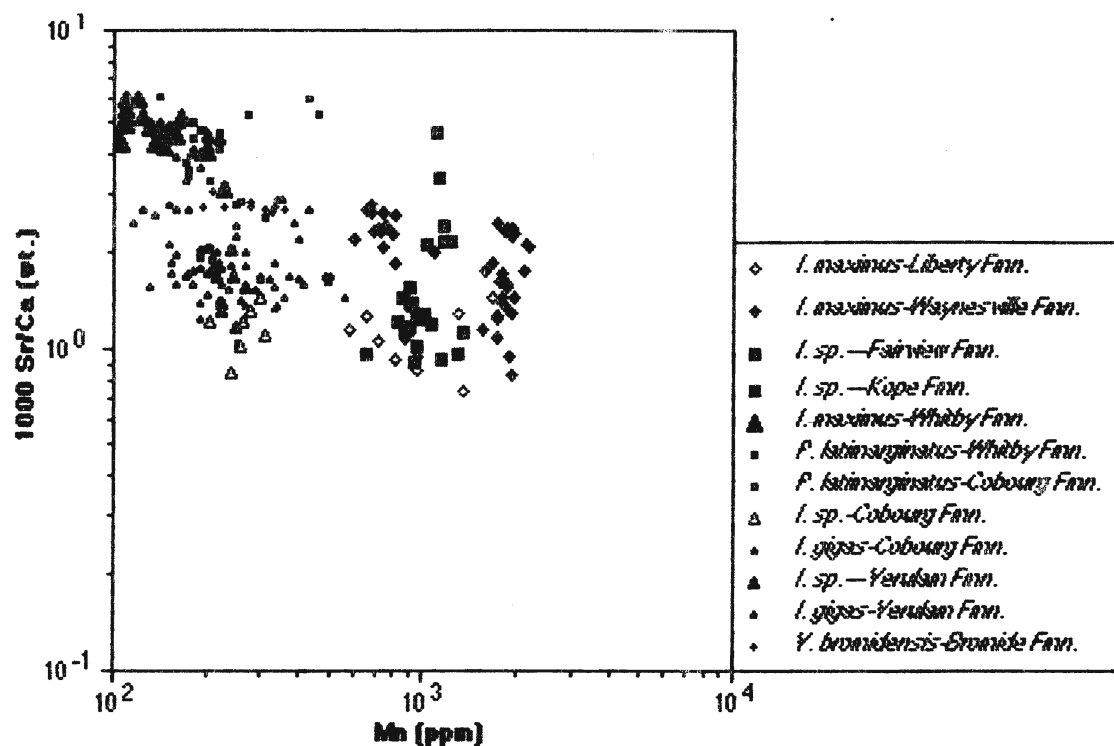


Figure 70: Scatter diagram of 1000 strontium/calcium ratios versus manganese concentrations in all Ordovician trilobites examined.

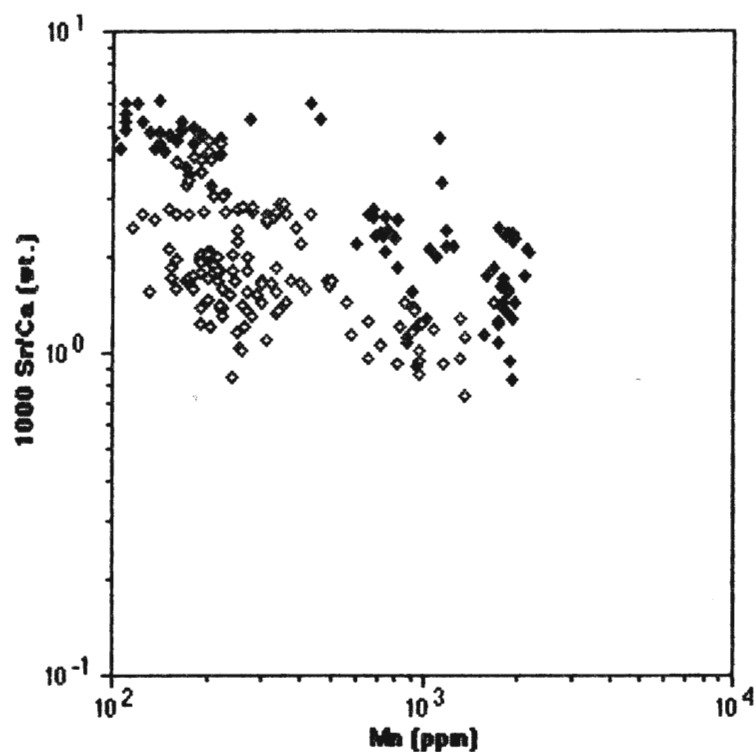


Figure 71: The influence of facies on Ordovician trilobite geochemistry is shown. Note the separation of strontium/calcium and manganese concentrations of trilobites from shale (solid symbols) and limestone (open symbols) facies.

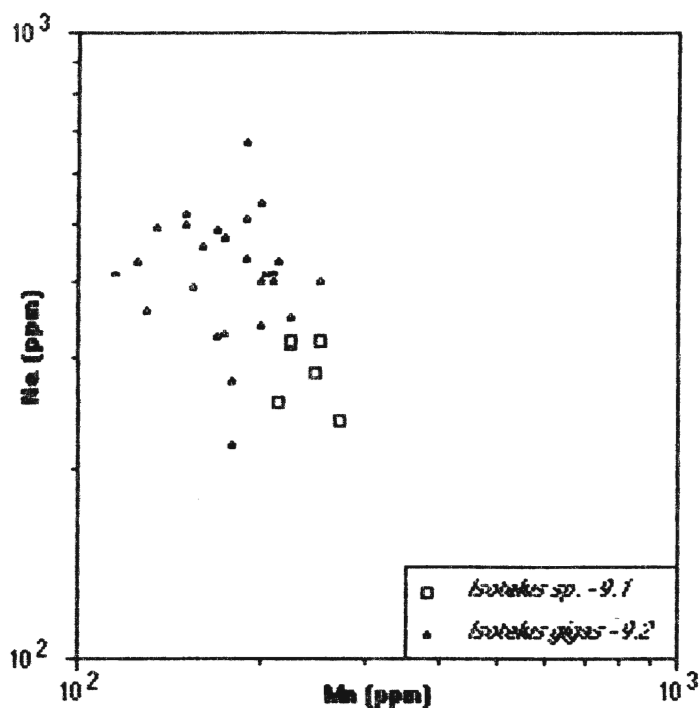


Figure 72: Stratigraphical variations in trilobite chemistry may be indicated by differences in manganese and sodium. Levels of sodium, as a diagenetic indicator, in *Isotelus* from the Yerulam Formation (9.1) are significantly lower (t-test -3.601, $p < 0.005$, $f=32$) than levels in *Isotelus* from the overlying Cobourg Formation (9.2), and suggest greater alteration in the Yerulam Formation.

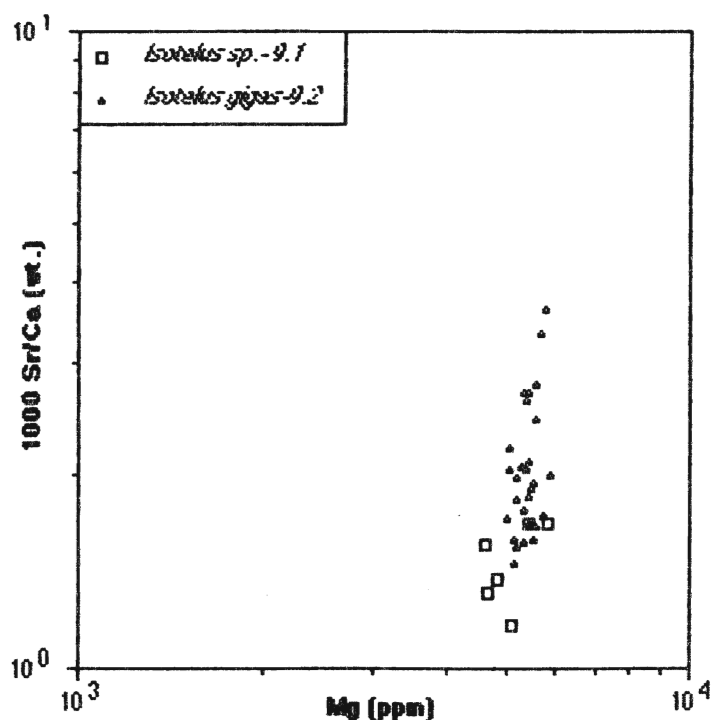
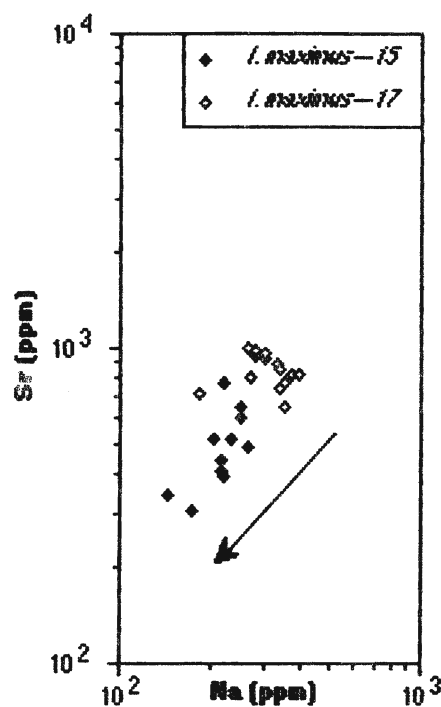


Figure 73: Stratigraphically differences in magnesium and strontium/calcium ratios in *Isotelus* from the Yerulam (9.1) and Cobourg (9.2) Formations.

have significantly lower concentrations of strontium (t-test -3.783, $p < 0.05$, $f = 32$; Appendix IV), sodium (t-test -3.601, $p < 0.05$, $f = 32$; Appendix IV), and magnesium (t-test -2.487, $p < 0.05$, $f = 32$; Appendix IV), and significantly higher concentrations of manganese (t-test 4.228, $p < 0.05$, $f = 32$; Appendix IV) than *Isotelus* from the Cobourg Formation. This suggests that at this locality specimens from the Verulam Formation are more altered than those of the overlying Cobourg Formation.

Geographically lateral variation in trilobite geochemistry was found in specimens of *Isotelus maximus* from the equivalent Trilobite Shale and *Treptoceras duseri* beds of the Waynesville Formation (Frey, 1987). Compared to Frey's (1987) *Treptoceras* Bed (loc. 15), significantly higher concentrations of the diagenetically controlled elements strontium (t-test -7.328, $p < 0.05$, $f = 23$; Appendix IV) and sodium (t-test -5.017, $p < 0.05$, $f = 23$; Appendix IV) (Fig. 74) in *Isotelus* from the Trilobite Shale (loc. 17) suggest less alteration in the latter's trilobites. An examination of the iron and manganese concentrations in *Isotelus* from these localities (see Appendix IV), suggests that the alteration fluid in the *Treptoceras* Bed was enriched in these elements, relative to that in the Trilobite Shale (Fig. 75). The trilobites from both units possess chemistries that are low in magnesium, strontium and sodium, relative to other specimens of *Isotelus* and are therefore considered geochemically altered.

Evidence for the resistance of cuticles to alteration may be found in a comparison of two *Isotelina* genera, *Isotelina bromidensis* from the 'Pooleville Member, Bromide Formation and *Isotelus gigas* from the Lower Verulam Formation. Analysis of the matrix revealed concentrations of iron (11 965 ppm) and magnesium (79 273 ppm) in the range of ferroan dolomite in the Bromide, and much lower concentrations in the Lower Verulam (890 ppm iron; 4060 ppm magnesium). The levels of these metals in the cuticular calcite of the trilobites were far lower than in the matrix, and concentrations of iron in the cuticles of *Isotelina* specimens were found to be significantly higher (t-test 12.703, $p < 0.05$, $f = 21$; Appendix IV) than that in *Isotelus* (Fig. 76), although they were reasonable for trilobites.



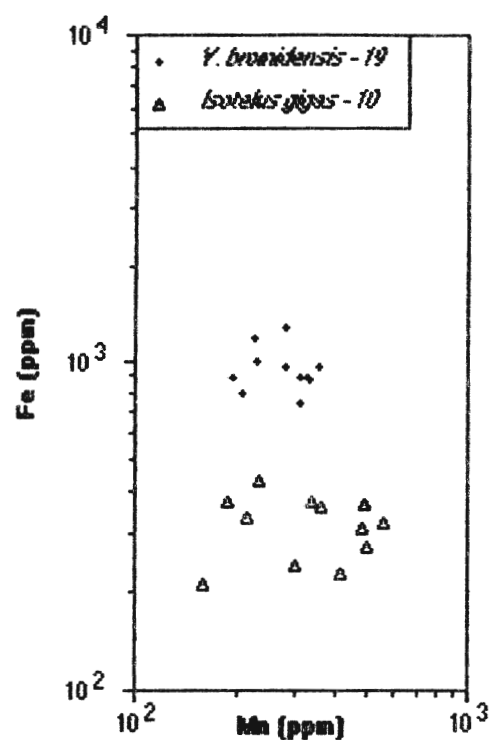


Figure 76: Scatter diagram of iron and manganese concentrations in specimens of *Yogdesia bromidensis* from the Bromide Formation (loc. 19), and *Isotelus gigas* from the Yerulam Formation (loc. 10).

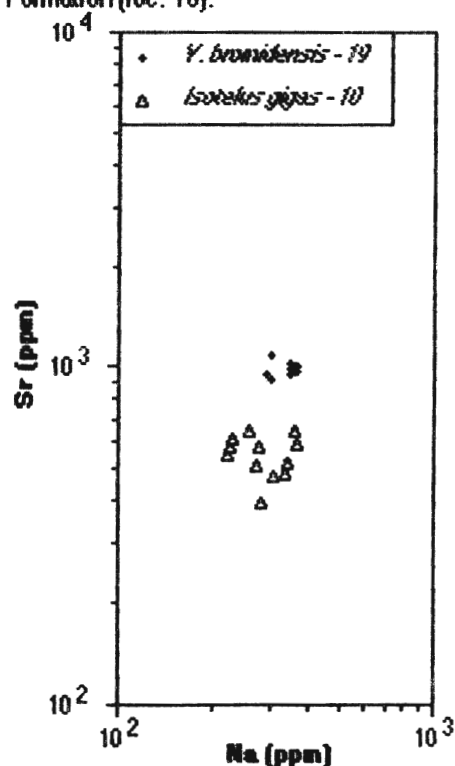


Figure 77: *Yogdesia* appears to be less altered than *Isotelus* due to significantly higher strontium (t-test 17.213, $p < 0.005$, $f=21$) and sodium (t-test 2.907, $p < 0.05$, $f=21$) concentrations.

The sodium values for both trilobites are far below what is consistent with pristine preservation. Microstructurally (Figs. 46 and 47) and geochemically (Fig. 77), *Magdalenia* was found to be less altered than *Aspidulus* and it can therefore be concluded that alteration of the cuticular calcite is occasionally independent of the alteration of the surrounding matrix.

Facies influence on trilobite cuticle geochemistries has to be considered while evaluating diagenetic effects on elemental re-distributions (Veizer, 1977; Brand, 1988). As demonstrated in this study, chemical trends in specimens from shales are more difficult to interpret due to high amounts of manganese in the depositional sediment, and the variation of this element with diagenetic alteration. This may be further complicated by the possibility that trilobites, similar to Recent arthropods, took up metals such as iron and manganese into their cuticles from the sediment. Variations in amounts of the metal in the sediment could result in a corresponding deviation in the concentration of metal in the pristine cuticular calcite of the trilobite (cf. Rainbow, 1988). Therefore, differences in cuticular pristine manganese concentrations between localities may represent localized conditions of the sediments. For this reason the preservation of trilobites from shales should not be evaluated solely by the level of manganese or other metal in their cuticular calcite, because this is likely influenced by the depositional environment/sediment. An example of this sediment influence, is most likely in trilobites from the brachiopodal pavement and black shale of the Whitby Formation (Maysvillian). It has been suggested that the brachiopodal pavement was formed from shale due to winnowing by storms (Westrop, pers. comm., 1989). Judging by the condition of the *Aspidulus* specimens, it is most likely that the brachiopods and trilobites were encased in the same sediment before winnowing occurred, because specimens migrating into the sediment after winnowing would not have been fragmented. Microstructurally pristine specimens of *Pseudogygites latimarginatus* obtained from the black shale facies (Fig. 6, loc. 6.1) possess significantly greater concentrations of manganese (t-test 3.771, $p < 0.05$, $f = 31$;

Appendix IV) and iron (t-test 3.29, $p < 0.05$, $f = 31$; Appendix IV) than the pristine specimens of *Isotelus maximus* obtained from the brachiopodal pavement (Fig. 6, loc. 6.2) (Fig. 78). If alteration was to be based solely upon the manganese concentration, pristine *Isotelus* would be found to be more geochemically altered than *Pseudogygites*. However, the diagenetically controlled elements strontium and sodium, which are not directly facies influenced, show all specimens from the Whitby Formation to possess similar preservations (Fig. 79), and are the least altered of the Ordovician trilobites (Fig. 80). The black shale matrix, in support of Rainbow's (1988) observations in Recent arthropods, possesses manganese concentrations of 890 ppm and iron concentrations of 4505 ppm, far higher than that found in the trilobite cuticular calcite (means of 223 ppm manganese, 965 ppm iron). The brachiopodal pavement matrix similarly possesses higher metal levels than was observed in the cuticular calcite, however the concentrations in this matrix are much lower than those in the black shale. It is therefore unlikely that the brachiopodal pavement was derived from the black shale sediment. Thus, it is possible that the elevated concentrations of manganese in the microstructurally and geochemically pristine specimens from the Whitby Formation reflect elevated metal concentrations in the surrounding sediment/environment at the time of cuticle formation. However, since *Isotelus* and *Pseudogygites* do not co-occur in the black shale or brachiopodal pavement, there is a possibility that differences in metal concentrations in *Isotelus* and *Pseudogygites* are taxonomic rather than environmental. Until co-occurring pristine specimens of *Isotelus* and *Pseudogygites* are found and analysed with matrix, no definite conclusion to this question can be drawn.

MINERALOGY

Few researchers have examined the composition of trilobite cuticular calcite in detail. Using X-ray diffraction (XRD), Stehli (1956) examined one trilobite pygidium from the Middle Pennsylvanian Boggy Formation of Oklahoma, and supported Bøggild's

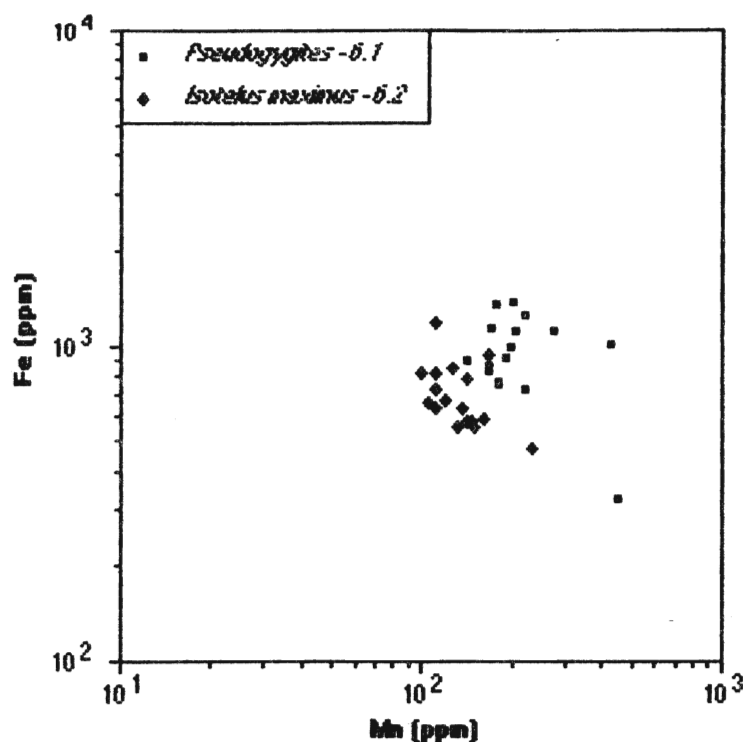


Figure 78: Possible original habitat differences are illustrated by significantly higher concentrations of iron (t-test 3.29, $p < 0.005$, $f=31$) and manganese (3.771, $p < 0.005$, $f=31$) in *Pseudogygites* compared to *Isotelus* from the Whitby Formation.

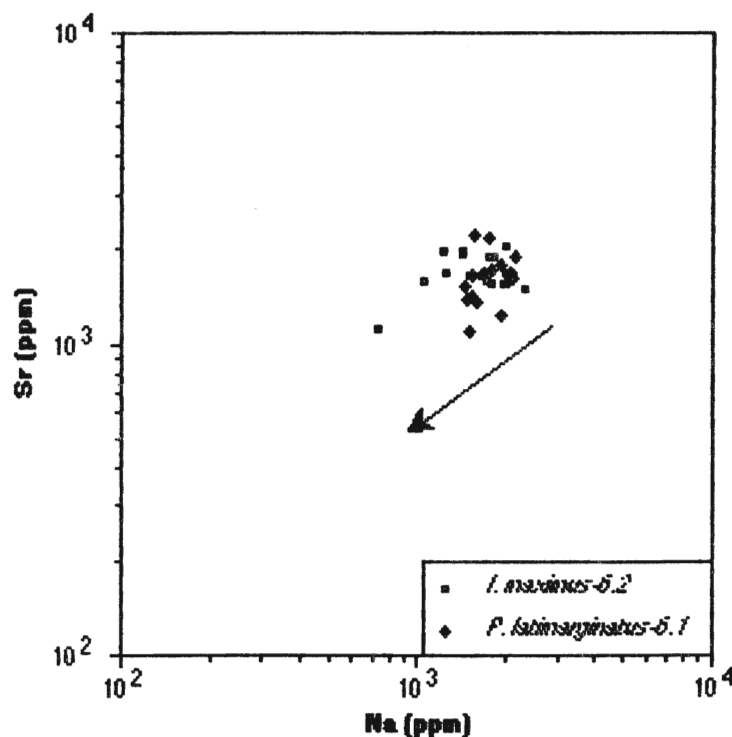


Figure 79: Similar concentrations of strontium and sodium in the trilobites *Isotelus* and *Pseudogygites* indicates the same degree of preservation. Arrow indicates the direction of alteration, to lower concentrations of sodium and strontium.

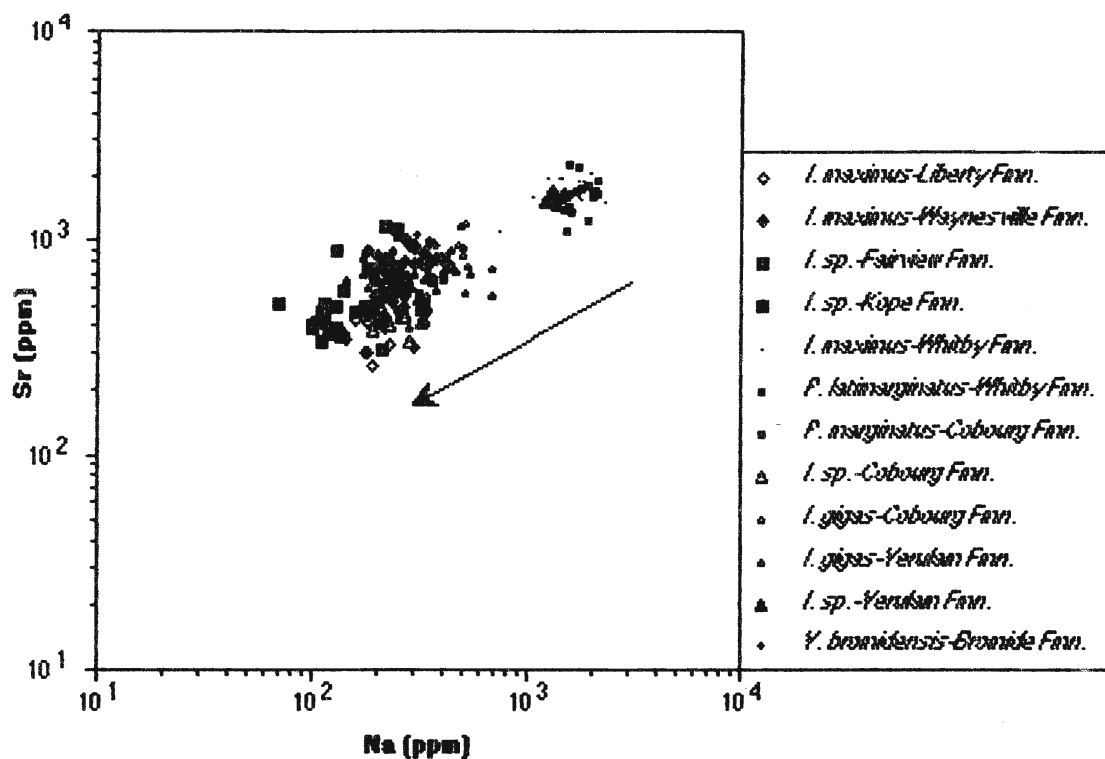


Figure 80: Loss of strontium and sodium in Ordovician trilobites. Arrow indicates direction of alteration.

(1930 in Stehli, 1956) suggestion of a calcitic trilobite cuticle. Lowenstam (1963) suggested a cuticular MgCO_3 composition of 2–14 mole% for Proetid trilobites (Lower Pennsylvanian). He noted that the data base was too limited to enable comment on the original mineralogy of other groups of arthropods and trilobites. Dalingwater (1973) and Towe (1973) also inferred an original calcite mineralogy for trilobite cuticles, whereas Richter and Füchtbauer (1978) suggested an original high magnesian calcite composition for trilobites because of their alteration to ferroan calcite. Kanip (1986) examined the elemental composition of ten trilobite fragments from the Kashong Shale of the Middle Devonian Hamilton Group and concluded that trilobite cuticles were originally low-Mg calcite.

The use of XRD examination (Appendix V) was limited by the resolution of the equipment. Although confirming the presence of calcite in cuticular powders, the amount of magnesium carbonate was not discernible, and therefore XRD data will not be considered further.

The present study has found that alteration of specimens can be determined by low strontium and sodium concentrations, and removal of altered specimens based on microstructural and geochemical considerations, yields essentially pristine specimens. Determination of mineralogies from these screened specimens indicates that the Devonian trilobite *Phacops rana* in shale possessed a pristine composition of between 5 000 and 7 000 ppm magnesium (1.73 – 2.43 mole % MgCO_3), and both Ordovician trilobites *Isotelus maximus* and *Pseudogygites latimarginatus*, also in shale, possessed magnesium values of 8000 to 9500 ppm (2.77 – 3.30 mole % MgCO_3) (Fig. 81). Since these trilobites are considered microstructurally and geochemically pristine, it is apparent that variable mineralogies for trilobites occurred in the Paleozoic. A possible hypothesis for this may be suggested by observations made of Recent arthropod reactions to salinity changes, and/or taxonomic influences on the secretion of magnesium calcite (see Chapter 3). In Recent marine arthropods, an increase in the

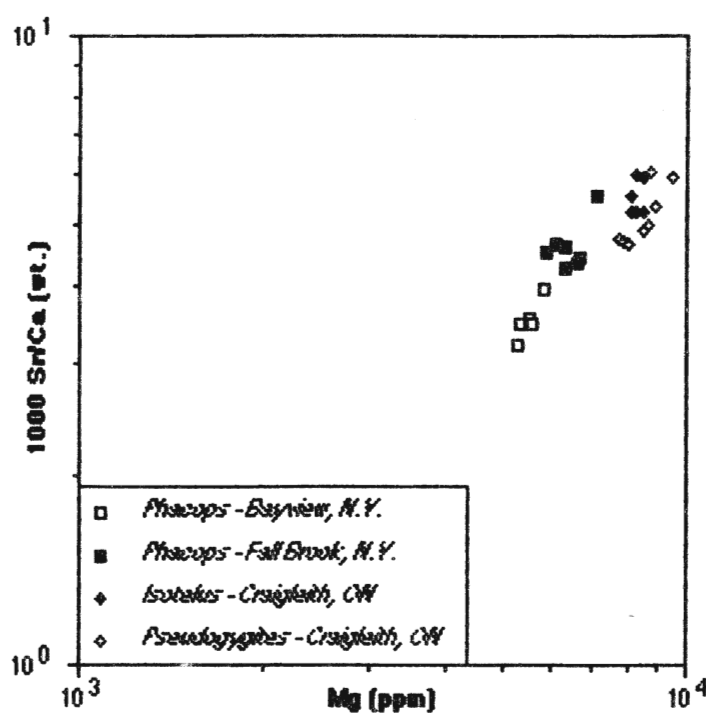


Figure 81: Geochemically and microstructurally pristine trilobites. Note separation of Devonian (*Phacops*) and Ordovician (*Isotelus* and *Pseudogygites*) trilobites.

cuticular magnesium concentration is the reaction to increased salinity. Assuming no taxonomic influence, it is possible that *Phacops* inhabited less saline waters than that by *Isotelus* and *Pseudopygites*. Further study of this possibility, and these trilobites is obviously required to prove or disprove this hypothesis.

STABLE ISOTOPES

The use of isotopes in the analysis of fossil material has proven beneficial in determining the fluids responsible for alteration, and in the case of pristine material, may yield paleoenvironmental information.

Diagenetic Evaluation

A suite of specimens was chosen for $\delta^{18}\text{O}$ and $\delta^{13}\text{C}$ analysis, to provide the greatest variety in preservation of the trilobite calcite and a good balance of samples from the different time periods (Figs. 82 and 83). There is only a slight difference in isotope values between the Ordovician specimens of *Isotelus* from the Whitby, Cobourg and Verulam Formations ($\Delta^{18}\text{O} = 1.03\text{ ‰}$; $\Delta^{13}\text{C} = 0.46\text{ ‰}$) (Fig. 82). This difference between the two populations may be a reflection of the secular variation of seawater composition and/or temperature (e.g. Knauth and Epstein, 1976; Brand, 1989). This conclusion, based on stable isotope values, is in agreement with their overall preservation as indicated by trace element analysis (Fig. 80). Overall, the slightly altered specimens from limestone (Cobourg and Verulam Formations) show a minimal increase in oxygen from the pristine specimens in shale (Whitby Formation). Carbon in specimens from the Cobourg Formation do not appear to be different from those from pristine specimens of the Whitby Formation, although specimens from the Verulam Formation are marginally higher (Fig. 82). This suggests that alteration of specimens from the Verulam Formation probably took place in the presence of marine-dominated

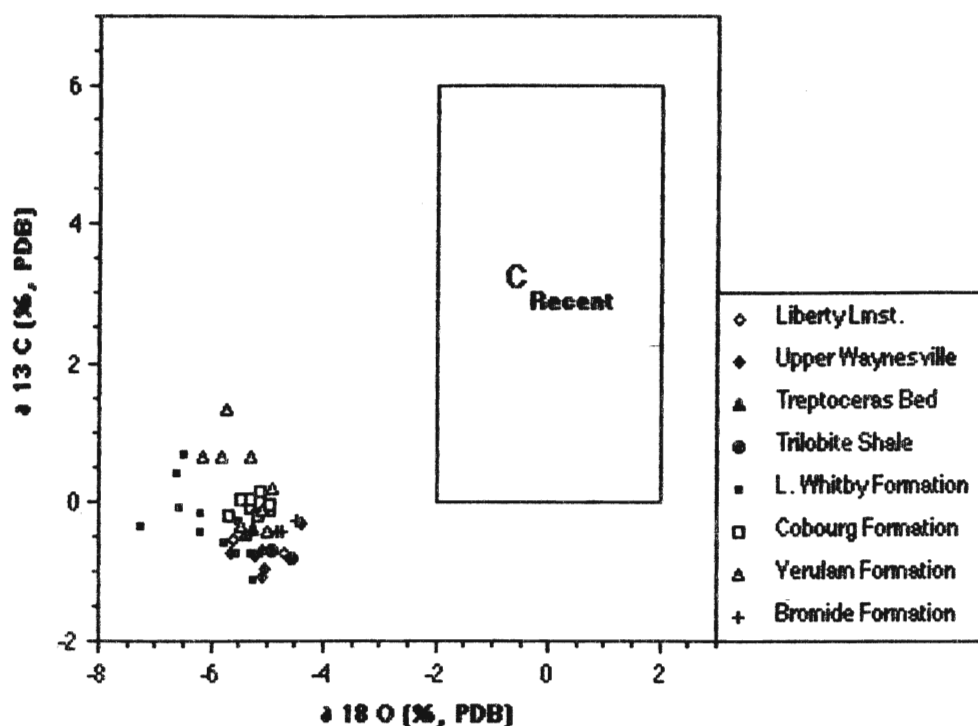


Figure 82: Carbon and oxygen isotopes in Ordovician trilobites. Defined field represents calcite precipitated in isotopic equilibrium with normal marine waters (Lowenstam, 1961; Brand, 1989).

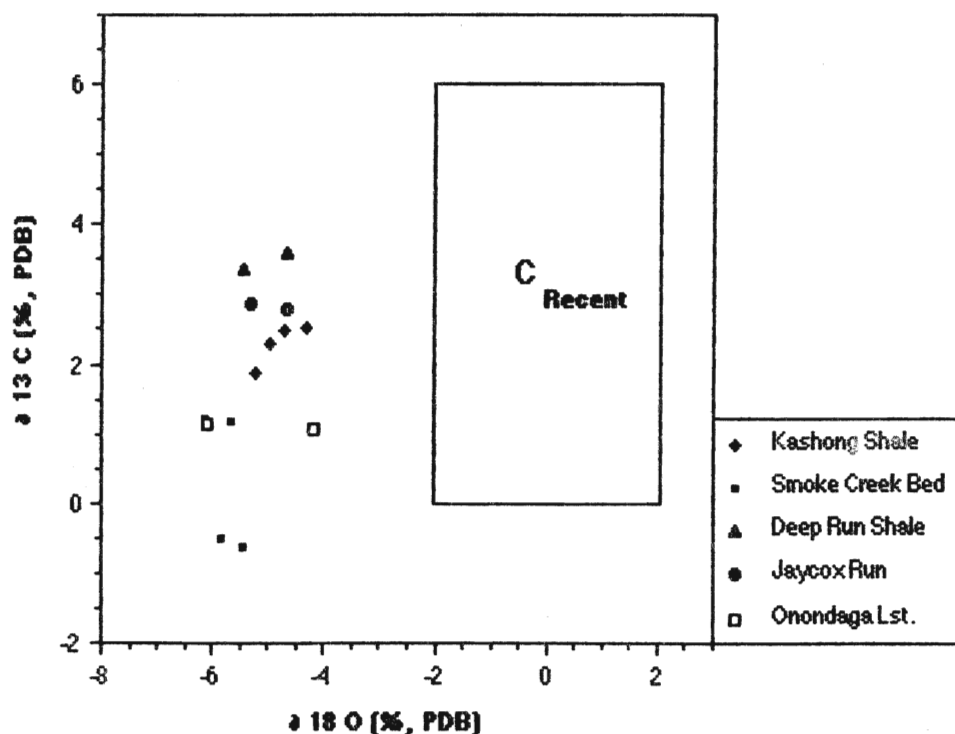


Figure 83: Carbon and oxygen isotopes in *Phacops* from the Devonian of New York State and Ontario. Defined field represents calcite precipitated in isotopic equilibrium with normal marine waters (Lowenstam, 1961; Brand, 1989).

mixed waters, while those of the Whitby and Cobourg Formation were subject to meteoric-dominated mixed waters.

Similar to the Ordovician samples, there is only a slight difference between Devonian trilobites from shales and limestones for carbon but not for oxygen (Fig. 83). The specimens from the Onondaga limestone with their textural and trace element features are indicative of extensive alteration (McAllister and Brand, 1989). The overall shift to slightly heavier carbon and oxygen values and the concomitant partial dolomitization of the matrix implies that waters of mixed origin were probably responsible for the observed diagenetic features and elemental as well as isotopic trends (e.g., Pingitore, 1976; Brand and Yeizer, 1980; Brand, 1989). Specimens of *Phacops rana* from the Moscow Formation (Deep Run Shale, Smoke Creek Bed, and Kashong Shale) illustrate a variety of preservations, and stable isotopic compositions. *Phacops* from the Smoke Creek Bed has been found to less altered than other Devonian trilobites. Altered specimens are characterized by lower strontium and sodium contents, as well as lighter $\delta^{13}\text{C}$ values (Figs. 61, and 83). It is postulated that alteration of the specimens from the Kashong and Deep Run shales occurred in the presence of marine-dominated mixed waters.

The average $\delta^{18}\text{O}$ values for the well-preserved Ordovician (-5.6 ‰, PDB) and Devonian (-5.5 ‰, PDB) trilobites are similar to those obtained from contemporaneous brachiopods (Popp *et al.*, 1986; Yeizer *et al.*, 1986; Brand, 1989). Several factors such as either extremely warm temperatures, dilution by isotopically-light water, and/or the secular variation of seawater may be responsible for the light values observed in the trilobite calcite. However, the shortage of data at this time limits the discussion on these different factors, and more data is obviously needed to address this question conclusively.

Chapter 5

Summary and Conclusions

The use of Recent arthropods in microstructural and geochemical investigations of trilobites has proven successful in many facets of this study, and problematic in others. Recent arthropods provide much needed data on the identification, origin and function of pristine microstructures in trilobites. Due to observations made in Recent arthropods, the dendritic microstructure, originally thought to be a diagenetic indicator, may in fact be suggestive of the delicate nature of diagenesis in trilobites. Microstructures, such as setae and tegumental gland duct openings, in like sized *Limulus* and Isotelina trilobites may indicate common ancestral origins for these organisms, or simply parallel cuticle evolutions. Due to a paucity of calcification in *Limulus*, a geochemical comparison was impossible. This in itself may indicate parallel evolution, and data to resolve this issue are urgently required.

Contrary to thin section observations made by Teigler and Towe (1975) and Towe (pers. comm., 1987), SEM examination of cuticle fragments of trilobites from the same unit/locality failed to detect the presence of a single laminae. Assuming no preparations errors, it is concluded that there is some inherent feature of SEM examination which may not allow detection of some features that are visible in thin sections, while features such as the dendritic microstructure are apparently visible only under SEM. Geochemical data from *Phacops* from Teigler and Towe's (1975) locality indicates that 1) not all trilobites have the same microstructural and geochemical preservation, and 2) that variations between trilobites are controlled by diagenetic rather than genetic factors, observations that dispute Teigler and Towe's (1975) findings.

The region of the cuticle sampled for examination is also a major influence in detecting pristine microstructures, as not all areas of trilobite and Recent arthropod cuticles will have microstructures identifiable in a SEM study. For example, the cephalons of trilobites are the most ideal area to examine because this is where setae were most abundant. Subtleties in the process of alteration, however, may leave pristine microstructures in cuticles that are partially silicified or dolomitized, and degree and type

of alteration may vary stratigraphically and longitudinally within a unit. It is therefore imperative that alteration be determined by both microstructural and geochemical analysis.

Environmental and sediment influences on Recent arthropod cuticle calcite can be documented, and comparisons made with extraneous chemistries in trilobites, eventually indicating possible environmental influences in pristine trilobite material. Natural processes in Recent arthropods, such as molting, also lead to variations in cuticle chemistries, apparently resulting in enrichment of the exuvia in some elements (iron, manganese and strontium), and a depletion in others (sodium). Variations are thought to reflect the area of concentration of the elements during calcification, and their subsequent reabsorption (or lack thereof) during ecdysis. Subsequent exposure to weathering was found to lead to leaching of mobile elements, such as sodium, from the cuticle. Environmental conditions, such as the salinity of water and metal content of the surrounding life medium, have been found to affect the composition of the cuticular calcite. Variable salinity produces distinctive results, specifically a lower salinity producing lower magnesium and higher calcium values. Therefore, observed differences in cuticular chemistries between individuals of the same taxon, such as *Hemigrapsus* or *Orconectes*, likely reflect salinity. Differences in magnesium between species, however, may be related to biological processes controlled by the individual organism, suggesting that all chemistry is uniform within a taxon and all variation is therefore intertaxic. This process remains to be fully understood.

The nature of the life habitat may be reflected in cuticular iron and manganese concentrations of Recent arthropods, and therefore would be applicable to pristine trilobites. Metal variations in pristine Ordovician trilobite cuticle appears to follow the constraints outlined for Recent arthropods, of regulation due to the chemistry of the surrounding medium (Rainbow, 1988). Variation of manganese concentration stratigraphically in pristine trilobites at Craigleith, necessitates caution in the use of this

element in determining diagenesis. Experimental studies into the responses of Recent taxa to variable environmental chemistries, and further study of pristine trilobites, is required to fully understand the processes responsible for metal variations.

In diagenetic analysis, sodium, strontium and magnesium proved most beneficial in determining altered trilobites. This follows observations made of high concentrations of these elements in Recent arthropods. Using this criterion, Ordovician specimens from shale generally showed the least amount of alteration (Fig. 80 and 81), with the majority of specimens from the Lower Whitby Formation being considered both geochemically and microstructurally pristine. Facies influence can therefore be considered to be the primary factor in cuticle preservation at the microstructural and geochemical level. Removing altered specimens from the data set gives a better indication of original mineralogy, with mineralogies of 1.7 — 2.4 mole % MgCO_3 (8000 to 9500 ppm magnesium; Fig. 81) for both *Isotelus maximus* and *Pseudogygites latimarginatus*, and 2.8 — 3.3 mole % MgCO_3 (5000 to 7000 ppm magnesium) for *Phacops*. This is slightly lower than the mineralogy of Recent marine arthropods (4.43 — 12.1 mole % MgCO_3), and slightly higher than that of fresh-water crayfish (0.96 — 1.82 mole % MgCO_3). Because of its metastable intermediate-magnesian calcite mineralogy, trilobite cuticle calcite is generally altered to low-magnesian calcite in the presence of meteoric or burial fluids. Stable isotope values and trends support the assertion that meteoric/burial fluids were responsible for the alteration observed in a number of the trilobite specimens. Pristine *Isotelus* and *Pseudogygites* from the Lower Whitby Formation possess $\delta^{18}\text{O}$ values of -7.3 — -5.31 ‰ PDB and -6.5 — -5.23 ‰ PDB respectively. These values are similar to those proposed by Brookfield (1988) to support his hypothesis of temperate rather than tropical Ordovician sea. However, application of the $\delta^{18}\text{O}$ values to formulas proposed by Brand (Lower Paleozoic waters to be corrected by -3.5 ‰ SMOW, pers. comm., 1988) yield paleotemperatures of 25 to 34 °C for *Isotelus* and 25 to 31 °C for *Pseudogygites*. These temperatures are much higher than would be expected in a

temperate sea. However, taking into consideration a less saline water (30 ‰ as apposed to 35.5 ‰) yields paleotemperatures of 18 to 27 °C and 17 to 23 °C for *Isotelus* and *Pseudogygites* respectively, which fall within the temperate realm. Since Recent arthropods have been excellent analogous organisms thus far, it is obvious that study into the isotopic composition of pristine trilobites and Recent arthropods should be persued, before further speculation into paleotemperatures from trilobites.

References

- Abele, L. G. 1982. Biogeography. // L. G. Abele, The Biology of the Crustacea Volume 1: Systematics, the Fossil Record, and Biogeography. Academic Press, New York, N. Y., pp. 241-304.
- Allison, P. A. 1986. Soft-bodied animals in the fossil record: The role of decay in fragmentation during transport. *Geology*, **14**, pp. 979-981.
- Allison, P. A. 1988a. Konservat-Lagerstätten: cause and classification. *Paleobiology*, **14** (4), pp. 331-344.
- Allison, P. A. 1988b. The role of anoxia in the decay and mineralization of proteinaceous macro-fossils. *Paleobiology*, **14** (2), pp. 139-154.
- Anstey, R. L., and Fowler, M. L. 1969. Lithostratigraphy and depositional environment of the Eden Shale (Ordovician) in the tri-state area of Indiana, Kentucky, and Ohio. *Journal of Geology*, **77**, pp. 668-682.
- Babcock, L. E. 1982. Original and diagenetic color patterns in two Phacopid trilobites from the Devonian of New York. Third North American Paleontological Convention, Proceedings vol. 1, pp. 17-22.
- Baird, G. C. 1979. Sedimentary relationships of Portland Point and associated Middle Devonian Rocks in central and western New York. New York State Museum Bulletin Number 433. 24 p.
- Barnes, C. R., Rexarod, C. B., and Miller, J. F. 1973. Lower Paleozoic conodont provincialism. Geological Society of America, Special Paper 141, pp. 157-190.
- Barnes, C. R., and Fahraeus, L. E. 1975. Provinces, communities, and the proposed nektobenthic habit of Ordovician conodontophorids. *Lethaia*, **8**, pp. 133-149.
- Barnes, C. R., Norford, B. S., and Skevington, D. 1981. The Ordovician System in Canada Correlation Chart and Explanatory Text. International Union of Geological Sciences, Pub. No. 8. 27 p.

- Bathurst, R. G. C. 1975. Carbonate Sediments And Their Diagenesis. Elsevier Science Publishers Inc., New York, N. Y. 658 p.
- Benton, A. G. 1935. Chitinovorous bacteria. *Journal of Bacteriology*, **29**, pp. 449-463.
- Bergström, J. 1975a. Functional morphology and evolution of xiphosurids. *Fossils and Strata*, **4**, pp. 291-305.
- Bergström, J. 1975b. Organization, life, and systematics of trilobites. *Fossils and Strata*, **4**, pp. 1-69.
- Bidwell, J. P., Paige, J. A., and Kuzirian, A. M. 1986. Effects of strontium on the embryonic development of *Aplysia californica*. *Biology Bulletin*, **170**, pp. 75-90.
- Brand, U. 1987a. Depositional analysis of the Breathitt Formation's marine horizons, Kentucky, U.S.A.: Trace elements and stable isotopes. *Chemical Geology (Isotope Geoscience Section)*, **65**, pp. 117-136.
- Brand, U., 1989. Biogeochemistry of Late Paleozoic North American brachiopods and secular variation of seawater composition. *Biogeochemistry*, **7**, pp. 159-193.
- Brand, U., Morrison, J. O., Brand, N. and Brand, E. 1986. Biogeochemical differentiation of the Cape Beale and Lucy Island marine invertebrates, British Columbia. Brock University Department of Geological Sciences, Research Report Series No. 27., Studies in Sedimentary Processes No. 3. pp. 14-40.
- Brand, U., Morrison, J. O., Brand, N. and Brand, E. 1987. Isotopic variation in the shells of Recent marine invertebrates from the Canadian Pacific Coast. *Chemical Geology (Isotope Geoscience Section)*, **65**, pp. 137-145.
- Brand, U. and Yeizer, J., 1980. Chemical diagenesis of a multicomponent carbonate system-1: Trace elements. *Journal of Sedimentary Petrology*, **50**, pp. 1219-1236.

- Brannon, A. C. and Rao, K. R. 1979. Barium, strontium and calcium levels in the exoskeleton, hepatopancreas and abdominal muscle of the grass shrimp *Palaemonetes pugio*: relation to molting and exposure to barite. *Comparative Biochemistry and Physiology*, **63 A**, pp. 261-274.
- Bray, R. G. 1972. The paleoecology of some Ludlowville brachiopod clusters (Middle Devonian), Erie County, New York. *International Geological Congress, 24th Session, Section 7*, pp. 66-73.
- Brett, C. E. 1974a. Contacts of the Windom Member (Moscow Formation) in Erie County, New York. // D. N. Peterson (editor) *New York State Geological Association 46th Annual Meeting, field trip guidebook*. pp. C1-C22.
- Brett, C. E. 1974b. Biostratigraphy and paleoecology of the Windom Shale Member (Moscow Formation) in Erie County, New York. // D. N. Peterson (editor) *New York State Geological Association 46th Annual Meeting, field trip guidebook*. pp. G1-G15.
- Brett, C. E. 1986. The Middle Devonian Hamilton of New York: An overview. // C. E. Brett, *Dynamic Stratigraphy and Depositional Environments of the Hamilton Group (Middle Devonian) in New York State, Part 1*. *New York State Museum Bulletin Number 457*, pp. 1-4.
- Brett, C. E. and Baird, G. C. 1981. Jaycox Run and Fall Brook, Genesee (Field trip guides). // *Devonian Biostratigraphy of New York Part 2, Subcommittee on Devonian Stratigraphy, July 1981*. pp. 28-34.
- Brett, C. E. and Baird, G. C. 1982. Upper Moscow-Genesee stratigraphic relationships in western New York: Evidence for regional erosive beveling in the Late Middle Devonian. // *Geology of the Northern Appalachian Basin Western New York, Edited by E. J. Buehler and P. E. Calkin*. *New York State Geological Association, 54th Annual Meeting, Buffalo, New York*. pp. 19-52.

- Brett, C. E., Speyer, S. E. and Baird, G. C. 1986. Storm-generated sedimentary units: tempestite proximity and event stratification in the Middle Devonian Hamilton Group of New York. // C. E. Brett, Dynamic Stratigraphy and Depositional Environments of the Hamilton Group (Middle Devonian) in New York State, Part 1. New York State Museum Bulletin Number 457, pp. 129-156.
- Brookfield, M. E. 1988. A mid-Ordovician temperate carbonate shelf — the Black River and Trenton Limestone Groups of southern Ontario, Canada. *Sedimentary Geology*, **60**, pp. 137-153.
- Brookfield, M. E. and Brett, C. E. 1988. Paleoenvironments of the Mid-Ordovician (Upper Caradocian) Trenton limestones of southern Ontario, Canada: Storm sedimentation on a shoal-basin shelf model. *Sedimentary Geology*, **57**, pp. 75-105.
- Broughton, J. G., Fisher, D. W., Isachsen, Y. W., and Rickard, L. V. 1973. Geology of New York: a short account. New York State Geological Survey Educational Leaflet No. 20.
- Brown, G. D., and Lineback, J. A. 1966. Lithostratigraphy of Cincinnati Series (Upper Ordovician) in southeastern Indiana. *Bulletin of the A. A. P. G.*, **50** (5), pp. 1018-1023.
- Buchardt, B. and Fritz, P. 1978. Strontium uptake in shell aragonite from the freshwater gastropod *Limnaea stagnalis*. *Science*, **199**, pp. 291-292.
- Campbell, L. L. and Williams, O. B. 1951. A study of chitin-decomposing microorganisms of marine origin. *Journal of General Microbiology*, **5**, pp. 894-905.
- Caster, K. E., Dalvé, E. A., and Pope, J. K. 1955. Elementary Guide to the Fossils and Strata of the Ordovician in the Vicinity of Cincinnati, Ohio. Cincinnati Mus. Nat. Hist., Cincinnati.
- Chlupáč, I. 1975. The distribution of phacopid trilobites in space and time. *Fossils and Strata*, no. 4, pp. 399-408.

- Copper, P. 1978. Paleoenvironments and paleocommunities in the Ordovician-Silurian sequence of Manitoulin Island. In *Geology of Manitoulin Island*. Edited by J. T. Sanford and R. E. Mosher. Michigan Basin Geological Society, Special Paper 3, pp. 47-61.
- Dalingwater, J. E. 1973. The cuticle of a eurypterid. *Lethaia*, **6**, pp. 179-186.
- Dalingwater, J. E. 1975a. Further observations on eurypterid cuticles. *Fossils and Strata*, **4**, pp. 271-279.
- Dalingwater, J. E. 1975b. Secondary microstructures in trilobite cuticles. *Fossils and Strata*, **4**, pp. 151-154.
- Dalingwater, J. E. and Miller, J. 1977. The laminae and cuticular organization of the trilobite *Asaphus raniceps*. *Palaeontology*, **20**, pp. 21-32.
- Dalla Via, G-J. 1987a. Effects of salinity and temperature on oxygen consumption in a freshwater population of *Palaemonetes antennarius* (crustacea, decapoda). *Comparative Biochemistry and Physiology*, **88 A**, pp. 229-305.
- Dalla Via, G-J. 1987b. Salinity responses in brackish water populations of the freshwater shrimp *Palaemonetes antennarius* — I. Oxygen consumption. *Comparative Biochemistry and Physiology*, **87 A**, pp. 471-478.
- Davenport, J. and Wong, T. M. 1987. Responses of adult mud crabs (*Scylla serrata*) (Forsk.) to salinity and low oxygen tension. *Comparative Biochemistry and Physiology*, **86 A**, pp. 43-47.
- Davis, R. A. (editor) 1981. *Cincinnati Fossils: An Elementary Guide to the Ordovician Rocks and Fossils of the Cincinnati, Ohio, Region*. Cincinnati Museum of Natural History, Cincinnati, Ohio. 58 p.
- Dendinger, J. E. and Alterman, A. 1983. Mechanical properties in relation to chemical constituents of postmolt cuticle of the Blue Crab, *Callinectes sapidus*. *Comparative Biochemistry and Physiology*, **75 A** (3), pp. 421-424.

- Dennell, R. 1960. Integument and exoskeleton. // T. H. Waterman, The Physiology of Crustacea, Volume I Metabolism and Growth. Academic Press, New York, N. Y., pp. 449-472.
- Driscoll, E. G., Hall, D. D., and Nussmann, D. G. 1965. Morphology, and paleoecology of the brachiopod *Leiorhynchus kelloggi* Hall, Middle Devonian, Ohio, Michigan, Ontario. Journal of Paleontology, **39** (5), pp. 916-933.
- Dunham, R. J. 1962. Classification of carbonate rocks according to depositional texture. // W. E. Ham (ed) Classification of Carbonate Rocks. A. A. P. G. Mem. No. 1, pp. 108-121.
- Eldredge, N. 1970. Observations on burrowing behaviour in *Limulus polyphemus* (Chelicerata, Merostomata), with implications on the functional anatomy of trilobites. American Museum Novitates, Num. 2436, pp. 1-17.
- Eldredge, N. 1974. Character displacement in evolutionary time. American Zoology, **14**, pp. 1083-1097.
- Engel, D. W. 1987. Metal regulation and molting in the Blue Crab, *Callinectes sapidus*. copper, zinc, and metallothionein. Biology Bulletin, **172**, pp. 69-82.
- Fay, R. O. 1969. Geology of the Arbuckle Mountains Along Interstate - 35. The Ardmore Geological Society, Ardmore, Oklahoma. 75 p.
- Fay, R. O., and Graffham, A. A. 1969. Bromide Formation on Tulip Creek and in the Arbuckle Mountains Region. // W. E. Ham, Regional Geology of the Arbuckle Mountains, Oklahoma. Oklahoma Geological Survey, Guidebook XVII. pp.37-39.
- Feldmann, R. M., and Tshudy, D. 1987. Ultrastructure in cuticle from *Hoploparia stokesi* (decapoda: nephropidae) from the Lopez de Bertodano Formation (Late Cretaceous-Paleocene) of Seymour Island, Antarctica. Journal of Paleontology, **61** (6), pp. 1194-1203.
- Florkin, M. 1960. Blood chemistry. // T. H. Waterman, The Physiology of Crustacea, Volume I Metabolism and Growth. Academic Press, New York. pp. 141-159.

- Ford, J. P. 1967. Cincinnati geology in southwest Hamilton County, Ohio. A. A. P. G. Bull., **51** (6), pp. 918-936.
- Frey, R. C. 1987. The paleoecology of a Late Ordovician shale unit from southwest Ohio and southeast Indiana. Journal of Paleontology, **61** (2), pp. 242-267.
- George, J. D. and George, J. J. 1979. Marine Life: An Illustrated Encyclopedia of Invertebrates in the Sea. John Wiley and Sons. 288 p.
- Goodwin, T. W. 1960. Biochemistry of pigments. // T. H. Waterman, The Physiology of Crustacea, Volume I Metabolism and Growth. Academic Press, New York. pp. 101-140.
- Gosner, K. L. 1978. A Field Guide To The Atlantic Seashore. The Peterson field guide series, Houghton Mifflin Co., Boston, Mass. 329 p.
- Gould, S. J. and Lewontin, R. C. 1979. The spandrels of San Marco and Panglossian paradigm: a critique of the adaptationist programme. Proceedings of the Royal Society of London, **B 205**, pp. 581-598.
- Greenaway, P. 1983. Uptake of calcium at the postmolt stage by the marine crabs *Callinectes sapidus* and *Carcinus maenas*. Comparative Biochemistry and Physiology, **75 A** (2), pp. 181-184.
- Halcrow, K. 1978. Modified pore canals in the cuticle of *Gammarus* (crustacea: amphipoda); a study by scanning and transmission electron microscopy. Tissue and Cell, **10** (4), pp. 659-670.
- Harbo, R. M. 1980. Tidepool and Reef: Marine life Guide to the Pacific Northwest Coast. Hancock House Publishers, Surrey, B. C. 57 p.
- Harland, W. B., Cox, A. Y., Llewellyn, Pickton, C. A. G., Smith, A. G., and Walters, R. 1982. A Geologic Time Scale. Cambridge University Press, Cambridge.

- Hay, H. 1977. Field trip no. 1, Cincinnati stratigraphy from Richmond to Aurora, Indiana. In J. K. Pope and W. D. Martin (editors), Field Guidebook to the Biostratigraphy and Paleoenvironments of the Cincinnati Series of Southeastern Indiana. S. E. P. M. 7th Annual Field Conference, Great Lakes Section. pp. 11-133.
- Huner, J. Y., Colvin, L. B. and Reid, B. L. 1979a. Postmolt mineralization of the exoskeleton of juvenile California Brown Shrimp, *Penaeus californiensis* (Decapoda: Penaeidae). Comparative Biochemistry and Physiology, **62 A**, pp. 889-893.
- Huner, J. Y., Colvin, L. B. and Reid, B. L. 1979b. Whole-body calcium, magnesium and phosphorous levels of the California Brown Shrimp, *Penaeus californiensis* (Decapod: Penaeidae) as functions of molt stage. Comparative Biochemistry and Physiology, **64 A**, pp. 33-36.
- Janssens, A. 1970. Middle Devonian Formations in the subsurface of northwestern Ohio. State of Ohio Department of Natural Resources Division of Geological Survey, Report of Investigations No. 78. 22 p.
- Johnson, D. E. 1932. Some observations on chitin-destroying bacteria. Journal of Bacteriology, **24**, pp. 335-340.
- Johnson, M. E., and Snook, H. J. 1967. Seashore Animals of the Pacific Coast. Dover Pub., New York. 659 p.
- Johnson, M. E. and Rong, J-Y. 1989. Middle to Late Ordovician rocky bottoms and rocky shores from the Manitoulin Island area, Ontario. Canadian Journal of Earth Sciences, **26** (4), pp. 642-653.
- Kanip, J. 1986. Fossil and facies geochemistry of the Middle Devonian Kashong Shale (Upper Hamilton Group), western New York. Unpublished B.Sc. thesis, Brock University, St. Catharines, Ontario. 71 pp.
- Kennaugh, J. 1965. Pore canals in the cuticle of *Hypoderma bovis* (Diptera). Nature (London), **207**, p. 205.

- Kinne, O. 1964. The effects of temperature and salinity on marine and brackish water animals: II. Salinity and temperature salinity combinations. *Oceanography and Marine Biology Annual Review*, **2**, pp. 281-339.
- Knauth, L. P., and Epstein, S. 1976. Hydrogen and oxygen isotope ratios in nodular and bedded cherts. *Geochimica et Cosmochimica Acta*, **40**, pp. 1095-1108.
- Laporte, L. F. 1971. Paleozoic carbonate facies of the central Appalachian shelf. *Journal of Sedimentary Petrology*, **41** (3), pp. 724-740.
- Liberty, B. A. 1967. Palaeozoic stratigraphy of the Kingston area, Ontario. In *Guidebook, Geology of Parts of Eastern Ontario and Western Quebec, Annual Meetings, Geological Association of Canada and Mineralogical Association of Canada, Kingston*. pp.167-182.
- Liberty, B. A. 1969. Paleozoic geology of the Lake Simcoe area, Ontario. *Geological Survey of Canada, Memoir 355*, 201 p.
- Lowenstam, H. 1961. Mineralogy, $^{18}\text{O}/^{16}\text{O}$ ratios and strontium and magnesium contents of Recent and fossil brachiopods and their bearing on the history of the oceans. *Journal of Geology*, **69**, pp. 241-260.
- Lowenstam, H., 1963. Biologic problems relating to the composition and diagenesis of sediments. *In: The Earth Sciences Problems and Progress in Current Research, edited by T. W. Donnelly*. University of Chicago Press. pp. 139-195.
- Marsaglia, K. M. and Klein, G. D. 1983. The paleogeography of Paleozoic and Mesozoic storm depositional systems. *Journal of Geology*, **91** (2), pp. 117-142.
- McAllister, J. E. 1987a. Trace element geochemistry of Ordovician and Devonian trilobite cuticles, Ontario and New York state. Unpublished B. Sc. thesis, Brock University, St. Catharines. 79 pp.

- McAllister, J. E., 1987b. Geochemistry of Lower Paleozoic trilobites: major implications for the paleoecology of marine invertebrates (Abstract). Canadian Paleontology and Biostratigraphy Seminar, Program with Abstracts. p. 5.
- McAllister, J. E. and Brand, U., 1987. Biogeochemistry of Lower Paleozoic trilobites from Ontario and New York: diagenetic and paleoenvironmental applications. Geol. Ass. Can. Joint Ann. Meeting, Program with Abstracts, **12**, p. 72.
- McAllister, J. E. and Brand, U. 1989. Primary and diagenetic microstructures in trilobites. *Lethaia*, **22**, pp. 101-111.
- McAllister, J. E. and Brand, U. (In press). Geochemistry of some Ordovician and Devonian trilobite cuticles from North America. *Chemical Geology*.
- Miller, J. 1975. Structure and function of trilobite terrace lines. *Fossils and Strata*, **4**, pp. 155-178.
- Miller, K. B., Brett, C. E., and Parsons, K. M. 1988. The paleoecologic significance of storm-generated disturbance within a Middle Devonian muddy epeiric sea. *Palaios*, **3**, pp. 35-52.
- Milliman, J. D. 1974. *Marine Carbonates*. Springer-Verlag, New York, N. Y. 375 p.
- Mitchell, S. W. 1967. Stratigraphy of the Silica Formation of Ohio and the Hungry Hollow Formation of Ontario, with paleogeographic interpretations. *Papers of the Michigan Academy of Science, Arts, and Letters*, **52**, pp. 175-196.
- Neville, A. C., and Berg, C. W. 1971. Cuticle ultrastructure of a Jurassic crustacean (*Eryma stricklandi*). *Palaeontology*, **14** (2), pp. 201-205.
- Neville, A. C., and Luke, B. M. 1969. Molecular architecture of adult locust cuticle at the electron microscope level. *Tissue and Cell*, **1** (2), pp. 355-366.
- Neville, A. C., Thomas, M. G., and Zelazny, B. 1969. Pore canal shape related to molecular architecture of arthropod cuticle. *Tissue and Cell*, **1** (1), pp. 183-200.

- Nussmann, D. G. 1975. Paleoecology and pyritization. // R. Y. Kesling and R. B. Chilman, *Strata and Megafossils of the Middle Devonian Silica Formation*. Museum of Paleontology Papers on Paleontology No. 8, Friends of The University of Michigan Museum of Paleontology, Inc. pp. 173-223.
- Osmólska, H. 1975. Fine morphological characters of some upper Palaeozoic trilobites. *Fossils and Strata*, **4**, pp. 201-207.
- Parkins, W. G. 1977. Onondaga Chert: Geological and Palynological Studies as Applied to Archaeology. Unpublished M. Sc. thesis, Brock University, St. Catharines, Ontario. 104 p.
- Passano, L. M. 1960. Molting and its control. // T. H. Waterman, *The Physiology of Crustacea, Volume I Metabolism and Growth*. Academic Press, New York. pp. 473-536.
- Pennak, R. W. 1953. *Fresh-Water Invertebrates of the United States*. The Ronald Press Co. 769 p.
- Pilkey, O. H. and Hower, J. 1960. The effect of environment on the concentration of skeletal magnesium and strontium in *Dendroaster*. *Journal of Geology*, **68**, pp. 203-214.
- Pingitore, N. E. 1976. Vadose and phreatic diagenesis: processes, products, and their recognition in corals. *Journal of Sedimentary Petrology*, **46**, pp. 985-1006.
- Plotnick, R. E. 1986. Taphonomy of a modern shrimp: Implications for the arthropod fossil record. *Palaos*, **1**, pp. 286-293.
- Popp, B. N. 1981. Coordinated textural, isotopic, and elemental analyses of constituents in some Middle Devonian limestones. M. Sc. thesis, University of Illinois, Urbana, Illinois, 105 p.
- Popp, B. N., Anderson, T. F., and Sanderberg, P. A. 1986. Brachiopods as indicators of original isotopic compositions in some Paleozoic limestones. *Geol. Soc. Am. Bulletin*, **97**, pp. 1262-1269.

- Price Sheets, W. C. and Dendinger, J. E. 1983. Calcium deposition into the cuticle of the Blue Crab, *Callinectes sapidus*, related to external salinity. *Comparative Biochemistry and Physiology*, **74 A** (4), pp. 903-907.
- Quackenbush, L. S. and Herrnkind, W. F. 1983. Regulation of the molt cycle of the spiny lobster, *Panulirus argus*: Effect of photoperiod. *Comparative Biochemistry and Physiology*, **76 A** (2), pp. 259-263.
- Rainbow, P. S. 1988. Trace metals in decapods. *In* A. A. Fincham and P. S. Rainbow, *Aspects of Decapod Crustacean Biology*, Symposia of the Zoological Society of London Number 59. Clarendon Press, Oxford England. pp.291-313.
- Reimann, I. G. 1940. A new restoration of *Terataspis*. Contributions by the Council of Scientific Societies of Western New York, first symposium. Bulletin of the Buffalo Society of Natural Science, **17** (3), pp.39-46.
- Richter, D. K. and Füchtbauer, H. 1978. Ferroan calcite replacement indicates former magnesian calcite skeletons. *Sedimentology*, **25**, pp. 843-860.
- Rickard, L. V. 1975. Correlation of the Silurian and Devonian rocks in New York State. New York State Museum and Science Service Map and Chart Series Number 24.
- Ricketts, E. F., and Calvin, J. 1962. *Between Pacific Tides*. Revised by J. W. Hedgpeth. Stanford University Press, Stanford, California. 516 p.
- Rolfe, W. D. I. 1962. The cuticle of some middle Silurian Ceratiocaridid Crustacea from Scotland. *Palaeontology*, **5**, pp. 30-51.
- Russell-Hunter, W. D. 1969. *A Biology of Lower Invertebrates*. The Macmillan Company Collier-Macmillan Limited, London. 224 p.
- Sabourin, T. D. 1984. The relationship between fluctuating salinity and oxygen delivery in adult blue crabs. *Comparative Biochemistry and Physiology*, **78 A**, pp. 109-118.

- Sanford, J. T. 1978. The stratigraphy of the Manitoulin Island area. // *Geology of the Manitoulin area. Edited by J. T. Sanford and R. E. Mosher. Michigan Basin Geological Society, Special Paper 3, pp. 3-28.*
- Scotese, C.R. and Denham, C.R. 1988. User's manual for Terra Mobilis: Plate tectonics for the Macintosh (Macintosh computer program). Earth in Motion Technologies, Houston, Texas, 43 p.
- Schramm, M. W. 1964. Paleogeologic and quantitative lithofacies analysis, Simpson Group, Oklahoma. *A. A. P. G. Bull.*, **48**, pp.1164-1195.
- Shaw, F. C. 1974. Simpson Group (Middle Ordovician) trilobites of Oklahoma. *Paleont. Soc., Mem. 6 (Journal of Paleontology, 48 (5) supp).* 54 p.
- Sheehan, P. M. 1973. The relation of Late Ordovician glaciation to the Ordovician-Silurian changeover in North American brachiopod faunas. *Lethaia*, **6**, pp. 147-154.
- Shumway, S. E. and Jones, M. B. 1981. Influence of salinity on the respiration of an estuarine mud crab, *Helice crassa* (Grapsidae). *Comparative Biochemistry and Physiology*, **70 A**, pp. 551-553.
- Sohn, I. G. 1958. Chemical constituents of ostracodes; some applications to paleontology and paleoecology. *Journal of Paleontology*, **32**, pp. 730-736.
- Speyer, S. E. 1985. Enrollment strategies in Middle Devonian trilobites. *Geological Society of America Abstracts with Programs*, **17**, p. 724.
- Speyer, S. E. 1988. Biostratinomy and functional morphology of enrollment in two Middle Devonian trilobites. *Lethaia*, **21**, pp. 121-138.
- Speyer, S. E. and Brett, C. E. 1984. Comparative taphonomy of Middle Devonian trilobite beds. *Geological Society of America Abstracts with Programs*, **16** (3), p. 198.

- Stehli, F. G. 1956. Shell mineralogy in Paleozoic invertebrates. *Science*, **123**, pp. 1031-1032.
- Stephens, G. C. 1955. Induction of molting in the crayfish, *Cambarus*, by modification of daily photoperiod. *Biology Bulletin*, **108**, pp. 235-241.
- Stockton, W. and Cowen, R. 1976. Stereoscopic vision in one eye: paleophysiology of the schizochroal eye of trilobites. *Paleobiology*, **2**, pp. 304-315.
- Størmer, L. 1980. Sculpture and microstructure of the exoskeleton in Chasmodonid and Phacopid trilobites. *Palaeontology*, **23**, pp. 237-271.
- Stürmer, W. and Bergström, J. 1973. New discoveries on trilobites by X-rays. *Paläont. Z.*, **47**, pp. 104-141.
- Teigler, D. J. and Towe, K. M. 1975. Microstructure and composition of the trilobite exoskeleton. *Fossils and Strata*, **4**, pp. 137-149.
- Thayer, C. W. 1979. Biological bulldozers and the evolution of marine benthic communities. *Science*, **203**, pp. 458-461.
- Towe, K. M. 1973. Trilobite eyes: calcified lenses in vivo. *Science*, **179**, pp. 1007-1009.
- Towe, K. M. 1975. Do trilobites have a typical arthropod cuticle? *Palaeontology*, **21**, pp. 456-461.
- Travis, D. F. 1954. The molting cycle of the spiny lobster *Panulirus argus* Latreille. I. Molting and growth in laboratory-maintained individuals. *Biology Bulletin*, **107**, pp. 433-450.
- Veizer, J. and Demovic, R., 1974. Strontium as a tool in facies analysis. *Journal of Sedimentary Petrology*, **44**, pp. 93-115.

- Veizer, J., Lemiex, J., Jones, B., Gibling, M. R., and Savelle, J., 1978. Paleosalinity and dolomitization of a Lower Paleozoic carbonate sequence, Somerset and Prince of Wales Islands, Arctic Canada. *Canadian Journal of Earth Sciences*, **15**, pp. 1448-1461.
- Veizer, J., Fritz, P. and Jones, B., 1986. Geochemistry of brachiopods: oxygen and carbon isotopic records of Paleozoic oceans. *Geochimica et Cosmochimica Acta*, **50**, pp. 1679-1695.
- Vigh, D. A. and Dendinger, J. E. 1982. Temporal relationships of postmolt deposition of calcium, magnesium, chitin and protein in the cuticle of the Atlantic Blue Crab, *Callinectes sapidus* Rathbun. *Comparative Biochemistry and Physiology*, **72 A** (2), pp. 365-369.
- Winder, C. G. 1960. Paleoeological interpretation of Middle Ordovician stratigraphy in southern Ontario, Canada. *International Geological Congress, XXI Session, Norden. Part VII, Ordovician and Silurian Stratigraphy and Correlations.* pp. 18-25.
- Wright, J. D., and Wright, E. P. 1961. A study of the Middle Devonian Widder Formation of southwestern Ontario. *Contributions from the Museum of Paleontology, The University of Michigan*, **16** (5), pp. 287-300.

Appendix I:**Species, Locality, Sample Information**

1.1 Species Numbers

Table 1: This table lists the different species of organisms of this study with their common name (if applicable) and assigned number. The numbers listed will appear in the first column (Sp) of the tables in Appendix III.

Species Number	Species
<i>Ordovician</i>	
10	<i>Isotelus</i> sp.
11	<i>Isotelus gigas</i>
12	<i>Isotelus maximus</i>
13	<i>Yogdesia bromidensis</i>
14	<i>Pseudogygites latimarginalus</i>
<i>Devonian</i>	
30	<i>Phacops</i> sp.
31	<i>Phacops rana</i>
32	<i>Greenops boothi</i>
33	<i>Terataspis grandis</i>
<i>Recent (marine)</i>	
70	<i>Cancer productus</i> (Red Rock Crab)
71	<i>Hemigrapsus nudis</i> (Purple Shore Crab)
72	<i>Cancer magister</i> (Dungeness Crab)
73	<i>Pugettia producta</i> (Kelp Crab)
74	<i>Limulus polyphemus</i> (Atlantic Horseshoe Crab)
75	<i>Parulirus argus</i> (Spiny Lobster)
76	<i>Callinectes sapidus</i> (Blue Crab)
77	<i>Callinectes</i> sp.
78	<i>Chelonibia patula</i> (Crab Barnacles)
<i>Recent (fresh water)</i>	
80	<i>Orconectes</i> sp. (Crayfish)
99	Matrix

1.11 Sample Numbers

Table 2: This table lists the fragment of cuticle sampled with its corresponding number. This number will appear immediately before the sample number in Appendix III.

First Two Digits	Meaning
11	cephalon (cephalothorax in lobsters)
12	thorax (dorsal carapace)
13	pygidium (tail)
14	hyperstoma
15	antennae
16	leg segment
17	left claw
18	right claw
19	unknown fragment
20	matrix
21	whole individual
22	ventral carapace
23	whole carapace

The sample numbers consist of essentially two numbers. The first two digits correspond to the segment or combination of segments that make up the sample. The next two to three digits are simply the number of the sample (ie. 01 to 500) and correspond to the order in which they were analyzed. The numbering of the samples for the present study will commence at 141. The data from McAllister (1987a) contains a symbol (*) immediately following the sample number. Where data from the previous study were used, the numbers for localities and species have been changed to reflect the new data set, with the numbers from McAllister (1987a) in parentheses. The old data has retained the previous numbering for the segment (s) that were analysed, and these

should be noted to avoid confusion. The mentioned numberings are listed in table 3 below.

Table 3: Shown is the meaning of the first two digits of the samples with the numbering from McAllister (1987).

First Two Digits	Old Data Set Meaning
14	whole trilobite
15	cephalon and thorax
16	thorax and pygidium
17	cephalon and pygidium
18	whole trilobite (eyes not included)

1.111 Locality Numbers

Table 4 includes: the age of the unit [given as the North American Stage, and the European equivalent (Barnes et al., 1981; Harland et al., 1982)]; the unit name; a general facies description; a hand specimen description (using Dunham's (1962) nomenclature); and a description of the locality of the sampled unit.

Table 4: Lists of localities of this study that correspond to the numbers in the second column in Appendix III, with reference to stratigraphic level of samples (i.e. locality X.2 is below X.3 and above X.1), the age of the unit, the name of formation, the general facies of the unit, and hand specimen descriptions (Dunham, 1962).

Locality #	Age	Formation	General Facies	Hand Specimen	Location
1.1	Middle Devonian Toughniogan (Givetian)	Demissa Bed	Calcareous gray shale	Mudstone	Exposed in a stream in the north end of the quarry
1.2 (1)		Smoke Creek Bed Windom Shale	Calcareous gray shale and limestone	Mudstone	Exposed in scattered pits in the north end of the quarry
1.3		Penn Dixie Bed Windom Shale Moscow Formation	Dark gray shale with pyrite	Mudstone	Exposed by entrance road Former Penn-Dixie Quarry Big Tree Rd., Bayview, NY
2 (2)	Middle Devonian Onesquethawian (Eifelian)	Edgecliff Member, Onondaga Formation	Dolomitic limestone	Wackestone	Quarry floor, Canadian Portland Cement Co., Quarry Rd., Port Colborne, ON (NTS 30 L/14. Grid Ref. 382490)
3 (3)	Middle Devonian Toughniogan (Givetian)	Smoke Creek Bed, Windom Member Moscow Formation	Medium gray calcareous shale	Mudstone	North face, Fall Brook Falls, 0.5 km east of US 20A and NY 39 Geneseo, Livingston Co., NY
4.1 (4)	Middle Devonian Toughniogan (Givetian)	Jaycox Sh. Member	Blue-gray calcareous shale	Wackestone/ mudstone	South Fork of Jaycox Creek, 0.4 km west of Rt. 39, 0.8 km north of Natons Rd., Geneseo, Livingston Co., NY
4.2 (5)		Deep Run Sh. Member Ludlowville Fmn.	Medium gray calcareous shale	Mudstone	
5.1	Middle Devonian Toughniogan (Givetian)	Upper Waukeah Sh	Calcareous shale	Mudstone	Exposed in Cazenovia Creek 2 m below the Tichenor Ls., west of the bridge, Northrup Rd., Exposed in Cazenovia Cr. east of the bridge, and below the waterfall (Tichenor Lmst.), Spring Brook, NY
5.2		Upper Waukeah Sh Ludlowville Formation	Calcareous shale	Mudstone	
6.1	Upper Ordovician Maysvillian (Caradocian)	Collingwood Member Whitby Formation	Bituminous black shale	Black shale	1 km east of Craighleith Prov. Park Hwy. 26, Craighleith Station, ON (NTS 41 A/9. Grid Ref. 5253112)
6.2 (6)			Bioclastic limestone	Brachiopodal grainstone	

Locality #	Age	Formation	General Facies	Hand Specimen	Location
7 (7)	Middle Ordovician Edenian (Caradocian)	Upper Member Cobourg Formation	Limestone	Packstone	Exposed outcrop on stream bed Lot 38, Con. VI Noltawasaga Twp., Collingwood, ON (NTS 41 A/8. Grid Ref. 660254)
8 (8)	Middle Ordovician Edenian (Caradocian)	Upper Member Cobourg Formation	Limestone	Packstone	Abandoned quarry, Lot 40, Con. VI Noltawasaga Twp., Collingwood, ON (NTS 41A/8. Grid Ref. 658266)
9.1 (9)	Middle Ordovician Trentonian (Caradocian)	Upper Member Verulam Formation	Limestone	Wackestone	Outcrop in north-east face of quarry (10 m level)
9.2 (10)		Lower Member Cobourg Formation	Limestone	Wackestone	Outcrop in the middle of quarry Ogden Point Quarry-St. Lawrence Cement Co., Colbourne, Ontario (NTS 30 N/13e, f. Grid Ref. 690737)
10	Middle Ordovician Trentonian (Caradocian)	Lower Member Verulam Formation	Argillaceous gray limestone	Wackestone	North face of the former Kirkfield Crushed Stone Ltd. Quarry 0.8 km east of the Kirkfield Liftlock, Kirkfield, ON (NTS 31 D/10. Grid Ref. 612387)
11 (11)	Middle Ordovician Trentonian (Caradocian)	Upper Member Verulam Formation	Argillaceous limestone	Mudstone	Junction of Hwy. 33 and Hwy. 401 north of Trenton, ON (NTS 31 C/4. Grid Ref. 925890)
12 (12)	Middle Ordovician Trentonian (Caradocian)	Middle Member Verulam Formation	Limestone	Wackestone/ packstone	Abandoned Belleville Quarry, S. of 401, W. bank of Moira River, Belleville, ON (NTS 31 C/3. Grid Ref. 088958)
13 (13)	Middle Ordovician Trentonian (Caradocian)	Lower Member Verulam Formation	Limestone	Wackestone/ packstone	Abandoned Canada Cement Co. Quarry, east of Lakefield, ON (NTS 31 D/8. Grid Ref. 187225)

Locality #	Age	Formation	General Facies	Hand Specimen	Location
14.1	Upper Ordovician Richmondian (Ashgillian)	Blanchester Member Waynesville Formation	Shale with limestone	Mudstone	East exposure of emergency spillway Caesar Creek State Park
14.2		Lower Member Liberty Formation	Limestone	Wackestone	Exposed on floor and walls of spillway, 5.2 km S of Rt. 73, Waynesville, Warren County, OH
15	Upper Ordovician Richmondian (Ashgillian)	Ft. Ancient Member Waynesville Formation (equil. Loc. 17)	Argillaceous limestone	Brachiopodal packstone	Talus slope, Rt. 42 (west road out), 4 km NE of junction with Rt. 73, Waynesville, Warren Co., OH
16	Upper Ordovician Edenian (Caradocian)	Kope Formation (Eden Shale) (Latonia Formation)	Blue shale with limestone partings and pyrite	Packstone	Talus slope, Rt. 68 (west road out) 5.7 km N of Junction with Rt. 52, Ripley, Brown Co., OH
17	Upper Ordovician Richmondian (Ashgillian)	Medial Member Waynesville Formation (Trilobite shale unit)	Shale with limestone partings	Wackestone	Bon Well Hill Section, Rt. 101 (NW road out), 2.1 km NE of Brookville, Franklin Co., IN
18	Upper Ordovician Maysvillian (Ashgillian)	Upper Member Fairview Formation	Argillaceous limestone	Brachiopodal packstone	Rt. 50 (south road out), 9.8 km W of Junction with Rt. 1, Aurora, Dearborn Co., IN
19	Middle Ordovician Black Riverian (Caradocian)	Pooleville Member Bromide Formation Simpson Group	Fine grained ferroan dolomite	Trilobital wackestone	Rock Crossing, Hickory Creek, SW of Ardmore, Carter Co., Oklahoma, Arbuckle Mtns. (general section in Fay, 1969 p.30 and Fay and Graffham, 1969 p. 37)
20	Middle Ordovician Trentonian (Caradocian)	Lower Member Cobourg Formation	Argillaceous limestone	Wackestone	Hwy. 33 and Wooler Rd. south of Trenton, ON (NTS 31 C/4. Grid Ref. 922837)
21.1	Middle Devonian Toughniogen (Givetian)	1.5 m below Murder Creek Bed	Shale	Mudstone	Mouth of 18 Mile Creek (north side) at Lake Erie Shoreline, near Wanakah, Erie Co., NY
21.2		Murder Creek Bed Wanakah Shale Ludlowville Fmn.	Shale	Mudstone	

Locality #	Age	Formation	General Facies	Hand Specimen	Location
22	Middle Devonian Toughniogen (Givetian)	Lower Member Widder Formation (Ludlowville equivalent)	Shale	Mudstone	Hungry Hollow, 3 km east of Arkona, ON (NTS 40 P/4. Grid Ref. 354695)
23	Middle Devonian Toughniogen (Givetian)	Kashong Shale Moscow Formation	Shale	Wackestone	International Salt Co., by railway tracks, 0.2 km S of Rt. 63, Retsof, Livingston Co., NY
24	Middle Devonian Toughniogen (Givetian)	Kashong Shale Moscow Formation	Shale	Wackestone	The bank of Wheeler Gully Rt. 39 East, 4.5 km NE of Geneseo, Livingston Co., NY
25	Middle Devonian Toughniogen (Givetian)	Silica Formation	Calcareous Shale	Wackestone	Medusa Portland Cement Co. Sylvania, Lucas Co., OH
27	Recent	N/A	Detrital fresh water environment		Severn River, Centre Branch, Washago, ON (NTS 31 D/14. Grid Ref. 322578)
28	Recent	N/A	Detrital marine environment		North Pacific Shore, Cape Beale lighthouse, Cape Beale, BC SW rim of Barkley Sound, approx. 145 km NW of Victoria, B. C. (NTS 92 C/14. Grid Ref. 374059) (loc. in Brand <i>et al.</i> , 1987)
29	Recent	N/A	Carbonate marine environment		Atlantic Ocean shore off US 1, Bahia Honda State Park, Bahia Honda Key, Florida approx. 185 km S of Miami, Fla.
30	Recent	N/A	Carbonate marine environment		Atlantic Ocean shore off US 1, Long Key State Park, Long Key, Florida approx. 139 km S of Miami, Fla.

Appendix II

Ecology of Recent Arthropods

CAPE BEALE, B. C.

Cancer magister (Dungeness Crab), a carnivore, is found intertidally in eel grass, and is often half-buried in the subtidal muddy sand (Harbo, 1980). The special arrangement of the gill chamber strains sand particles out of the water (Johnson and Snook, 1967), and allows the crab to burrow deeply into the sediment. Immature specimens of *C. magister* may stray from their usual deep water habitat into intertidal areas (Ricketts and Calvin, 1962). The average life span for this species is approximately eight years, and individuals do not become sexually active until their fourth or fifth year (Ricketts and Calvin, 1962).

Cancer productus (Red Rock Crab) is found in both intertidal and in shallow subtidal areas of the north-east Pacific Ocean (George and George, 1979) and on rocky and eel grass-covered substrates (Harbo, 1980). Unlike *C. magister*, *C. productus* lacks a mechanism for filtering fine debris out of its gill chamber (Ricketts and Calvin, 1962), and is therefore confined to relatively rocky terrain.

Hemigrapsus nudis (Purple Shore Crab) is a dominant species of the middle tide-pool region (Ricketts and Calvin, 1962) and is commonly found under intertidal rocks (Harbo, 1980), or on mud flats along the Pacific Coast (Johnson and Snook, 1967).

By contrast, *Pugettia producta* (Kelp Crab) is found clinging to or around kelp (Harbo, 1980) but only one specimen of this rare species was obtained at Cape Beale.

MIDDLE FLORIDA KEYS, FLORIDA

Panulirus argus (Spiny Lobster) is most common at water depths of approximately 20 m in rocky and sandy areas (George and George, 1979), but it ranges from shallow subtidal areas to the edge of the continental shelf. It also ventures into slightly brackish water with salinities of 20 to 25‰ (Gosner, 1978).

Callinectes sapidus (Blue Crab) is omnivorous and found on muddy sand sediments in shallow water (George and George, 1979). A euryhaline organism, it is

most common in estuaries but also ranges into fresh water and may be found in normal marine environments at depths of at least 36m (Gosner, 1978). *C. sapidus* is an avid burrower, producing pits ranging in size from 3 to 9 cm deep (Plotnick, 1986).

Callinectes sp. is morphologically similar to *C. sapidus*, but it has a more tapered carapace. It probably inhabits an environment similar to that of *C. sapidus*.

Specimens of the crab barnacle, *Chekonibia patula*, were found affixed to the carapaces of *Callinectes sp.* and therefore matured in a similar environment.

Limulus polyphemus (Atlantic Horseshoe Crab) is a sediment feeder, and is known to produce extensive bioturbation (Plotnick, 1986). Predominantly a nocturnal species, it spends the daylight hours covered by a thin layer of substratum (Eldredge, 1970). Its functional morphology is similar to that of trilobites (Eldredge, 1970) and it has therefore been used as a model for both trilobite circulatory systems (Bergström, 1975a) and feeding mechanisms (Thayer, 1979).

NORTH-CENTRAL ONTARIO

Orconectes sp. (common crayfish) is generally omnivorous (Pennak, 1953) and is usually restricted to shallow waters, of less than 1 to 2 m, but, some species have been found as deep as 36 m (Pennak, 1953). As nocturnal feeders, crayfish remain in burrows or under rocks during the day but they venture out into the open and even on to shore at night (Pennak, 1953). Most species are able to tolerate wide ranges in temperature, hydrogen ion concentration, and free and bound carbon dioxide (Pennak, 1953).

Appendix III
Geochemical Data

Geochemical data for Recent specimens of *Cancer productus*, *Cancer magister* and *Pugettia producta* sampled from the detrital marine environment off of Cape Beale, British Columbia. (I.R.—insoluble residue, L—length, W—width; all elemental values are in ppm—parts per million; isotopes are expressed in per mille)

Sp. #	Loc. #	Sample #	I.R. %	Ca ppm	Mg	Sr	Mn	Na	Fe	Al	$\delta^{13}\text{C}$ ‰, PDB	$\delta^{18}\text{O}$	L cm	W
<i>Cancer productus</i> (detrital)														
70	28	12 142	13.9	330260	19465	2700	16	7330	170				4.7	6.5
70	28	12 143	6.8	330940	18550	3270	20	6305	60				4.7	6.5
70	28	12 150	17.6	318530	20400	4005	15	6955	185					
70	28	12 151	7.7	309030	18640	3230	20	6235	75					
70	28	17 152	15.3	306960	19205	3615	21	7825	145				3.5	2.0
70	28	17 153	16.2	305670	18110	3785	19	8360	130				3.5	2.0
70	28	17 154	16.8	317680	18530	3900	19	9300	95				3.5	2.0
70	28	17 155	15.2	312470	15470	4180	16	8750	85				3.5	2.0
70	28	17 159	11.8	338930	15630	3870	18	7075	70				3.5	1.7
70	28	12 163	25.2	327730	17645	4115	13	7820	155				7.0	9.4
70	28	18 168	21.0	335870	12760	3900	16	5590	75					
70	28	18 168	20.4	286210	18150	3905	12	12575	75				3.3	1.6
70	28	18 169	32.1	271480	16070	3520	8	14485	60				3.3	1.6
70	28	18 170	19.2	307470	14760	3905	10	9950	50				3.3	1.6
70	28	18 171	11.9	292380	18500	3365	19	9115	100				3.9	
70	28	17 172	8.9	258100	18640	3315	18	8460	85				3.9	1.7
70	28	17 173	15.7	293770	19620	3725	18	7870	80				3.9	1.7
70	28	18 174	14.8	278400	18340	3735	18	6920	130				3.6	1.8
70	28	18 175	18.1	286180	17775	3750	17	8570	110				3.6	1.8
70	28	18 176	16.0	281240	19055	3770	16	8890	85				3.6	1.8
70	28	18 177	14.7	333670	17960	3835	20	5740	80				1.9	1.3
70	28	12 185	7.8	274240	17950	3670	18	6160	90					
70	28	17 186	12.0	289250	15960	4000	15	9170	75					
70	28	18 187	13.0	305780	15455	4230	14	7810	70					
<i>Cancer magister</i> (detrital)														
72	28	12 146	27.4	326480	17250	4400	10	7205	105				4.6	7.0
72	28	12 147	28.6	349040	17610	4250	12	6640	200				4.6	7.0
72	28	12 156	23.5	305780	17180	4120	21	9985	125				3.8	5.9
72	28	17 157	22.0	350170	19560	4195	24	5720	340				3.5	1.7
72	28	17 158	6.8	331660	18535	3565	26	6140	70				3.5	1.7
72	28	12 160	18.6	330640	17000	4480	17	7915	90				5.5	7.5
72	28	12 164	22.1	337700	14790	3840	19	6020	135				3.0	4.7
72	28	18 165	25.5	302900	14610	3680	18	14220	245				2.4	1.1
72	28	17 166	20.3	313730	14900	3645	17	12500	155				2.4	1.0

72	28	17 286	0.6	308870	20390	3645	11	11420	80				2.0	1.3
Sp. #	Loc. #	Sample #	I.R. %	Ca ppm	Mg	Sr	Mn	Na	Fe	Al	$\delta^{13}\text{C}$ ‰, PDB	$\delta^{18}\text{O}$	L cm	W
72	28	17 287	0.3	305950	19370	3535	11	11215	85				2.7	1.7
72	28	17 288	2.8	316660	17060	2980	12	10150	60					
<i>Pezomachus prolixus</i> (detrital)														
73	28	21 184	32.5	306190	15430	3945	30	3750	305				2.2	1.8

Geochemical data for Recent specimens of *Hemigrapsus nudis* from a detrital, lagoonal environment at Cape Beale, B. C. (I. R.—insoluble residue, L—length, W—width; all elemental values are in ppm—parts per million; isotopes are expressed in permille)

Sp. #	Loc. #	Sample #	I.R. %	Ca ppm	Mg	Sr	Mn	Na	Fe	Al	$\delta^{13}\text{C}$ ‰, PDB	$\delta^{18}\text{O}$	L cm	W
<i>Hemigrapsus nudis</i> (detrital)														
71	28	21 141	20.8	366200	13390	2855	20	6190	190				1.7	2.0
71	28	21 144	22.3	359640	14335	4070	18	5130	90				2.1	2.3
71	28	21 145	26.3	273680	14785	4290	14	8550	205				1.6	1.9
71	28	21 148	15.1	328480	16010	3880	15	11190	270				1.8	2.1
71	28	12 149	21.4	343480	14800	4005	15	6615	100				3.0	3.6
71	28	12 161	25.2	381320	14065	3840	13	7305	80				3.5	4.0
71	28	22 162	19.4	304350	14700	3820	14	6670	90				3.5	4.0
71	28	21 178	15.9	307080	16570	3350	25	7860	140	280				
71	28	21 179	17.7	328120	13200	3345	20	7375	160	280				
71	28	18 180	8.8	305830	15595	3715	10	5745	80				2.0	1.1
71	28	18 181	21.0	284570	18060	4070	10	7915	100				2.2	1.3
71	28	17 182	16.7	313600	15570	4205	12	5460	100				1.8	1.1
71	28	18 183	14.8	306370	18530	3990	18	7055	190				1.9	1.1
71	28	12 281	7.2	323310	15690	3650	11	8740	70				3.0	2.5
71	28	12 282	3.0	319170	13090	2800	14	8815	70				2.2	1.8
71	28	12 283	9.9	340900	14090	3685	12	13455	110				1.8	1.4
71	28	12 284	3.3	296710	18625	3090	10	17335	70				2.7	2.5

Geochemical data for Recent specimens of *Limulus polyphemus* and *Paralimulus argus* from the carbonate environment off the Atlantic coast of Florida. (I. R.—insoluble residue, L—length, W—width; all elemental values are in ppm—parts per million; isotopes are expressed in permille)

Sp. #	Loc. #	Sample #	I. R. %	Ca ppm	Mg	Sr	Mn	Na	Fe	Al	$\delta^{13}\text{C}$ ‰, PDB	$\delta^{18}\text{O}$	L cm	W
<u><i>Limulus polyphemus</i> (carbonate)</u>														
74	29	11 189	97.8	32655	34515	2470	245	54890	160	4870			10.3	7.3
74	29	13 190	94.1	13275	25460	910	140	149150	190	3360				
74	30	11 321	83.7	86680	19670	700	16	1680	200				14.6	10.3
74	30	11 322	88.8	14370	16770	520	1	6810	30					
<u><i>Paralimulus argus</i> (carbonate)</u>														
75	29	11 188	23.6	267870	26035	4070	19	10800	40					
75	29	11 203	22.2	266200	26590	3610	11	6740	45					
75	29	15 204	42.1	242860	34970	3645	8	17530	50					
75	29	16 205	34.6	274100	30300	4080	12	10255	65					
75	30	15 298	9.1	259670	20355	2650	12	17790	20					
75	30	16 299	16.6	246000	20500	3180	8	25110	25					
75	30	11 300	12.0	276270	24750	3305	12	23080	20					
75	30	11 301	13.9	292000	18125	2895	5	12450	20					
75	30	15 302	18.1	280460	20395	3180	6	18405	30					
75	30	11 303	11.9	291810	17170	3250	9	14955	30					
75	30	11 307	42.2	153630	25135	2635	8	51270	70					
75	30	11 308	43.0	156050	30395	2180	8	37705	50					
75	30	11 309	40.6	175280	24405	2645	9	34380	80					

Geochemical data for Recent specimens of *Callinectes sapidus*, *Callinectes* sp. and the attached crab barnacle *Chelonibia patula* from the carbonate environment off the Atlantic coast of Florida. (I.R.—insoluble residue, L—length, W—width; all elemental values are in ppm—parts per million; isotopes are expressed in permille)

Sp. #	Loc. #	Sample #	I.R. %	Ca ppm	Mg	Sr	Mn	Na	Fe	Al	$\delta^{13}\text{C}$ ‰, PDB	$\delta^{18}\text{O}$	L cm	W
<u><i>Callinectes sapidus</i> (carbonate)</u>														
76	29	17 191	15.6	300450	20580	4495	14	7750	60				5.0	1.6
76	29	17 192	15.5	357830	21485	4665	66	5620	120				5.0	1.6
76	29	17 193	14.2	262920	20195	4240	30	11015	100				5.0	1.6
76	29	17 194	17.1	321430	19745	4480	34	9025	50				5.0	1.6
76	29	17 195	13.6	343684	21175	3935	40	8630	90				5.0	1.6
76	29	18 196	16.5	276550	21280	4150	18	10865	60				5.0	1.6
76	29	18 197	9.3	297950	19320	3440	50	6445	50				5.0	1.6
76	29	18 198	9.5	297630	19115	3440	30	7065	70					
76	29	18 199	12.5	289080	20390	3730	40	9110	45					
76	29	12 200	14.4	266920	20860	3945	14	10250	40					
76	29	12 201	7.5	299180	18380	3410	45	7690	40					
76	29	16 202	28.0	243400	21805	3720	40	16405	50					
<u><i>Callinectes</i> sp. (carbonate)</u>														
77	29	23 206	20.7	279870	20840	4105	15	8027	30				4.9	10.0
77	29	17 207	15.8	257070	19585	3670	10	10715	30					
77	29	18 208	21.6	251270	19950	3900	11	9860	40				6.1	1.8
77	29	16 209	36.7	214920	21595	3730	11	17150	50					
77	29	22 210	19.5	273930	21040	3950	11	7765	35					
<u><i>Chelonibia patula</i> (carbonate)</u>														
78	29	21 211	3.1	351840	5130	3450	20	8340	40	210			1.6	1.4
78	29	21 212	2.8	332070	5105	3235	17	9910	40	210			1.1	0.9
78	29	21 213	0.7	365890	5370	3140	6	7590	40				1.2	0.9

Geochemical data for Recent specimens of the fresh water crayfish *Oreomunus* sp. from the Great Lakes region of Ontario. (I.R.—insoluble residue, L—length, W—width; all elemental values are in ppm—parts per million; isotopes are expressed in permille)

Sp. #	Loc. #	Sample #	I.R. %	Ca ppm	Mg	Sr	Mn	Na	Fe	Al	$\delta^{13}\text{C}$ ‰, PDB	$\delta^{18}\text{O}$	L cm	W
<i>Oreomunus</i> sp. (fresh water-detrital)														
80	27	17 248	10.3	338200	5030	680	60	2470	35				4.0	2.0
80	27	17 249	12.4	338840	3545	650	45	3440	30				4.5	2.0
80	27	17 250	11.1	366520	2770	750	130	1030	225				2.7	1.0
80	27	17 251	11.4	341490	3755	595	70	3660	30				4.0	1.9
80	27	18 252	8.9	319690	4475	650	35	3240	35				3.3	1.8
80	27	11 254	10.2	319110	4470	920	160	320	120				4.3	1.7
80	27	11 255	8.2	346700	3845	620	65	1100	80				4.0	2.0
80	27	11 258	8.7	323760	4030	680	45	965	45				4.0	2.1
80	27	11 264	9.3	311060	5215	725	85	7205	35					
80	27	18 265	4.7	313500	5240	760	85	6960	45				3.5	1.3
80	27	16 266	10.6	285320	4530	750	130	6880	60					
80	27	18 268	14.6	355480	5150	820	195	2125	390				2.6	1.0
80	27	17 269	13.1	355630	4450	710	180	1420	350				2.8	1.0
80	27	13 270	22.4	315710	5010	840	510	1280	1460				4.0	1.3

Geochemical data for the trilobite *Phacops rana* from the Middle Devonian Ludlowville Formation. (I. R.—insoluble residue, L—length, W—width; all elemental values are in ppm—parts per million; isotopes are expressed in permille)

Sp. #	Loc. #	Sample #	I.R. %	Ca ppm	Mg	Sr	Mn	Na	Fe	Al	Zn	$\delta^{13}\text{C}$ ‰, PDB	$\delta^{18}\text{O}$ ‰, PDB	L cm	W
<i>Phacops rana</i>															
31	1.1	21 225	9.5	369100	4365	1060	1905	905	2710	290					
31	1.1	12 226	5.9	380950	3995	920	2240	690	2540	210		-0.55	-5.94	1.0	1.8
31	1.1	11 227	6.9	371030	4385	910	2255	730	2220	195				1.5	2.5
31	1.1	12 228	15.8	366670	4165	920	2500	730	2765	325				1.8	2.2
31	1.1	21 229	12.8	370050	4085	845	2415	690	3095	265		-0.70	-5.54	2.4	2.0
31 (1)	4.1 (4)	11 11*	32.8	328380	3660	1280	1110	940	6470	140	7				
31 (1)	4.1 (4)	13 12*	29.6	380330	4550	1430	1250	990	4150	280	5				
31 (1)	4.1 (4)	16 13*	29.3	393870	4145	1175	1115	920	3740	250	4				
31 (1)	4.1 (4)	12 94*	28.9	424660	3990	820	2290	610	2915	535	7	+2.87	-5.31		
31 (1)	4.1 (4)	11 107*	25.2	385490	3520	880	1350	720	3910	220	6				
31 (1)	4.1 (4)	12 108*	22.7	379570	4160	1020	1300	900	3470	240	7				
31 (1)	4.1 (4)	13 109*	27.7	396480	3990	850	1420	690	3530	225	8	+2.78	-4.65		
31	4.1	21 395	46.8	380720	4310	935	1390	740	2710	590				3.8	2.2
31	4.1	11 397	12.9	393610	5090	1110	1415	880	2320	395					
31	4.1	13 398	5.9	358510	6330	1465	1225	1200	1770	240				1.2	2.0
31	4.1	13 399	11.2	368080	6760	1330	1405	920	1860	460				1.2	2.0
31	4.1	13 400	24.4	352730	4250	950	1595	740	2500	450				1.0	1.9
31	4.1	13 402	40.9	360540	4200	980	1170	1055	2760	315				1.1	2.0
31	4.1	11 403	20.9	327090	5665	1100	1220	995	2185	410				1.1	1.9
31	4.1	11 404	26.6	360330	7100	1470	1370	1275	2640	725				1.0	1.8
31	4.1	11 405	18.1	364760	4570	875	1850	780	2895	580				1.1	1.7
31 (1)	4.2 (5)	11 15*	28.6	365550	4050	1275	990	890	4770	375	3	+3.60	-4.68		
31 (1)	4.2 (5)	16 16*	39.3	403820	4790	1620	1020	1160	3270	285	4				
31 (1)	4.2 (5)	11 106*	16.7	387920	3815	900	1480	640	2550	60	9	+3.36	-5.45		
31	4.2	11 406	22.2	367500	3970	750	1610	650	3540	450				2.2	3.8
31	4.2	13 407	25.5	365530	4795	925	1065	795	3020	515				1.3	2.9
31	4.2	11 408	24.2	398560	4370	1150	1160	610	2775	375				1.9	3.7
31	4.2	11 409	10.7	395110	4440	890	1285	625	4200	420				1.5	2.2
31	4.2	11 412	20.4	391140	4295	1000	1250	580	2330	370				1.7	4.0
31	4.2	11 413	21.0	385860	4310	1140	1055	660	2405	445					
31	4.2	11 414	19.0	394780	4000	920	1595	620	2905	420					
31	4.2	12 415	26.3	390990	4775	1205	890	810	2300	410				1.3	3.9
31	4.2	11 417	20.1	401210	3960	785	1510	500	3245	445				1.3	3.0
31	4.2	11 418	24.7	392840	3770	830	1500	515	5440	340				1.9	3.9
31	4.2	11 423	30.4	317780	3770	870	1070	730	3190	325					

Sp. #	Loc. #	Sample #	L.R. %	Ca ppm	Mg	Sr	Mn	Na	Fe	Al	Zn	$\delta^{13}\text{C}$ ‰, PDB	$\delta^{18}\text{O}$ ‰, PDB	L cm	W
31	5.1	12 424	31.5	360960	6630	1535	1410	970	2520	550				1.2	2.2
31	5.1	13 425	18.4	371500	6615	1455	1420	865	2290	560				1.0	2.2
31	5.1	11 426	21.5	373640	6080	1310	1660	845	2600	550				1.0	2.2
31	5.1	12 428	30.8	358090	6710	1510	1400	885	2500	510				1.5	1.7
31	5.1	13 429	10.9	367650	4705	1130	1515	1005	2430	480					
31	5.1	11 430	19.4	360240	4835	1330	1505	950	2860	500					
31	5.1	11 431	37.9	369910	5750	1450	1820	870	3510	995				1.2	1.7
31	5.1	11 432	27.4	385490	4810	1525	1855	820	2570	910				1.2	1.7
31	5.1	11 433	38.8	374190	5780	1160	1989	900	2760	570				0.8	1.4
31	5.1	21 434	34.9	380070	6390	1720	1585	810	3210	690				2.5	1.1
31	5.1	11 435	22.2	361460	5125	1250	1760	770	2840	490					
31	5.1	11 436	36.6	383990	6000	1605	1280	1140	3325	570					
31	5.1	11 437	26.9	318090	4560	1135	1570	835	2885	440					
31	5.1	11 438	23.1	371950	5470	1400	1710	800	2300	355				1.0	1.8
31	5.1	11 439	18.8	365730	5620	1530	1610	840	2670	365					
31	5.2	11 440	22.0	366340	5530	1550	1830	825	2210	205				1.0	1.8
31	5.2	11 442	21.9	377290	5960	1670	1710	1060	2220	435					
31	5.2	12 443	33.4	332110	6495	1860	1730	1040	2730	790				1.5	1.5
31	5.2	11 444	28.6	284630	5415	1230	1370	1030	2250	440					
31	21.1	21 216	14.6	386950	4685	1045	995	860	3420	315					
31	21.1	21 217	22.1	369980	5045	1170	945	750	3130	510					
31	21.1	11 218	19.6	356740	4920	1120	1135	775	3240	675				1	1.9
31	21.1	11 219	18.5	376730	5365	1250	1025	1010	2875	490				0.9	1.8
31	21.1	11 220	16.2	361420	5210	1290	1095	870	3130	440				1.3	2.2
31	21.1	21 221	20.5	371960	5340	1160	1100	825	3190	590				2	1.6
31	21.2	12 493	11.9	366160	4320	840	1570	770	3665	310		+1.81	-5.26	1.9	1.0
31	21.2	12 494	8.3	347340	4240	900	1505	705	3655	310				1.4	1.2
31	21.2	13 496	7.4	352380	5130	1090	1460	920	3260	310					
31	21.2	21 497	9.7	365970	4260	810	1620	880	3875	185		+1.95	-4.97		
31	21.2	11 498	9.5	357710	4570	930	1780	785	3710	330					
31	21.2	21 499	11.6	353470	4680	820	1700	790	4545	430					
31	21.2	12 505	13.4	368130	5350	515	945	115	2525	220				2.3	1.8
<u>Matrix</u>															
99	1.1	20 224	54.1	336360	2555	510	2525	395	4930	730					
99 (5)	4.1 (4)	20 14*	42.2	390990	1940	320	1720	230	3725	375	4				

Sp. #	Loc. #	Sample #	I.R. %	Ca ppm	Mg	Sr	Mn	Na	Fe	Al	Zn	$\delta^{13}\text{C}$ ‰, PDB	$\delta^{18}\text{O}$ ‰, PDB	L cm	W
99 (5)	4.1 (4)	20 18*	53.8	363520	2235	395	990	375	3925	505	8				
99	5.1	20 427	90.0	214490	4545	945	910	820	10070	6105					
99	5.2	20 441	85.4	269660	4225	690	1260	1200	6470	2900					
99	21.1	20 222	83.2	310590	7790	525	860	640	10170	3425					
99	21.2	20 495	50.5	322470	3980	390	2000	445	4985	660					

Geochemical data for the trilobite *Phacops rana* from the Middle Devonian Silica Formation. (I.R.—insoluble residue, L—length, W—width; all elemental values are in ppm—parts per million; isotopes are expressed in per mille)

Sp. #	Loc. #	Sample #	I.R. %	Ca ppm	Mg	Sr	Mn	Na	Fe	Al	Zn	$\delta^{13}\text{C}$ ‰, PDB	$\delta^{18}\text{O}$ ‰, PDB	L cm	W
<u><i>Phacops rana</i> sp.</u>															
31	25	11 472	6.5	363990	3720	390	685	350	510	0		-1.19	-5.35	2.1	2.7
31	25	11 474	5.1	358610	4610	510	1050	490	855	0				1.5	2.7
31	25	12 475	4.1	329460	3790	370	790	300	500	14		+1.02	-5.63	3.1	2.3
31	25	12 476	11.3	376290	4220	455	935	440	960	50				2.7	2.6
31	25	13 477	7.0	341980	4510	410	640	435	440	100		+1.48	-5.39	2.0	3.5
31	25	11 478	4.7	371690	4000	345	985	400	565	75				1.0	2.2
31	25	11 479	7.3	375840	4740	490	690	390	475	0				1.2	2.6
31	25	11 480	3.2	354700	4430	545	730	415	340	0				1.3	3.2

Matrix

99	25	20 473	33.9	354750	5120	285	830	400	660	260					
----	----	--------	------	--------	------	-----	-----	-----	-----	-----	--	--	--	--	--

Geochemical data for the trilobite *Phacops rana* from the Middle Devonian Moscow Formation. (I. R.—insoluble residue, L—length, W—width; all elemental values are in ppm—parts per million; isotopes are expressed in permille)

Sp. #	Loc. #	Sample #	I. R. %	Ca ppm	Mg	Sr	Mn	Na	Fe	Al	Zn	$\delta^{13}\text{C}$ ‰, PDB	$\delta^{18}\text{O}$ ‰, PDB	L cm	W cm
<i>Phacops rana</i>															
31 (1)	1.2 (1)	16 01*	8.6	365430	5530	1305	1650	1510	3585	180	9				
31 (1)	1.2 (1)	16 02*	7.0	360370	4615	880	2020	1090	3020	350	11				
31 (1)	1.2 (1)	16 03*	4.3	361340	5260	1170	1970	1345	2620	120	17				
31 (1)	1.2 (1)	16 04*	5.8	389130	4630	1110	2745	920	3700	180	5				
31 (1)	1.2 (1)	18 05*	4.6	395170	5590	1380	2040	1230	2695	120	6				
31 (1)	1.2 (1)	16 06*	4.7	330250	4830	1180	2320	1020	3140	210	10				
31 (1)	1.2 (1)	16 07*	4.1	375490	5060	1215	2175	950	3640	200	18				
31 (1)	1.2 (1)	16 08*	5.5	398720	5320	1395	1940	1090	3370	160	5				
31 (1)	1.2 (1)	14 09*	11.3	383820	5850	1520	2040	1465	3465	295	7				
31 (1)	1.2 (1)	16 10*	3.4	398040	3835	1045	2215	1000	2570	170	12				
31 (1)	1.2 (1)	11 30*	5.2	375060	4630	1115	1925	790	3400	170	13				
31 (1)	1.2 (1)	14 96*	13.1	398770	3920	855	3560	590	2290	210	60	-0.62	-5.46		
31 (1)	1.2 (1)	14 97*	11.5	422420	4380	980	2840	850	1365	330	12				
31 (1)	1.2 (1)	16 98*	10.1	422290	4060	875	3240	690	2160	315	20	-0.51	-5.84		
31 (1)	1.2 (1)	14 99*	9.2	413960	3855	830	3650	545	2255	360	20				
31	1.3	21 454	3.0	359770	4550	775	1850	725	1330	0		-2.04	-4.72	1.3	2.5
31	1.3	21 456	10.0	350660	4635	760	1680	790	1765	20		-2.30	-5.50	2.4	1.8
31	1.3	13 457	6.3	354600	4420	790	1425	885	1300	0				0.8	1.9
31	1.3	13 458	9.4	332590	4680	840	1610	940	1485	0				0.9	1.8
31	1.3	11 459	11.5	350680	4710	830	1565	960	1555	0				1.1	2.6
31	1.3	13 460	4.8	369400	4195	735	2005	900	1615	0				1.1	2.2
31	1.3	21 461	17.7	354040	4600	615	1920	700	2350	0				3.2	1.3
31	1.3	11 462	8.5	332600	4470	710	1845	670	1510	0				1.0	1.9
31	1.3	12 465	19.1	362990	4465	620	2105	720	1925	0				0.5	1.3
31	1.3	12 466	18.0	343020	4375	660	2230	620	2285	0				1.2	2.0
31	1.3	13 467	9.3	324550	4580	810	1975	825	1420	16				0.9	1.6
31 (1)	3	11 88*	11.4	349240	6360	1620	2730	1355	1830	425	12				
31 (1)	3	11 90*	21.6	411550	5880	1180	2550	1075	2450	855	16				
31 (1)	3	17 91*	11.1	411560	6180	1930	2905	1170	2350	410	5	+1.27	-6.36		
31 (1)	3	11 100*	13.3	369130	6700	1650	2595	1260	2260	330	12				
31 (1)	3	14 101*	5.1	353620	6110	1645	2095	1380	2115	120	35				
31 (1)	3	14 103*	7.7	368510	5905	1675	2010	1310	2960	65	5				
31 (1)	3	14 104*	5.7	380310	5440	1420	2150	1150	3680	0	6	+1.17	-5.66		
31 (1)	3	11 105*	21.4	376810	6360	1610	1800	1485	3290	800	7				
31	3	13 391	10.4	392260	6930	1445	2240	1420	2130	365					
31	3	11 392	12.3	380670	6620	1660	2005	1350	2890	400					

Sp. #	Loc. #	Sample #	I.R. %	Ca ppm	Mg	Sr	Mn	Na	Fe	Al	Zn	$\delta^{13}\text{C}$ ‰, PDB	$\delta^{18}\text{O}$ ‰, PDB	L cm	W
31	3	11 393	10.9	354070	6225	1490	2005	1320	2680	355				0.9	1.9
31	3	13 394	10.3	377800	7150	2110	2120	1460	2550	455					
31	23	13 445	38.7	284560	5760	1400	1805	1650	3170	280		2.48	-4.70		
31	23	12 446	14.5	251810	5900	1740	1700	1400	3770	180		2.53	-4.31		
31	23	12 447	19.0	364530	6080	1385	1360	1845	3250	200					
31	23	13 448	33.3	367390	6620	1440	1820	1660	3230	480					
31	23	19 449	17.7	387910	6300	1310	1600	1795	3745	205					
31	23	19 450	12.0	380290	5535	1160	1765	1490	4320	235					
31	23	19 451	16.0	386520	6080	1200	1845	1590	4700	180					
31	23	13 452	39.1	349090	6100	1170	2075	2070	3530	365					
31	24	19 214	22.0	352320	5385	1190	1365	970	2150	540		2.31	-4.98		
31	24	19 215	13.7	369130	4955	1280	1860	930	3095	240		1.88	-5.25		
31	24	11 469	28.7	363210	5290	1250	1230	1300	2585	500				1.5	2.0
31	24	11 470	36.4	362820	5345	1160	1135	1460	2450	520					
31	24	13 500	9.3	295590	5975	1175	1300	1555	2940	240				1.1	2.7
31	24	11 502	21.0	307010	5815	1165	1290	1460	3100	465					
31	24	19 503	25.5	352340	6350	1350	1310	1760	3215	595					

Matrix

99 (5)	1.2 (1)	20 31*	33.8	350510	2400	210	2100	265	4550	470	12
99 (5)	1.2 (1)	20 32*	38.5	336120	2480	260	2090	345	3800	455	10
99 (5)	1.2 (1)	20 33*	42.8	340040	2605	280	2265	360	3200	445	10
99	1.3	20 455	23.5	377900	2910	150	1930	170	2060	245	
99 (5)	3	20 89*	45.6	330000	3360	460	3785	390	3830	765	10
99 (5)	3	20 102*	11.7	366370	1515	7805	3140	90	4760	0	9
99	23	20 453	30.5	378190	3545	370	4885	845	7470	455	
99	24	20 501	63.2	325010	5090	425	1680	530	5285	970	
99	26	20 471	76.0	330590	4205	360	1560	505	5355	1945	

Geochemical data for the Devonian trilobite *Greenops boothi* from the Middle Devonian of New York and Ontario. (I.R.—insoluble residue, L—length, W—width; all elemental values are in ppm—parts per million; isotopes are expressed in permille)

Sp. #	Loc. #	Sample #	I.R. %	Ca ppm	Mg	Sr	Mn	Na	Fe	Al	Zn	$\delta^{13}\text{C}$ ‰, PDB	$\delta^{18}\text{O}$ ‰, PDB	L cm	W cm
<i>Greenops boothi</i>															
32 (2)	1.2 (1)	14 92*	22.4	428000	3725	790	3155	700	1945	495	675				
32	1.2	13 223	19.6	359310	3870	885	2355	710	3290	470		-1.01	-6.35		
32 (2)	4.1 (4)	16 17*	24.2	373710	3955	1050	1050	790	4000	290	4				
32	4.1	13 401	30.9	370740	4985	1215	1300	1080	2570	570		+3.69	-4.14	2.0	3.2
32	4.2	13 411	37.2	377390	3370	900	1760	650	4550	800				2.9	3.4
32	4.2	13 420	17.3	405710	3715	900	1150	500	2370	310				2.5	3.5
32	4.2	13 421	26.8	378780	5170	1190	1120	875	1935	610		+3.22	-4.84		
32	4.2	13 422	27.6	370290	4115	980	1260	710	3025	450					
32	22	13 619	7.5	370900	2950	360	2055	540	5745	300				1.3	2.0
32	22	13 620	9.7	378470	2865	325	2360	405	5665	420				0.9	1.3
32	22	21 621	9.7	354260	2875	290	1960	500	5725	330		+0.54	-6.35	2.0	1.4
32	22	11 623	7.7	368130	2780	280	2230	415	4965	375		+0.86	-5.72		
32	22	13 624	16.1	350580	2800	275	1715	415	5450	475					
32	22	11 625	13.6	357180	2880	330	1970	345	4935	550					
32	22	13 626	11.7	355490	2820	290	1810	470	5240	630					
32	22	11 627	11.6	380220	2910	255	2130	490	6330	680					
32	22	13 628	13.0	359330	2780	280	2010	400	4845	535					
32	22	13 629	11.7	344450	2870	520	1815	395	4650	380					
<i>Matrix</i>															
99 (5)	1.2 (1)	20 31*	33.8	350510	2400	210	2100	265	4550	470	12				
99 (5)	1.2 (1)	20 32*	38.5	336120	2480	260	2090	345	3800	455	10				
99 (5)	1.2 (1)	20 33*	42.8	340040	2605	280	2265	360	3200	445	10				
99 (5)	4.1 (4)	20 14*	42.2	390990	1940	320	1720	230	3725	375	4				
99 (5)	4.1 (4)	20 18*	53.8	363520	2235	395	990	375	3925	505	8				
99	22	20 622	53.8	357960	3445	230	2860	340	6825	800					

Geochemical data for the Devonian trilobites *Phacops rana* and *Terataspis grandis* from the Onondaga Formation. (I. R.—insoluble residue, L—length, W—width; all elemental values are in ppm—parts per million; isotopes are expressed in permille)

Sp. #	Loc. #	Sample #	I.R. %	Ca ppm	Mg	Sr	Mn	Na	Fe	Al	Zn	$\delta^{13}\text{C}$ ‰, PDB	$\delta^{18}\text{O}$ ‰, PDB	L cm	W cm
<u>Phacops rana</u>															
31 (1)	2	13 81*	9.8	391430	6030	390	560	310	120	95	14	+1.13	-6.09		
31 (1)	2	11 83*	10.6	327070	16250	280	135	295	295	70	13				
31 (1)	2	13 84*	9.8	312250	12110	380	145	560	275	70	20				
31 (1)	2	11 85*	6.5	361520	5470	310	550	280	115	100	6	+1.07	-4.18		
31 (1)	2	13 93*	13.3	418780	12930	285	175	220	200	210	19				
<u>Terataspis grandis</u>															
33 (8)	2	12 67*	13.5	381550	6485	275	260	230	120	100	7	+1.18	-5.57		
33 (8)	2	12 68*	15.2	375260	7950	280	280	270	140	135	8				
33 (8)	2	13 69*	9.9	368100	5960	165	265	220	100	80	13				
33 (8)	2	13 70*	4.8	421740	7230	230	225	180	110	130	13	+0.79	-4.96		
33 (8)	2	11 71*	14.2	445190	11285	350	525	270	190	200	8				
33 (8)	2	11 72*	2.1	384000	11600	280	525	190	180	180	6				
33 (8)	2	11 73*	15.7	431340	12870	330	505	240	220	255	8				
33 (8)	2	19 76*	14.1	435520	10090	390	305	320	280	190	7				
33 (8)	2	19 77*	14.0	419100	10120	410	295	360	290	220	8				
33 (8)	2	13 79*	13.5	424770	11150	415	340	370	200	270	6				
33 (8)	2	19 80*	10.6	368040	8690	330	540	330	270	205	7				
33	2	19 376	12.3	395290	10795	385	310	480	770	0					
33	2	11 377	8.8	407320	7295	440	270	435	635	0					
33	2	11 378	13.0	382970	11920	480	445	530	910	0					
33	2	11 379	15.6	378510	13315	490	335	465	1000	0					
33	2	11 380	15.2	389570	12790	390	340	490	920	0					
33	2	19 381	14.2	382000	11440	370	280	340	700	270					
<u>Matrix</u>															
99 (5)	2	20 75*	34.5	375630	45935	275	245	240	420	635	14				
99 (5)	2	20 78*	44.1	283040	63270	360	380	285	480	825	9				
99 (5)	2	20 82*	14.1	360310	6515	195	460	165	80	120	13				

Geochemical data for specimens of *Vogdesia bromidensis* from the Middle Ordovician (Black River) Bromide Formation. (I. R.—insoluble residue, L—length, W—width; all elemental values are in ppm—parts per million; isotopes are expressed in permille)

Sp. #	Loc. #	Sample #	I. R. %	Ca ppm	Mg	Sr	Mn	Na	Fe	Al	Zn	$\delta^{13}\text{C}$ ‰, PDB	$\delta^{18}\text{O}$ ‰, PDB	L cm	W cm
<i>Vogdesia bromidensis</i>															
13	19	11 481	2.0	358620	6250	990	280	350	1270	0					
13	19	13 482	1.1	339530	5590	965	280	360	960	0				2.8	3.8
13	19	13 484	1.0	380260	4615	1020	310	350	890	0				2.9	4.7
13	19	13 485	1.4	364390	4545	995	330	360	865	0					
13	19	21 486	2.2	360860	4695	950	325	350	890	0				6.7	3.1
13	19	13 487	2.3	354660	4575	920	310	305	735	0	-0.42	-4.81		2.8	3.2
13	19	11 488	4.6	357170	4735	960	355	370	960	0				4.0	N/A
13	19	13 489	5.0	366310	3990	995	195	365	880	60					
13	19	11 490	1.0	347120	4305	1070	225	305	1170	45		-0.42	-4.75	2.5	4.0
13	19	11 491	2.4	355890	4210	980	230	350	990	50		-0.26	-4.46	2.6	4.7
13	19	11 492	1.9	303490	4030	940	210	290	790	30				2.6	4.7
<i>Matrix</i>															
99	19	20 483	16.4	267220	79273	760	480	280	11965	115					

Geochemical data for specimens of *Isotelus* sp. and *Isotelus gigas* from the Verulam Formation. (I. R.—insoluble residue, L—length, W—width; all elemental values are in ppm—parts per million; isotopes are expressed in permille)

Sp. #	Loc. #	Sample #	I. R. %	Ca ppm	Mg	Sr	Mn	Na	Fe	Al	Zn	$\delta^{13}\text{C}$ ‰, PDB	$\delta^{18}\text{O}$ ‰, PDB	L cm	W cm
<i>Isotelus</i> sp.															
10 (4)	9.1 (9)	11 118*	9.0	360750	5120	420	250	320	640	165	3	-0.43	-4.99		
10 (4)	9.1 (9)	11 120*	7.6	393260	4830	540	225	315	550	110	6				
10 (4)	9.1 (9)	11 121*	6.8	386240	4665	505	225	320	490	40	6				
10	9.1	19 346	8.3	376220	5420	630	215	255	785	230					
10	9.1	19 348	4.3	375230	4625	585	270	240	550	210					
10	9.1	19 349	13.9	370590	5835	625	245	285	1020	520		-0.11	-5.08		

Sp. #	Loc. #	Sample #	I.R. %	Ca ppm	Mg	Sr	Mn	Na	Fe	Al	Zn	$\delta^{13}\text{C}$ ‰	$\delta^{18}\text{O}$ PDB	L cm	W
<i>Isotefus gigas</i>															
11	10	11 630	7.9	349220	4710	585	300	370	240	210		+0.66	-5.31		
11	10	13 632	8.5	361080	4670	575	410	275	225	190					
11	10	11 633	8.0	346040	4750	470	340	310	375	250					
11	10	13 634	7.4	340240	4490	485	360	335	360	310					
11	10	11 635	7.5	365880	4365	610	500	230	270	250					
11	10	11 636	9.0	346670	4165	580	480	225	310	240					
11	10	11 637	9.4	340350	4250	550	490	220	365	355					
11	10	11 638	11.2	354880	4460	510	560	270	320	295					
11	10	13 639	4.9	357970	4790	640	215	360	330	420					
11	10	12 640	5.8	326410	4310	640	160	260	210	230				3.2	1.0
11	10	13 641	9.0	322460	4250	395	190	280	370	310					
11	10	13 642	12.1	341000	4560	520	235	340	430	330		+0.66	-5.79		
11	11	11 122*	6.4	387220	4365	550	220	220	560	50	6				
11	11	11 123*	6.1	388630	4280	540	190	200	550	80	4				
11 (3)	11	13 125*	8.9	387450	4205	640	400	250	675	150	6				
11 (3)	11	13 126*	8.7	376960	4045	690	330	295	730	280	6				
11	11	13 362	3.7	353190	4270	635	240	195	480	0				2.7	3.5
11	11	19 365	8.3	354420	4580	610	180	180	680	105				2.2	1.0
11	11	13 366	7.9	355980	4600	780	400	310	570	150				5.5	6.0
11	11	13 367	4.6	324000	4570	795	380	315	620	180					
11	11	11 368	7.3	283270	4350	565	270	210	630	140				2.6	2.5
11	12	11 127*	6.7	380090	4335	520	270	200	460	210	5	-0.34	-5.48		
11	12	11 129*	6.9	393330	4200	675	155	190	200	30	5	+0.63	-6.16		
11	12	13 130*	5.9	360930	4240	550	290	685	395	210	9				
11	12	11 370	1.1	244010	4700	660	160	200	60	6				5.5	6.8
11	12	11 372	2.5	238730	4570	820	175	170	245	30					
11	12	11 373	4.3	229670	4700	910	160	235	190	25					
11	12	13 382	6.7	381040	4425	530	220	195	650	185					
11	12	12 361	4.8	357210	4270	860	250	230	480	0				3.5	0.8
11	13	11 86*	5.6	363270	5060	985	425	350	160	100	6				
11	13	11 132*	8.4	344710	5845	700	190	250	810	330	5	+1.34	-5.72		
11	13	19 133*	8.4	353720	4405	495	260	175	820	290	4				
11	13	12 134*	8.0	353440	4600	580	300	230	1040	380	4				
11	13	19 135*	13.3	350810	4780	580	320	255	840	455	4				
11	13	11 136*	6.7	348610	4435	580	370	275	690	155	4	+0.17	-4.91		
11	13	19 325	15.5	366420	4700	570	330	510	1120	470					
11	13	12 327	11.1	362070	4475	480	330	245	1150	345					
11	13	11 350	8.4	363650	4810	735	200	210	625	170					

Sp. #	Loc. #	Sample #	I.R. %	Ca ppm	Mg	Sr	Mn	Na	Fe	Al	Zn	$\delta^{13}\text{C}$ ‰, PDB	$\delta^{18}\text{O}$ ‰, PDB	L cm	W
11	13	12 351	6.1	371910	4680	660	210	145	510	80				4.2	0.9
11	13	12 352	11.1	359290	4730	1040	340	250	670	100				2.1	0.6
11	13	19 354	8.5	357780	4430	1030	350	275	460	0					
11	13	19 356	3.3	339380	4060	870	310	175	610	0					
11	13	19 357	6.8	368600	4720	700	190	170	530	0				3.5	1.1
11	13	19 369	10.5	277790	4850	500	270	180	640	270				3.5	2.0

Matrix

99 (5)	9.1 (9)	20 119*	39.2	347270	10410	475	305	470	1590	845	8				
99	10	20 631	26.1	346630	4060	495	370	400	890	610					
99 (5)	11	20 124*	11.6	386030	3525	410	230	95	740	210	6				
99 (5)	12	20 128*	26.6	381740	5370	565	260	430	870	490	5				
99 (5)	13	20 87*	26.2	368030	4735	640	455	250	260	430	7				
99 (5)	13	20 131*	24.7	349190	9870	625	330	260	1890	580	5				

Geochemical data for specimens of *Isotelus gigas*, *Isotelus* sp. and *Pseudogigiles latimarginalis* from the Middle Ordovician Cobourg Formation. (I.R.—insoluble residue, L—length, W—width; all elemental values are in ppm—parts per million; isotopes are expressed in permille)

Sp. #	Loc. #	Sample #	I.R. %	Ca ppm	Mg	Sr	Mn	Na	Fe	Al	Zn	$\delta^{13}\text{C}$ ‰, PDB	$\delta^{18}\text{O}$ ‰, PDB	L cm	W
<u><i>Isotelus gigas</i></u>															
11 (3)	9.2 (10)	11 37*	6.7	328500	5420	555	200	340	585	150	4				
11 (3)	9.2 (10)	12 38*	8.3	381830	5730	660	180	220	670	250	7				
11 (3)	9.2 (10)	13 39*	5.8	316200	5060	700	250	400	720	135	3				
11 (3)	9.2 (10)	11 41*	5.5	355530	5340	955	175	475	670	170	14	-0.20	-5.18		
11 (3)	9.2 (10)	11 42*	5.9	345190	5580	845	115	415	625	160	7				
11 (3)	9.2 (10)	11 43*	6.2	336290	5420	910	125	435	580	150	4	-0.13	-4.97		
11 (3)	9.2 (10)	11 44*	9.3	331660	5580	925	150	500	840	210	11	+0.02	-5.45		
11 (3)	9.2 (10)	11 45*	5.3	321630	5410	840	135	495	600	130	8				
11 (3)	9.2 (10)	11 46*	11.5	370440	5885	740	190	670	975	280	115				
11 (3)	9.2 (10)	11 47*	6.6	357850	5435	750	150	520	700	175	9				

Sp. #	Loc. #	Sample #	I.R. %	Ca ppm	Mg	Sr	Mn	Na	Fe	Al	Zn	$\delta^{13}\text{C}$ ‰, PDB	$\delta^{18}\text{O}$ ‰, PDB	L cm	W
11 (3)	9.2 (10)	11 48*	8.4	334090	5265	690	200	540	1030	250	4				
11 (3)	9.2 (10)	11 49*	10.6	331430	5780	1205	190	510	835	290	5	+0.02	-5.28		
11 (3)	9.2 (10)	11 51*	9.5	346930	5700	1155	170	490	925	210	14	+0.15	-5.13		
11 (3)	9.2 (10)	11 52*	5.7	443720	5355	780	190	440	370	70	8				
11 (3)	9.2 (10)	11 53*	13.4	448830	5510	710	160	460	305	20	5				
11 (3)	9.2 (10)	11 54*	4.1	434910	5140	690	225	350	305	30	5				
11 (3)	9.2 (10)	11 55*	6.3	452750	5170	830	155	390	320	3	7				
11 (3)	9.2 (10)	12 56*	5.4	438680	5200	680	130	360	370	95	4				
11 (3)	9.2 (10)	12 57*	6.6	440630	5330	690	180	275	605	85	16				
11 (3)	9.2 (10)	11 58*	4.6	443310	5025	760	175	330	450	80	5				
11 (3)	9.2 (10)	11 59*	3.0	445830	5150	650	200	400	320	20	7				
11 (3)	9.2 (10)	11 60*	4.3	391250	5050	800	205	410	305	70	14				
11 (3)	9.2 (10)	11 61*	5.3	377700	5170	745	215	435	345	60	8				
11 (3)	9.2 (10)	13 62*	6.2	382770	5460	730	210	415	110	75	8				
11 (3)	9.2 (10)	13 63*	7.6	386810	5430	720	210	400	120	95	7				
11 (3)	9.2 (10)	13 64*	6.7	378990	5390	770	205	410	130	90	7				
11 (3)	9.2 (10)	13 65*	7.1	384110	5535	750	190	440	160	150	9				
11 (3)	9.2 (10)	19 66*	6.5	391890	5610	650	170	325	165	120	8				
<i>Isotefus</i> sp.															
10 (4)	7	13 110*	7.8	369380	4310	380	260	190	755	155	45	-0.19	-5.66		
10 (4)	7	19 111*	8.3	350660	6830	500	300	340	1110	75	4				
10 (4)	7	11 112*	6.8	355200	4070	430	205	325	640	150	13	-0.08	-5.29		
10 (4)	8	19 114*	6.8	367390	5350	480	280	330	705	60	4				
10 (4)	8	19 115*	7.9	358490	5330	435	265	270	740	110	5				
10 (4)	8	19 116*	8.0	361380	5650	400	310	230	980	130	8	-0.06	-4.95		
10	8	13 390	3.9	396170	5280	335	240	280	630	75				2.7	1.8
10	20	11 339	1.6	375620	7885	1510	190	1205	510	70				6.8	2.3
10	20	11 340	2.6	371600	7830	1670	220	1290	750	45					
10	20	11 341	3.4	370490	7955	1585	200	1360	610	60					
10	20	11 342	1.6	364240	8080	1465	205	1350	580	70					
10	20	11 343	3.3	362910	7990	1650	200	1490	570	100					
10	20	11 344	3.2	375850	7140	1525	180	1265	870	130					
10	20	11 359	2.2	375530	4435	680	220	195	315	0				3.3	1.5
10	20	11 360	4.0	365580	4580	735	240	255	315	0				2.9	1.5

Sp. #	Loc. #	Sample #	I.R. %	Ca ppm	Mg	Sr	Mn	Na	Fe	Al	Zn	$\delta^{13}\text{C}$ ‰, PDB	$\delta^{18}\text{O}$ ‰, PDB	L cm	W
<i>Pseudograptus latimarginatus</i>															
14	7	13 374	5.8	202660	5120	570	250	310	790	25				3.5	4.8
14	7	13 375	3.2	196640	5750	560	260	270	1030	60					
14	8	11 389	2.7	410300	7330	430	255	275	930	45				2.1	1.5
<i>Metix</i>															
99 (5)	7	20 113*	23.5	356770	4990	330	440	265	915	290	5				
99 (5)	8	20 117*	16.6	350550	5950	270	265	190	940	220	5				
99 (5)	9.2 (10)	20 40*	34.5	312660	9730	555	275	470	1970	535	6				
99 (5)	9.2 (10)	20 50*	37.5	349930	8425	840	205	650	2010	800	7				
99	20	20 345	9.6	375030	4170	870	175	380	1205	160					

Geochemical data for specimens of *Isotelus maximus* and *Pseudograptus latimarginatus* from the lower member of the Upper Ordovician Whitby Formation. (I.R.—insoluble residue, L—length, W—width; all elemental values are in ppm—parts per million; isotopes are expressed in per mille)

Sp. #	Loc. #	Sample #	I.R. %	Ca ppm	Mg	Sr	Mn	Na	Fe	Al	Zn	$\delta^{13}\text{C}$ ‰, PDB	$\delta^{18}\text{O}$ ‰, PDB	L cm	W
<i>Isotelus maximus</i>															
12	6.2 (6)	19 19*	2.6	356230	6210	1110	230	735	470	100	2	-0.60	-5.76		
12	6.2 (6)	11 20*	2.7	331150	8450	1980	120	1410	670	60	4	-0.29	-5.51		
12	6.2 (6)	19 21*	3.3	326620	8255	1960	110	1215	635	70	3	-0.34	-7.26		
12	6.2 (6)	11 22*	2.1	371780	8255	1945	110	1425	815	80	3	-0.42	-6.20		
12	6.2 (6)	11 23*	4.6	368800	8120	2050	110	1980	730	90	2	-0.73	-5.31		
12	6.2 (6)	19 24*	5.2	365490	8510	1915	125	1810	845	100	3				
12	6.2 (6)	12 25*	4.8	362990	8110	1905	165	1730	940	135	2	-0.73	-5.54		
12	6.2 (6)	11 27*	3.6	361430	8200	1700	100	1240	820	95	2	-0.09	-6.59		
12	6.2 (6)	11 28*	4.6	320600	6805	1600	110	1040	1190	125	3	-0.15	-6.20		

Sp. #	Loc. #	Sample #	I.R. %	Ca ppm	Mg	Sr	Mn	Na	Fe	Al	Zn	$\delta^{13}\text{C}$ ‰, PDB	$\delta^{18}\text{O}$ ‰, PDB	L cm	W
12	6.2	19605	3.1	335840	8090	1640	140	1510	785	18					
12	6.2	11609	3.5	339580	8565	1650	130	1660	550	0					
12	6.2	19610	3.0	347140	8220	1490	105	2290	660	0					
12	6.2	19611	2.8	359050	8145	1560	135	1965	630	0					
12	6.2	19614	1.9	348800	8040	1570	140	1780	570	0					
12	6.2	11615	1.3	354050	8170	1700	150	1970	550	0					
12	6.2	11616	2.2	364130	8010	1550	145	1985	580	0					
12	6.2	11617	0.9	345860	7865	1590	160	1700	590	0					

Pseudosyrinx latimarginatus

14 (7)	6.1	1336*	5.5	360490	8690	2195	140	1735	890	100	8				
14 (7)	6.1	1395*	7.1	418690	8850	2240	455	1570	330	310	10				
14	6.1	13595	3.3	318890	9455	1910	430	2130	1010	170		-1.10	-5.23		
14	6.1	11596	6.9	313560	7640	1685	275	2060	1110	310					
14	6.1	13598	6.1	346980	7180	1240	175	1920	1345	190				1.5	2.3
14	6.1	11599	2.4	338210	8035	1585	220	2005	720	195					
14	6.1	13600	10.7	333920	7090	1390	220	1460	1260	250					
14	6.1	11601	2.1	328490	6100	1090	205	1510	1120	175					
14	6.1	13602	7.6	355650	7875	1680	195	1680	1000	265					
14	6.1	13603	6.9	341850	7740	1630	190	2100	915	250					
14	6.1	13604	6.2	340240	7385	1420	200	1535	1365	245		+0.41	-6.64		
14	6.1	13606	3.4	338390	6990	1535	180	1440	775	210					
14	6.1	13607	6.8	351170	8500	1730	165	1770	870	0					
14	6.1	13608	2.0	355770	7220	1360	170	1590	1145	0		+0.70	-6.49		
14	6.1	13612	3.7	359230	8650	1800	180	1920	750	0					
14	6.1	13280	5.2	366210	7880	1650	165	1540	830	120					

Matrix

99	6.1	20597	42.4	291760	8605	630	890	585	4505	840					
99 (5)	6.2 (6)	2026*	30.4	360410	8740	1420	260	575	3335	380	4				
99 (5)	6.2 (6)	2029*	8.2	365760	5920	1710	95	830	1380	90	2				

Geochemical data for specimens of the trilobite *Isotelus maximus* from the Upper Ordovician Waynesville Formation. (I. R.—insoluble residue, L—length, W—width; all elemental values are in ppm—parts per million; isotopes are expressed in per mille)

Sp. #	Loc. #	Sample #	I. R. %	Ca ppm	Mg	Sr	Mn	Na	Fe	Al	Zn	$\delta^{13}\text{C}$ ‰, PDB	$\delta^{18}\text{O}$ ‰, PDB	L cm	W
<i>Isotelus maximus</i>															
12	14.1	12 526	2.1	339740	3250	835	1720	215	4350	185		-0.95	-5.02	2.7	1.4
12	14.1	12 527	2.9	343610	3250	790	1810	300	3975	175		-1.09	-5.08	3.4	1.5
12	14.1	12 528	1.8	353490	3280	840	1865	200	4305	185				2.7	1.3
12	14.1	12 529	9.7	362980	3180	625	2110	260	5425	0				3.8	1.7
12	14.1	12 530	2.2	355690	3195	655	1670	230	4625	0					
12	14.1	12 531	2.5	350540	3240	800	1965	210	4705	0					
12	14.1	12 532	2.4	377490	3365	890	1910	180	4395	0		-0.68	-5.06		
12	14.1	12 533	2.0	349460	3360	780	1910	230	4495	0					
12	14.1	19 534	6.7	359660	3660	570	1845	270	4950	0					
12	14.1	19 535	4.5	352340	3685	720	2170	220	4915	0					
12	14.1	19 536	1.8	343390	3420	580	1785	210	4400	0		-0.30	-4.40		
12	14.1	19 537	2.2	359090	2830	555	1860	195	4420	0					
12	14.1	19 538	2.4	370200	3180	470	1930	180	4140	0					
12	14.1	19 539	3.8	338880	3200	455	1865	180	4775	110		-0.74	-5.64		
12	14.1	19 540	4.1	340690	3195	420	1735	200	4980	100		-0.77	-5.20		
12	15	11 553	4.3	369030	2785	305	1930	175	2100	115					
12	15	19 555	4.5	366980	3360	770	2160	220	4250	175					
12	15	19 556	4.5	363720	3610	390	1735	220	4570	190					
12	15	14 557	5.0	364440	2920	520	1945	235	3715	170		-0.45	-5.36	3.2	2.5
12	15	14 558	6.5	354990	2635	490	1790	265	3655	150					
12	15	19 559	3.8	366760	2840	345	1900	145	3470	130					
12	15	19 560	5.7	357050	3820	410	1550	215	3760	140					
12	15	19 561	8.5	353290	5015	440	1725	215	4760	210					
12	15	19 562	7.5	372970	2340	600	1765	250	4420	145		-0.39	-5.27		
12	15	12 563	8.3	363720	2550	520	1780	205	4305	270				2.0	1.0
12	15	19 564	8.2	371340	4125	645	1575	250	3735	260					
12	17	11 565	6.4	346280	3500	750	605	340	2160	150					
12	17	11 566	7.2	353090	3895	920	820	300	2720	270					
12	17	11 570	2.2	355480	3540	940	750	280	2225	150				3.0	4.5
12	17	11 571	4.1	367810	3410	855	735	335	1740	170		-0.69	-4.91	2.2	3.0
12	17	12 572	3.8	375990	3335	770	740	350	1890	240				3.5	0.9
12	17	11 573	3.2	356680	3410	1005	675	265	2015	165		-0.80	-4.55	5.5	8.5
12	17	11 574	2.4	368460	3280	990	660	280	1910	230				5.5	8.5
12	17	11 575	3.0	363700	3410	960	685	300	2005	250				5.5	8.5
12	17	11 576	2.7	365700	3325	885	760	330	2070	60				5.5	8.5
12	17	11 577	3.3	353690	3380	820	695	390	2320	110				5.5	8.5

Sp. #	Loc. #	Sample #	I.R. %	Ca ppm	Mg	Sr	Mn	Na	Fe	Al	Zn	$\delta^{13}\text{C}$ ‰, PDB	$\delta^{18}\text{O}$ ‰, PDB	L cm	W
12	17	11 578	3.3	350700	3290	830	715	370	2090	105				5.5	8.5
12	17	11 580	6.7	355900	3865	805	805	270	2570	230				2.0	3.5
12	17	11 581	1.9	356570	3660	655	810	350	2775	125					
12	17	12 582	2.2	365090	3690	720	1090	185	1440	95				4.5	1.0

Matrix

99	14.1	20 541	38.5	359740	9555	510	1720	235	6540	450					
99	15	20 554	15.5	369560	2790	245	2140	140	2790	210					
99	17	20 579	13.7	347730	3950	740	870	370	2600	320					

Geochemical data for specimens of the trilobite *Isotelus maximus* from the Upper Ordovician Liberty Formation. (I.R.—insoluble residue, L—length, W—width; all elemental values are in ppm—parts per million; isotopes are expressed in permille)

Sp. #	Loc. #	Sample #	I.R. %	Ca ppm	Mg	Sr	Mn	Na	Fe	Al	Zn	$\delta^{13}\text{C}$ ‰, PDB	$\delta^{18}\text{O}$ ‰, PDB	L cm	W
12	14.2	19 542	3.6	355990	2890	410	580	180	2860	55					
12	14.2	19 543	2.7	343370	3080	430	660	160	3070	75					
12	14.2	11 544	6.8	350830	3090	370	715	140	3030	125				1.3	3.7
12	14.2	11 546	4.7	329060	2625	305	820	180	2790	20				3.8	3.2
12	14.2	11 547	3.9	360770	2790	390	870	125	2700	80					
12	14.2	19 548	1.6	359460	3455	460	1295	200	3640	80					
12	14.2	11 549	3.8	339920	3000	485	1660	205	4630	65					
12	14.2	19 550	3.3	370640	2980	320	950	300	3580	100	-0.53	-5.60		3.1	1.0
12	14.2	11 551	5.4	349990	3025	330	955	230	3710	160	-0.72	-4.67			
12	14.2	12 552	2.5	355680	3070	260	1350	190	5005	200					

Matrix

99	14.2	20 545	8.7	359040	4375	690	510	905	1935	195					
----	------	--------	-----	--------	------	-----	-----	-----	------	-----	--	--	--	--	--

Geochemical data for specimens of the trilobite *Isotelus* sp. from the Upper Ordovician Kope Formation. (I. R.—insoluble residue, L—length, W—width; all elemental values are in ppm—parts per million; isotopes are expressed in permille)

Sp. #	Loc. #	Sample #	I. R. %	Ca ppm	Mg	Sr	Mn	Na	Fe	Al	Zn	$\delta^{13}\text{C}$ ‰, PDB	$\delta^{18}\text{O}$ ‰, PDB	L cm	W
<i>Isotelus</i> sp.															
10	16	11 504	5.8	335240	4470	460	920	160	1150	110					
10	16	19 507	10.4	371840	5480	1995	1240	1595	6115	700					
10	16	11 508	8.4	375350	3595	460	970	110	1870	510				1.5	1.0
10	16	11 509	6.3	355900	3675	510	860	70	1160	360					
10	16	19 510	21.5	367640	4785	440	1070	260	4380	750		-0.91	-5.34	2.1	2.5
10	16	19 511	6.5	371960	3045	500	930	130	1040	230				4.0	1.4
10	16	19 512	12.2	358100	3375	405	1335	100	2615	260					
10	16	19 513	9.4	381660	3690	390	950	130	1500	400					
10	16	11 516	7.0	381340	3600	370	1290	120	2245	280					
10	16	19 518	4.9	361420	3240	440	825	115	970	170					
10	16	19 519	3.2	370850	3680	355	655	135	885	235					
10	16	19 520	9.8	342850	3755	395	885	100	1250	410					
10	16	14 521	3.4	364750	2730	335	1135	110	1495	340		-0.62	-5.05	5.0	5.0
10	16	14 522	3.3	366330	3035	510	905	115	1295	170				5.0	5.0
10	16	14 523	3.7	367580	3785	410	870	105	1480	205				5.0	5.0
10	16	14 524	3.8	354690	4450	410	900	110	1450	215				5.0	5.0

Matrix

99	16	20 525	15.6	337720	16835	705	1060	280	3920	390					
----	----	--------	------	--------	-------	-----	------	-----	------	-----	--	--	--	--	--

Geochemical data for specimens of the trilobite *Isotelus* sp. from the Upper Ordovician Fairview Formation. (I. R.—insoluble residue, L—length, W—width; all elemental values are in ppm—parts per million; isotopes are expressed in permille)

Sp. #	Loc. #	Sample #	I. R. %	Ca ppm	Mg	Sr	Mn	Na	Fe	Al	Zn	$\delta^{13}\text{C}$ ‰, PDB	$\delta^{18}\text{O}$ ‰, PDB	L cm	W
<i>Isotelus</i> sp.															
10	18	19 583	11.8	357420	3370	760	1230	210	5005	270					
10	18	19 584	4.0	356580	2900	745	1030	180	4040	170		-0.89	-4.91		
10	18	19 585	11.3	358640	3610	765	1155	250	4950	320					
10	18	12 587	2.8	246930	3120	1150	1100	220	5145	250				2.0	1.0

Sp. #	Loc. #	Sample #	I.R. %	Ca ppm	Mg	Sr	Mn	Na	Fe	Al	Zn	$\delta^{13}\text{C}$ ‰, PDB	$\delta^{18}\text{O}$	L cm	W
10	18	19 588	1.1	379460	2130	590	900	140	3530	160					
10	18	19 589	2.8	386170	4080	495	1010	175	2940	170					
10	18	19 591	6.5	371220	2090	890	1170	130	4240	220		+1.40	-6.20		
10	18	12 592	4.4	382500	2550	470	960	190	2920	270				2.7	1.0
10	18	19 593	12.2	349590	4605	315	940	210	3955	470					
10	18	12 594	3.8	335470	2770	1125	1120	250	5765	265				1.8	1.2
<u>Matrix</u>															
99	18	20 586	23.1	360560	4780	760	1050	385	4750	450					

Appendix IV:**Statistical Data**

RESULTS OF FACTOR ANALYSIS

Oreonectes sp. from Central Ontario

Orthogonal Transformation Solution-Varimax

	Factor 1	Factor 2	Communality
log I. R.	0.705	-0.254	0.561
log Ca	0.089	-0.849	0.729
log Mg	0.212	0.826	0.727
log Sr	0.790	0.343	0.742
log Mn	0.945	0.127	0.910
log Na	-0.498	0.568	0.572
log Fe	0.941	-0.158	0.910

Factor	Eigenvalue	Pct. of Var.
1	3.211	45.9
2	1.939	27.7
3	0.795	11.4

Hemigrapsus nudis from Cape Beale, B. C.

Orthogonal Transformation Solution-Varimax

	Factor 1	Factor 2	Factor 3	Communality
log I. R.	0.832	-0.170	0.429	0.905
log Ca	0.016	-0.822	0.043	0.678
log Mg	-0.026	0.860	-0.230	0.741
log Sr	0.877	0.334	-0.101	0.891
log Mn	0.034	-0.424	0.812	0.840
log Na	-0.695	0.490	-0.027	0.723
log Fe	0.111	0.232	0.908	0.890

Factor	Eigenvalue	Pct. of Var.
1	2.521	36.0
2	1.797	25.7
3	1.351	19.4

STUDENT T-TEST

Recent Arthropods

Differences between the exuvia and non-molts of the crayfish *Cyconectes* sp.

Element	Condition	Mean (ppm)	Ranges (ppm)	Std. Dev. (ppm)	Num. Obs.	t-stat.	Degrees of Freedom	Significance
I. R.	non-molt	9.4	4.7 - 12.4	2.2	9	-2.627	12	0.022
	exuvia	14.3	10.2 - 22.4	4.9	5			
Ca	non-molt	324284	285320 - 346700	19477	9	-1.565	12	0.143
	exuvia	342490	315710 - 366520	23349	5			
Mg	non-molt	4407	3545 - 5240	650	9	0.088	12	0.932
	exuvia	4370	2770 - 5150	948	5			
Sr	non-molt	679	595 - 760	57	9	-3.5	12	0.004
	exuvia	808	710 - 920	82	5			
Mn	non-molt	69	35 - 130	29	9	-3.2	12	0.008
	exuvia	235	130 - 510	156	5			
Na	non-molt	3991	965 - 7005	2457	9	2.421	12	0.032
	exuvia	1235	320 - 2125	653	5			
Fe	non-molt	44	30 - 80	16	9	-2.661	12	0.021
	exuvia	509	120 - 1460	542	5			

Differences between *Hemigrapsus nalis* (71) versus *Cancer productus* (70), and *Cancer magister* (72).

Element	Species Num.	Mean (ppm)	Ranges (ppm)	Std. Dev. (ppm)	Num. Obs.	t-stat.	Degrees of Freedom	Significance
I. R.	71	16.1	3.0-26.2	7.0	18	+0.420 -0.136	39 28	0.677 0.893
	70	15.3	6.8-32.1	5.7	23			
	72	16.5	0.3-28.6	10.7	12			
Ca	71	323260	273680-381320	28124	18	+2.661 -0.004	39 28	0.011 0.997
	70	302378	258100-338930	22167	23			
	72	323298	302900-350170	16771	12			
Mg	71	15215	13090-18625	1808	18	-5.004 -3.108	39 28	0.000 0.004
	70	17821	12760-20400	1526	23			
	72	17355	14610-20390	1907	12			
Sr	71	3698	2800-4290	441	18	-0.121 -0.998	39 28	0.904 0.327
	70	3713	2700-4230	354	23			
	72	3861	2980-4480	437	12			
Mn	71	15	10-25	4	18	-1.455 -0.963	39 28	0.154 0.344
	70	17	8-21	3	23			
	72	16	10-26	5	12			
Na	71	8166	5130-17335	3091	18	-0.209 -0.829	39 28	0.835 0.414
	70	8333	5590-14485	2008	23			
	72	9094	5720-14220	2864	12			
Fe	71	122	70-270	58	18	+1.572 -0.743	39 28	0.124 0.463
	70	98	50-185	37	23			
	72	141	60-340	84	12			
¹³ C	71	-1.845	-1.53 — -2.25	0.365	3	-2.212 -2.519	3 3	0.114 0.066
	70	-0.808	-0.30 — -1.32	0.725	2			
	72	-1.085	-0.91 — -1.26	0.247	2			
¹⁸ O	71	-2.08	-1.62 — -2.46	0.426	3	+0.288 -2.494	3 3	0.792 0.088
	70	-2.40	-0.97 — -3.83	2.022	2			
	72	-1.09	-0.77 — -1.41	0.453	2			

Differences between *Cancer productus* (70) and *Cancer asgister* (72).

Element	Species Num.	Mean (ppm)	Ranges (ppm)	Std. Dev. (ppm)	Num. Obs.	t-stat.	Degrees of Freedom	Significance
I.R.	70	15.3	6.8-32.1	5.7	23	-0.463	33	0.647
	72	16.5	0.3-28.6	10.7	12			
Ca	70	302378	258100-338930	22167	23	-2.862	33	0.007
	72	323298	302900-350170	16771	12			
Mg	70	17821	12760-20400	1526	23	0.788	33	0.437
	72	17355	14610-20390	1907	12			
Sr	70	3713	2700-4230	354	23	-1.086	33	0.285
	72	3861	2980-4480	437	12			
Mn	70	17	8-21	3	23	0.015	33	0.988
	72	16	10-26	5	12			
Na	70	8333	5590-14485	2008	23	-0.917	33	0.366
	72	9094	5720-14220	2864	12			
Fe	70	98	50-185	37	23	-2.102	33	0.043
	72	141	60-340	84	12			
¹³ C	70	-0.808	-0.30 — -1.32	0.725	2	0.512	2	0.659
	72	-1.085	-0.91 — -1.26	0.247	2			
¹⁸ O	70	-2.40	-0.97 — -3.83	2.022	2	-0.89	2	0.466
	72	-1.09	-0.77 — -1.41	0.453	2			

T-test statistical differences between *Cancer* and *Callinectes*

Element	Species	Mean (ppm)	Ranges (ppm)	Std. Dev. (ppm)	Num. Obs.	t-stat.	Degrees of Freedom	Significance
I.R.	<i>Cancer</i>	15.7	0.6-32.1	7.7	35	-0.56	50	0.578
	<i>Callin.</i>	16.9	7.5-36.7	7.1	17			
Ca	<i>Cancer</i>	309551	258100-350170	22593	35	3.099	50	0.003
	<i>Callin.</i>	284358	214920-357830	35747	17			
Mg	<i>Cancer</i>	17661	12760-20400	1653	35	-6.379	50	0.000
	<i>Callin.</i>	20432	18380-21805	969	17			
Sr	<i>Cancer</i>	3764	2700-4480	385	35	-1.573	50	0.122
	<i>Callin.</i>	3941	3410-4665	377	17			
Mn	<i>Cancer</i>	16.5	8-26	4	35	-3.903	50	0.000
	<i>Callin.</i>	28.2	10-66	17	17			
Na	<i>Cancer</i>	8594	5590-14485	2323	35	-1.321	50	0.192
	<i>Callin.</i>	9611	5620-17150	3115	17			
Fe	<i>Cancer</i>	113	50-340	60	35	3.723	50	0.001
	<i>Callin.</i>	56	30-120	25	17			
¹³ C	<i>Cancer</i>	-0.946	-1.32 — -0.30	0.470	4	.677	6	0.524
	<i>Callin.</i>	-1.728	-3.82 — 0.47	2.261	4			
¹⁸ O	<i>Cancer</i>	-1.745	-3.83 — -0.77	1.415	4	0.150	6	0.886
	<i>Callin.</i>	-1.895	-4.00 — -1.01	1.412	4			

T-test statistical differences between crayfish *Cyproendras* sp. and lobster *Paralithorus argus*.

Element	Species	Mean (ppm)	Ranges (ppm)	Std. Dev. (ppm)	Num. Obs.	t-stat.	Degrees of Freedom	Significance
I. R.	crayfish	11.1	4.7 - 22.4	4.0	14			
	lobster	25.4	9.1 - 43.0	13.2	13	-3.854	25	0.001
Ca	crayfish	330786	311060 - 366520	21984	14			
	lobster	244785	1536 - 292000	49830	13	5.878	25	0.000
Mg	crayfish	4394	2770 - 5240	733	14			
	lobster	24548	18125 - 34970	5241	13	-14.261	25	0.000
Sr	crayfish	725	595 - 920	90	14			
	lobster	3179	2180 - 4080	575	13	-15.779	25	0.000
Mn	crayfish	128	35 - 510	122	14			
	lobster	9	5 - 19	4	13	3.506	25	0.002
Na	crayfish	3007	320 - 7205	2393	14			
	lobster	21575	6740 - 51270	12757	13	-5.353	25	0.000
Fe	crayfish	210	30 - 1460	380	14			
	lobster	42	20 - 80	20	13	1.592	25	0.124
¹³ C	crayfish	-3.270	-4.70 — -2.08	1.326	3			
	lobster	0.212	-1.01 — 1.38	0.794	6	-5.043	7	0.001
¹⁸ O	crayfish	-8.295	-8.44 — -8.02	0.238	3			
	lobster	-4.605	-6.63 — -0.96	1.975	6	-3.117	7	0.017

Devonian

Statistical differences between *Alacops rana* specimens from the Demissa Bed (Ludlowville Formation) at Bayview (loc. 1.1) and Spring Brook, N. Y. (loc. 5.2).

Element	Locality Num.	Mean (ppm)	Ranges (ppm)	Std. Dev. (ppm)	Num. Obs.	t-stat.	Degrees of Freedom	Significance
I. R.	1.1	10	5.9 - 15.8	4	5			
	5.2	27	21.9 - 33.4	6	4	-5.059	7	0.001
Ca	1.1	371560	366670 - 380950	5493	5			
	5.2	340093	284630 - 377290	41683	4	1.699	7	0.532
Mg	1.1	4199	3995 - 4385	172	5			
	5.2	5850	5415 - 6495	490	4	-7.115	7	0.000
Sr	1.1	931	845 - 1060	79	5			
	5.2	1577	1230 - 1670	264	4	-5.264	7	0.001
Mn	1.1	2263	1905 - 2415	228	5			
	5.2	1660	1370 - 1830	200	4	6.267	7	0.004
Na	1.1	749	690 - 905	89	5			
	5.2	989	825 - 1060	110	4	-3.620	7	0.009
Fe	1.1	2666	2220 - 3095	320	5			
	5.2	2353	2210 - 2730	252	4	1.594	7	0.155
Al	1.1	257	195 - 325	54	5			
	5.2	467	205 - 790	177	4	-1.922	7	0.001

Statistical differences between *Phacops rana* specimens from the Smoke Creek Bed (Moscow Formation) at Bayview (loc. 1.2) and Fall Brook, N. Y. (loc. 3).

Element	Locality Num.	Mean (ppm)	Ranges (ppm)	Std. Dev. (ppm)	Num. Obs.	t-stat.	Degrees of Freedom	Significance
I.R.	1.2	7.2	3.4 - 13.1	3.1	15			
	3	11.8	5.1 - 21.6	5.2	12	-2.813	25	0.009
Ca	1.2	386017	330250 - 422420	25383	15			
	3	377127	349240 - 411560	20500	12	0.983	25	0.335
Mg	1.2	4758	3835 - 5850	665	15			
	3	6322	5440 - 7150	478	12	-6.842	25	0.000
Sr	1.2	1124	830 - 1520	215	15			
	3	1620	1180 - 2110	238	12	-5.674	25	0.000
Mn	1.2	2422	1650 - 3650	632	15			
	3	2267	1800 - 2905	343	12	0.762	25	0.453
Na	1.2	1005	545 - 1510	294	15			
	3	1311	1075 - 1485	127	12	-3.349	25	0.003
Fe	1.2	2885	1365 - 3700	678	15			
	3	2599	1830 - 3680	532	12	1.196	25	0.243
Al	1.2	225	120 - 360	83	15			
	3	382	0 - 855	257	12	-2.237	25	0.034
Zn	1.2	15	5 - 60	13	15			
	3	12	5 - 35	10	8	0.506	21	0.618
¹³ C	1.2	-0.565	-0.62 — -0.51	0.078	2			
	3	1.19	+1.17 — +1.27	0.028	2	-29.988	2	0.001
¹⁸ O	1.2	-5.65	-5.84 — -5.46	0.269	2			
	3	-5.905	-6.36 — -5.66	0.346	2	0.822	2	0.497

Stratigraphical differences between *Phacops rana* specimens from the Demissa Bed (1.1), and the Smoke Creek (1.2) and Penn Dixie Beds at Bayview, N. Y.

Element	Locality Num.	Mean (ppm)	Ranges (ppm)	Std. Dev. (ppm)	Num. Obs.	t-stat.	Degrees of Freedom	Significance
I.R.	1.1	10.2	5.9 - 15.8	4	5			
	1.2	7.2	3.4 - 13.1	3.1	15	1.687	18	0.109
	1.3	10.7	3.0 - 19.1	5.4	11	-0.186	14	0.855
Ca	1.1	371560	366670 - 380950	5493	5			
	1.2	386017	330250 - 422420	25383	15	-1.242	18	0.230
	1.3	348627	324550 - 369400	14002	11	3.487	14	0.004
Mg	1.1	4199	3995 - 4385	172	5			
	1.2	4758	3835 - 5850	665	15	-1.826	18	0.084
	1.3	4516	4195 - 4710	151	11	-3.744	14	0.002
Sr	1.1	931	845 - 1060	79	5			
	1.2	1124	830 - 1520	215	15	-1.928	18	0.070
	1.3	740	615 - 840	80	11	4.426	14	0.001
Mn	1.1	2263	1905 - 2415	228	5			
	1.2	2422	1650 - 3650	632	15	-0.542	18	0.594
	1.3	1837	1425 - 2230	245	11	3.28	14	0.005
Na	1.1	749	690 - 905	89	5			
	1.2	1005	545 - 1510	294	15	-1.891	18	0.075
	1.3	794	620 - 960	116	11	-0.767	14	0.456
Fe	1.1	2666	2220 - 3095	320	5			
	1.2	2885	1365 - 3700	678	15	-0.688	18	0.500
	1.3	1685	1300 - 2350	361	11	5.196	14	0.000
Al	1.1	257	195 - 325	54	5			
	1.2	225	120 - 360	83	15	0.812	18	0.428
	1.3	3	0 - 20	7	11	15.827	14	0.000
¹³ C	1.1	-0.625	-0.70 — -0.55	0.106	2			
	1.2	-0.565	-0.62 — -0.51	0.078	2	0.645	2	0.585
	1.3	-2.17	-2.30 — -2.04	0.184	2	10.294	2	0.009
¹⁸ O	1.1	-5.74	-5.94 — -5.54	0.283	2			
	1.2	-5.65	-5.84 — -5.46	0.269	2	-0.362	2	0.775
	1.3	-5.11	-5.50 — -4.72	0.552	2	-1.437	2	0.287

Stratigraphical differences between *Alacops rana* specimens from the Smoke Creek (1.2) and Penn Dixie Beds (1.3) at Bayview, N.Y.

Element	Locality Num.	Mean (ppm)	Ranges (ppm)	Std. Dev. (ppm)	Num. Obs.	t-stat.	Degrees of Freedom	Significance
I.R.	1.2	7.2	3.4 - 13.1	3.1	15			
	1.3	10.7	3.0 - 19.1	5.4	11	-2.05	24	0.051
Ca	1.2	386017	330250 - 422420	25383	15			
	1.3	348627	324550 - 369400	14002	11	4.404	24	0.000
Mg	1.2	4758	3835 - 5850	665	15			
	1.3	4516	4195 - 4710	151	11	1.175	24	0.252
Sr	1.2	1124	830 - 1520	215	15			
	1.3	740	1425 - 2230	80	11	5.596	24	0.000
Mn	1.2	2422	1650 - 3650	632	15			
	1.3	1837	1425 - 2230	245	11	2.898	24	0.008
Na	1.2	1005	545 - 1510	294	15			
	1.3	794	620 - 960	116	11	2.251	24	0.034
Fe	1.2	2885	1365 - 3700	678	15			
	1.3	1685	1300 - 2350	361	11	5.321	24	0.000
Al	1.2	225	120 - 360	83	15			
	1.3	3	0 - 20	7	11	8.825	24	0.000
¹³ C	1.2	-0.565	-0.62 - -0.51	0.078	2			
	1.3	-2.17	-2.30 - -2.04	0.184	2	11.37	2	0.008
¹⁸ O	1.2	-5.65	-5.84 - -5.46	0.269	2			
	1.3	-5.11	-5.50 - -4.72	0.552	2	-1.245	2	0.339

Ordovician

T-test statistical differences stratigraphically between *Isotakis gigas* from the Cobourg Fmn. (locality 9.1) and *Isotakis* sp. from the underlying Yerulam Fmn. (locality 9.2).

Element	Species	Mean (ppm)	Ranges (ppm)	Std. Dev. (ppm)	Num. Obs.	t-stat.	Degrees of Freedom	Significance
I.R.	9.1	8.3	4.3 - 13.9	3.2	6			
	9.2	6.9	3.0 - 13.4	2.3	28	1.302	32	0.202
Ca	9.1	377048	360750 - 393260	11477	6			
	9.2	382170	316200 - 448830	45228	28	-0.272	32	0.787
Mg	9.1	5083	4625 - 5835	475	6			
	9.2	5398	5025 - 5885	228	28	-2.487	32	0.018
Sr	9.1	551	420 - 625	80	6			
	9.2	782	555 - 1205	144	28	-3.783	32	0.001
Mn	9.1	238	215 - 270	20	6			
	9.2	180	115 - 250	32	28	4.228	32	0.000
Na	9.1	289	240 - 320	35	6			
	9.2	423	220 - 670	89	28	-3.601	32	0.001
Fe	9.1	672	490 - 1020	199	6			
	9.2	505	110 - 1030	273	28	1.419	32	0.166
Al	9.1	212	40 - 520	166	6			
	9.2	129	3 - 290	79	28	1.886	32	0.068
Zn	9.1	5	3 - 6	1.7	3			
	9.2	11	3 - 115	20.6	28	-0.542	29	0.592
¹³ C	9.1	-0.27	-0.43 - -0.11	0.226	2			
	9.2	-0.028	-0.20 - +0.15	0.138	5	-1.811	5	0.130
¹⁸ O	9.1	-5.035	-5.08 - -4.99	0.064	2			
	9.2	-5.202	-5.45 - -4.97	0.178	5	1.233	5	0.273

Statistical differences between *Isotekus maximus* specimens from the Trilobite Shale (17) and Frey's (1987) *Traptoceras dusseri* bed (15).

Element	Locality Num.	Mean (ppm)	Ranges (ppm)	Std. Dev. (ppm)	Num. Obs.	t-stat.	Degrees of Freedom	Significance
I.R.	15 17	6.1 3.7	3.8-8.5 1.9-7.2	1.8 1.8	11 14	3.261	23	0.003
Ca	15 17	364026 359653	353290-372970 346280-375990	6486 8232	11 14	1.443	23	0.163
Mg	15 17	3273 3499	2340-5015 3280-3895	808 204	11 14	-1.014	23	0.321
Sr	15 17	494 850	305-770 720-1005	138 105	11 14	-7.328	23	0.000
Mn	15 17	1805 753	1550-2160 605-1090	174 115	11 14	18.211	23	0.000
Na	15 17	217 310	145-265 185-390	34 53	11 14	-5.017	23	0.000
Fe	15 17	3885 2138	2100-4760 1440-2775	729 369	11 14	7.818	23	0.000
Al	15 17	178 168	115-270 60-270	51 66	11 14	0.408	23	0.687
¹³ C	15 17	-0.42 -0.745	-0.45 - -0.39 -0.80 - -0.69	0.042 0.078	2 2	5.188	2	0.035
¹⁸ O	15 17	-5.315 -4.73	-5.36 - -5.27 -4.91 - -4.55	0.064 0.255	2 2	-3.153	2	0.088

T-test statistical differences between *Vogdesia bromidensis* from locality 19 (Bromide Fmn.) and *Isotekus gigas* from locality 10 (Yerulam Fmn.).

Element	Species	Mean (ppm)	Ranges (ppm)	Std. Dev. (ppm)	Num. Obs.	t-stat.	Degrees of Freedom	Significance
I.R.	<i>Vogdesia</i> <i>I. gigas</i>	2.3 8.4	1.0-5.0 4.9-12.1	1.3 2.0	11 12	-8.479	21	0.000
Ca	<i>Vogdesia</i> <i>I. gigas</i>	353482 346017	303490-380260 322460-365880	19587 13086	11 12	1.084	21	0.291
Mg	<i>Vogdesia</i> <i>I. gigas</i>	4685 4481	3990-6250 4165-4790	677 215	11 12	0.995	21	0.331
Sr	<i>Vogdesia</i> <i>I. gigas</i>	980 547	920-1070 470-640	41 74	11 12	17.213	21	0.000
Mn	<i>Vogdesia</i> <i>I. gigas</i>	277 353	195-355 160-560	54 136	11 12	-17.34	21	0.098
Na	<i>Vogdesia</i> <i>I. gigas</i>	341	290-370 220-370	28 53	11 12	2.907	21	0.008
Fe	<i>Vogdesia</i> <i>I. gigas</i>	945 317	735-1270 210-430	156 68	11 12	12.703	21	0.000
Al	<i>Vogdesia</i> <i>I. gigas</i>	16.8 283	0-60 190-420	24 66	11 12	-12.495	21	0.000
¹³ C	<i>Vogdesia</i> <i>I. gigas</i>	-0.367 0.660	-0.42 - -0.26 0.66 - 0.86	0.092 0.000	3 2	-14.911	3	0.001
¹⁸ O	<i>Vogdesia</i> <i>I. gigas</i>	-4.673 -5.55	-4.81 - -4.46 -5.79 - -5.31	0.187 0.339	3 2	3.864	3	0.031

T-test statistical differences between *Acrotylus* (14) and *Isotakis maxinus* (12) from the base of the Whitby Finn.

Element	Sample Num.	Mean (ppm)	Ranges (ppm)	Std. Dev. (ppm)	Num. Obs.	t-stat.	Degrees of Freedom	Significance
I. R.	14 12	5.4 3.1	2.0 - 10.7 0.9 - 5.2	2.4 1.2	16 17	3.498	31	0.001
Ca	14 12	347984 350561	313560 - 418690 320600 - 371780	23999 15412	16 17	-0.369	31	0.714
Mg	14 12	7830 8001	6100 - 9455 6210 - 8565	851 599	16 17	-0.671	31	0.507
Sr	14 12	1634 1701	1090 - 2240 1110 - 2050	310 237	16 17	-0.702	31	0.488
Mn	14 12	223 134	140 - 455 100 - 230	91 32	16 17	3.771	31	0.001
Na	14 12	1748 1614	1440 - 2130 735 - 2290	242 400	16 17	1.151	31	0.259
Fe	14 12	965 708	330 - 1365 470 - 1190	265 178	16 17	3.29	31	0.003
Al	14 12	174 61	0 - 310 0 - 135	104 59	16 17	3.862	31	0.001
Zn	14 12	9 3	8 - 10 2 - 4	1.4 0.7	2 9	9.92	9	0.000
^{13}C	14 12	+0.003 -0.418	-1.10 — 0.70 -0.73 — -0.09	0.966 0.247	3 8	1.233	9	0.249
^{18}O	14 12	-6.120 -6.046	-6.49 — -5.23 -7.26 — -5.31	0.774 0.653	3 8	-0.16	9	0.877

Appendix Y

XRD Evaluation

For reference, the following XRD values for different minerals are given (Milliman, 1974).

<u>Mineral</u>	<u>Value</u>
aragonite std.	26.24
alpha quartz	26.66
calcite (LMC)	29.43
dolomite	32.00
pyrite	33.07 and 56.34

Interpretation as to the mineralogy of the specimen is based on geochemical analysis, and with respect to the above values for XRD analysis (in parentheses). Original geochemical mineralogies are low magnesium calcite (LMC; 0—4 mol % Mg), intermediate magnesium calcite (IMC; 4—7 mol % Mg) and high magnesium calcite (HMC; > 7 mol % Mg) (Millimay, 1974). Detailed XRD mineralogies are difficult to assign due to the age and relative inaccuracy of the equipment used, however, the machine was able to detect low magnesium calcite, quartz (Qtz) and pyrite peaks.

Table 5: Results of XRD analysis.

<u>Sample Number</u>	<u>XRD Value</u>	<u>MgCo₃ (mol %)</u>	<u>Interpretation</u>
RECENT			
<i>Cancer productus</i>			
70, 28, 18 170	No strong peak	5.12	IMC (N/A)
70, 28, 18 171	29.6 (weak)	6.42	IMC (LMC)
<i>Cancer magister</i>			
72, 28, 17 288	29.8	5.92	IMC (LMC)
<i>Oreconectes</i> sp.			
80, 27, 17 249	29.7 (weak)	1.23	LMC (LMC)
80, 27, 17 264	No strong peak	1.81	LMC (N/A)
DEVONIAN			
<i>Phacops rana</i>			
31, 1.1, 12 228	26.7 (weak) and 29.7 (weak)	1.44	LMC (Qtz and LMC)
31, 1.1, 21 229	26.6 (weak) and 29.5 (weak)	1.42	LMC (Qtz and LMC)
31 (1), 1.2 (1), 16 06	29.9	1.68	LMC (LMC)
31 (1), 1.2 (1), 11 30	29.4	1.61	LMC (LMC)
31 (1), 1.2 (1), 14 96	29.8	1.36	LMC (LMC)
31 (1), 1.2 (1), 16 98	29.5	1.41	LMC (LMC)
31, 1.3, 21 456	26.6 and 29.6	1.61	LMC (Qtz and LMC)
31, 1.3, 13 458	26.6 (weak) and 29.5	1.62	LMC (Qtz and LMC)
31, 1.3, 13 467	26.5 (weak) and 29.5	1.59	LMC (Qtz and LMC)
31 (1), 2, 11 85	26.8 and 29.6	1.90	LMC (Qtz and LMC)
31 (1), 3, 17 91	29.4	2.14	LMC
31 (1), 3, 14 104	29.5	1.89	LMC
31 (1), 4.1 (4), 11 11	26.7, 29.5 and 56.3	1.27	LMC (Qtz, IMC and pyrite)
31 (1), 4.1 (4), 13 12	26.7 and 29.5	1.58	LMC (Qtz and LMC)
31, 4.1, 21 395	26.9 and 29.7	1.50	LMC (Qtz and LMC)
31, 4.1, 13 398	26.6 and 29.4	2.20	LMC (Qtz and LMC)
31 (1), 4.2 (5), 16 16	26.7 and 29.7	1.86	LMC (Qtz and LMC)
31, 4.2, 11 418	26.8 and 29.7	1.31	LMC (Qtz and LMC)
31, 4.2, 11 408	30.1 (weak)	1.52	LMC (LMC)
31, 24, 13 500	29.3	2.07	LMC (LMC)
31, 25, 13 477	29.7	1.56	LMC (LMC)

Terataspis grandis

33(8), 2, 12 67	26.7 and 29.5	2.25	LMC (Qtz and LMC)
33(8), 2, 12 68	29.9 and 31.3	2.76	LMC (HMC/ dolomite)
33(8), 2, 11 73	27.0 and 29.9	4.46	LMC (Qtz and LMC)

ORDOVICIAN

Isotelus gigas

11(3), 9.2(10), 12 38	29.4	1.99	LMC (LMC)
11(3), 9.2(10), 11 43	29.7	1.88	LMC (LMC)
11, 10, 11 638	29.5	1.55	LMC (LMC)
11, 10, 13 641	29.7	1.47	LMC (LMC)

Isotelus maximus

12, 6.2(6), 19 24	29.9	2.95	LMC (LMC)
12, 6.2(6), 11 27	29.5	2.84	LMC (LMC)
12, 6.2, 19 609	29.5	2.97	LMC (LMC)
12, 6.2, 19 610	29.5	2.85	LMC (LMC)
12, 14.1, 12 526	29.7	1.13	LMC (LMC)
12, 14.1, 19 538	30.1(weak)	1.10	LMC (LMC)
12, 14.2, 11 547	29.4	0.97	LMC (LMC)
12, 14.2, 11 551	29.4	1.05	LMC (LMC)
12, 15, 14 557	29.6	1.01	LMC (LMC)
12, 17, 11 576	29.7	1.15	LMC (LMC)
12, 17, 11 577	29.8	1.17	LMC (LMC)

Pseudogygites latimarginatus

14, 6.1, 13 608	29.5	2.50	LMC (LMC)
-----------------	------	------	-----------